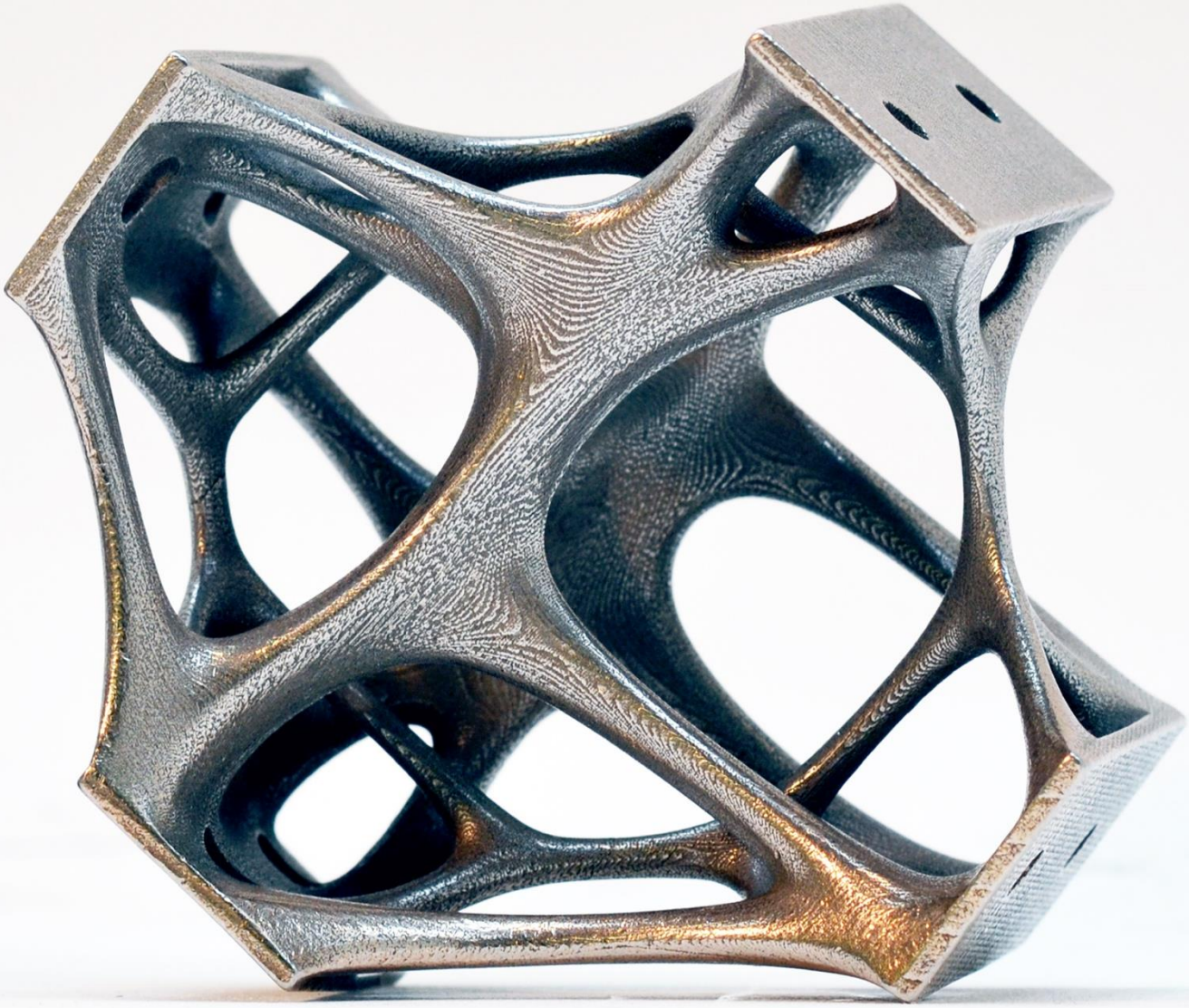

3F3D

3F3D: Form Follows Force with 3D printing

Topology Optimization for Free-form Building Envelope design with Additive Manufacturing

Student:
Bayu Prayudhi

Student number:
4416368

Contact:
bayu.prayudhi@gmail.com

Members of graduation committee:

Dr. M. Turrin
Architectural Engineering +Technology
Design Informatics

Prof.dr.ing. U. Knaack
Architectural Engineering +Technology
Design of Construction

Shibo Ren
Guest supervisor from ARUP Amsterdam

Delft University of Technology
Faculty of Architecture and the Built Environment
Master track of Building Technology

Start date: November 5, 2015
Graduation date: June 30, 2016

ARUP TUDelft

ACKNOWLEDGEMENT

The graduation project represents the end of my study journey in Delft. I am very grateful for a high value of unforgettable 2 years of learning experience. I would like to express my gratitude to the people who have supported me intellectually, financially, and mentally.

The project would not be possible without the support and trust of all my mentors. Michela Turrin, who is always available for discussions, guidance, and keeping me on track since the very beginning of the project. Ulrich Knaack, who inspires me to push the boundaries and challenge me to do something beyond my expectation for the project. Shibo Ren, my guest supervisor from ARUP Amsterdam who inspires me to choose the topic and always provide useful information and technical solution.

Special thanks for Mathew Vola from ARUP for his helpful feedbacks. Marcel Bilow for helping me build the prototype structure with his Bucky Lab tools. Aaron Bislip for his amazing Leeuwenhoek 3D printer. And also for people at ALTAIR for providing me a full license of Hyperworks Suite for the project.

I would like to express my deepest gratitude for Indonesia Endowment Fund for Education (LPDP) with the Ministry of Finance of Indonesia for the scholarship which allows me to pursue my master study including funding for this project.

Finally, thanks to my family back home for all the support. My dearest Monica and all my friends in Delft for all the fun and stressful times together. It has been a great two years.

TABLE OF CONTENTS

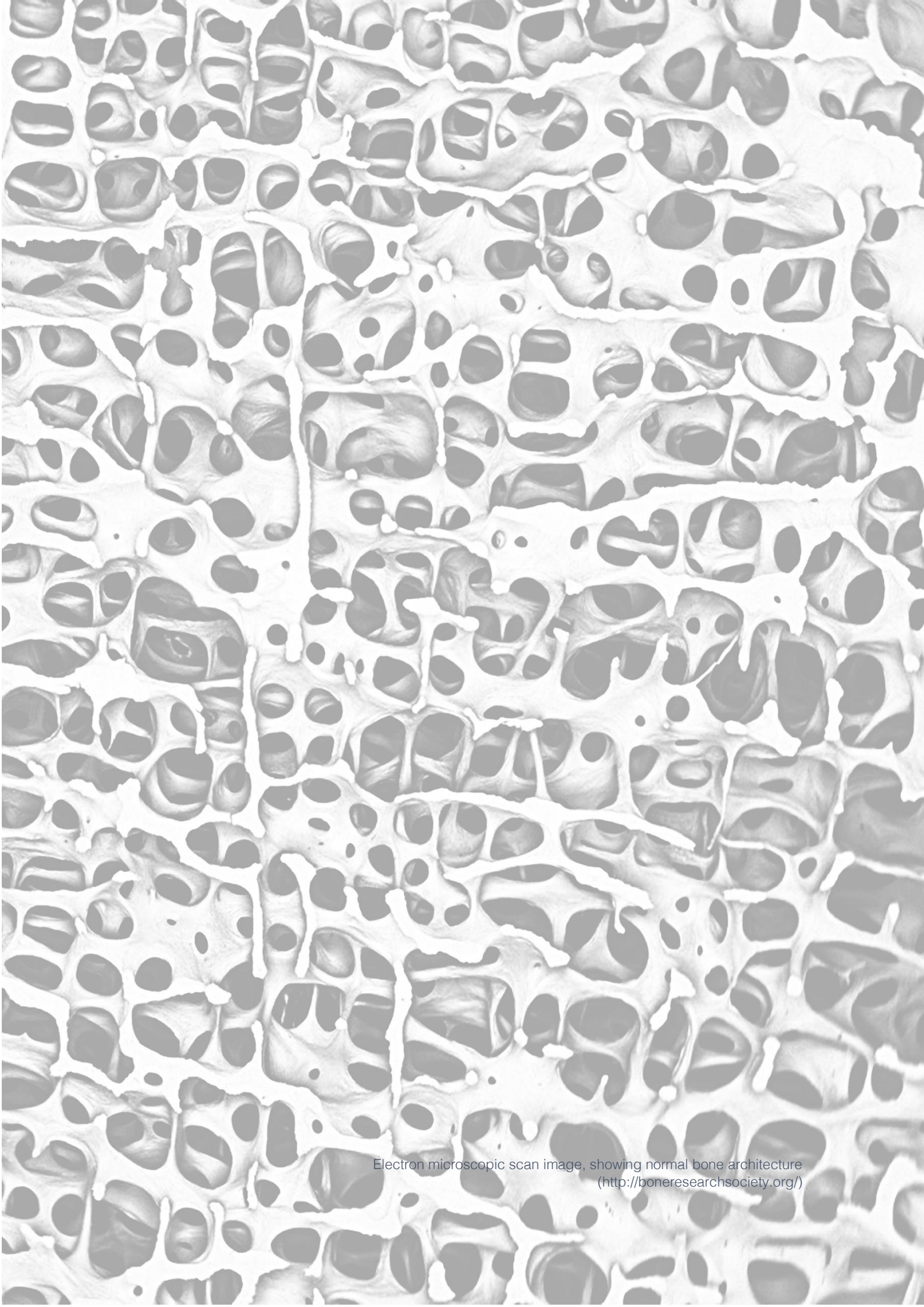

Electron microscopic scan image, showing normal bone architecture
(http://boneresearchsociety.org/)

INTRO
DUCTION

1

INTRODUCTION

1.1 Problem statement

The development of Computer Aided Design (CAD) as a design tool gives a lot of new opportunities and freedom for architects and designers to create a new innovative type of building envelope with complex freeform geometry. This advancement comes in parallel with the progress of digital fabrication, which enable a seamless 'file-to-factory' process that allows designers to create manufactured products from digital design directly (Strauss, Knaack, & Techen, 2012).

However, most of the standard fabrication tools today are subtractive-based process. The main drawbacks of this method is a significant amount of material waste compare to the exact amount of material that is actually being used for the final product. For example, CNC milling machine uses a block of material and removes unnecessary excess until only the desired shape remains.

Figure 1-1 Gradation of material density in bone structure, optimized for structural function (Pawlyn, 2011)

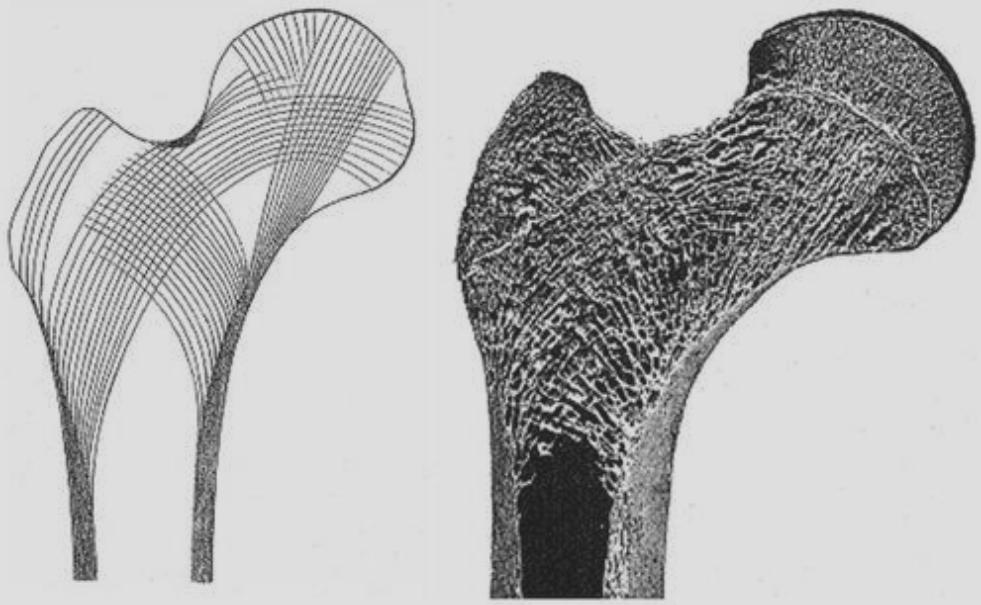

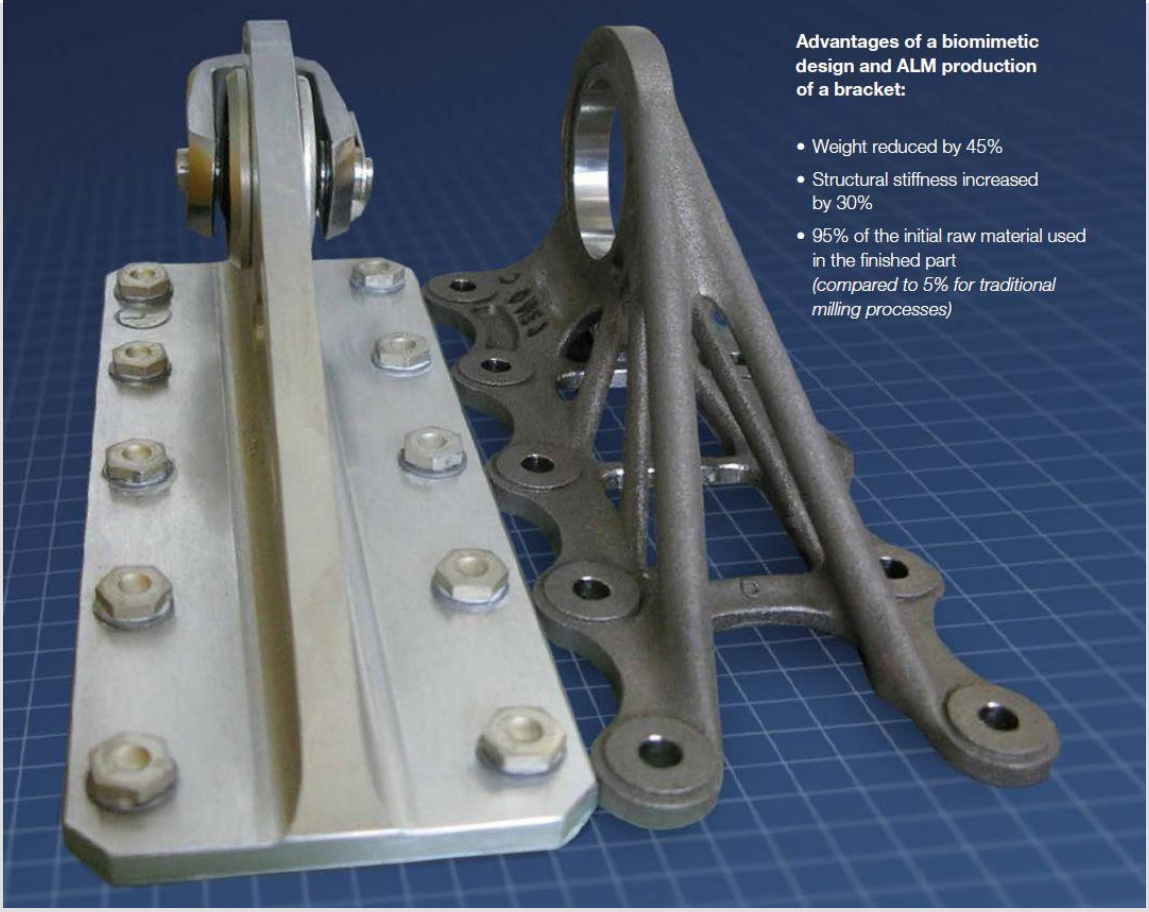

Figure 1-2 Airbus topology optimized bracket design, manufactured with metal 3d printing technology (Airbus technical magazine, January 2015)

If we compare the way we build our products today with the growth process that happens in the nature system, we could say that our conventional manufacturing system is tremendously inefficient. The optimization of material usage plays a necessary role in nature; the principle is 'materials are expensive and shape is cheap' as opposed to current technology in our manufacturing industry, the opposite tend to be the case (Pawlyn, 2011).

Recent development in Topology Optimization and Additive Manufacturing could play an important role in changing the way we design and manufacture our products considering of how the process mimics the nature system of manufacturing and design, so-called biomimicry design.

Topology Optimization (TO) method provides an answer to the following structural design question: Given a specified design domain including loads, supports and constraints; how should material be distributed? Such that the performance of the resulting structure is the most efficient, relative to the aim of the optimization (Bendsoe & Sigmund, 2003). Additive Manufacturing (AM) is the natural counterpart to TO, which the emphasis is on its capability to fabricate complex geometry, sometimes described in terms of providing 'complexity for free' (Gibson, Rosen, & Stucker, 2015). AM technology has been used in several industries such as aerospace and automotive, where minimizing the self-weight is crucial for cost saving. Although the development of AM in Architecture industry is still at the early stage, the technology offers the potential to revolutionize the methods of design and fabrication.

1.2 Research objective

The objective of this research is to design a structural system for free-form envelope of building by utilizing the potential of additive manufacturing and using topology optimization as a design method to optimize the structural performance and reducing the amount of structural material in comparison to the existing design and manufacturing process.

1.3 Research question

What are the design strategies to optimize structural performance and material efficiency in freeform envelope structure by utilizing the advantages of additive manufacturing?

Sub questions

- What is topology optimization and how to apply the method on free-form envelope design?
- What type of additive manufacturing process, including which material is suitable for the optimized structure design?
- What is the new design method of free-form envelope structure by utilizing the potentials of topology optimization and additive manufacturing?

1.4 Relevance

The current general perception of Additive Manufacturing in the building industry is that it still has a very high cost compare to the conventional method. However, the general cost is decreasing over time and new technology of AM emerges every year, with the emphasis on more efficiency, lower cost, and availability of the technology for everyone. The advantage of 'complexity is free' offered by AM, gives architects and designers opportunities to focus on design performance and innovation, rather than restricted by manufacturing constraint. Realizing this opportunities, Topology Optimization is the natural counterpart as a design method for AM technology (Langelaar & Keulen, 2015). It helps designers distribute structural material in the most efficient way, relative to the aim of structural optimization. The process gives designer even more freedom to focus on design performance. While topology optimization method has been used extensively in the aerospace industry, the architecture industry is mostly still using conventional approach in its structural design system. A typical building typology that can maximize the potential of TO and AM technology are freeform structure. Freeform geometry in architecture was made popular following the availability of complex CAD tools available for designers. This research will investigate the potential of TO and AM to minimize the labour intensive and high material inefficiency in the highly complex design and fabrication of freeform structure.

1.5 Research methodology

The scheme of the research thesis will mainly divided into three phase: Literature study, Research analysis, and Design. First, the literature study focus in the latest state of the art development in Additive Manufacturing process for structural design. The research will focus on the conventional proven material for AM process (metal) and study on available alternative material as an option to replace metal in AM for structure, such as polymers and composites.

Theoretical background research on Topology Optimization will conducted by studying the basic principle of TO process. Tests on general TO cases are done by utilizing a commercially available TO tools which are available for academic purposes. The research are done on theoretical load case scenarios to study different behaviours of TO method according to each cases. On the other hand, theoretical background research on freeform envelope is conducted by studying the design methodology of some built projects by studying the design process for its structural performance while also considering its choice of manufacturing process.

The research analysis phase will use the information gathered from literature study to define the design methodology and direction in the design phase. A simple design process of topology optimized design for AM is conducted using a theoretical case of a simple TO design. This process will include a research on design optimization method for AM, such as minimizing support material. The result of this theoretical design process will be used as a reference model to research the current market cost of metal AM. Analysis on material options will also be done be doing mechanical test on selected metal materials or alternatives material such as composite.

A case study of freeform envelope built project will be selected. After that, an analysis will be conducted on a new design method on the freeform envelope design using the same boundary conditions on the case study with the new design methodology utilizing the potential of TO and AM process.

The design phase will start after the case study is selected and the design method is defined. The design process will conducted from a macro level of the whole geometry of freeform envelope surface until the micro level of connection detail of AM-produced parts. The design process is done with the structural performance, material efficiency, and fabrication method as main objective criteria.

After the design of the new structure is defined, a prototype will be made. The prototype will be the proof of concept which shows not only the result of TO geometry fabricated with AM process, but the general assembly and its practicality and feasibility in the context of architecture.

The design result of the new freeform envelope structure and the prototype result will be used evaluate the research question, generates a conclusion and possible suggestion for further research on the similar topic.

The general framework of the research method is described:

1. Literature study
    a. Topology Optimization (TO) principle and methods
    b. Relevant Additive Manufacturing (AM) method for structure
        i. Market research for AM metal cost
        ii. Alternative method for AM metal
    c. Principle of freeform envelope structure
2. Research and analysis
    a. TO software learning (OptiStruct)
    b. Design optimization method for AM
    c. Potential utilization research of TO in freeform structure
3. Design phase
    a. Define case study
    b. TO design domain, boundary conditions, and load cases definition
    c. TO calculation process
    d. Design optimization for AM
    e. FEM analysis and possible reiteration
    f. Design for construction
4. Prototype definition and manufacturing
5. Result
    a. Analysis and comparison
    b. Design adjustment
    c. General recommendations and final report.

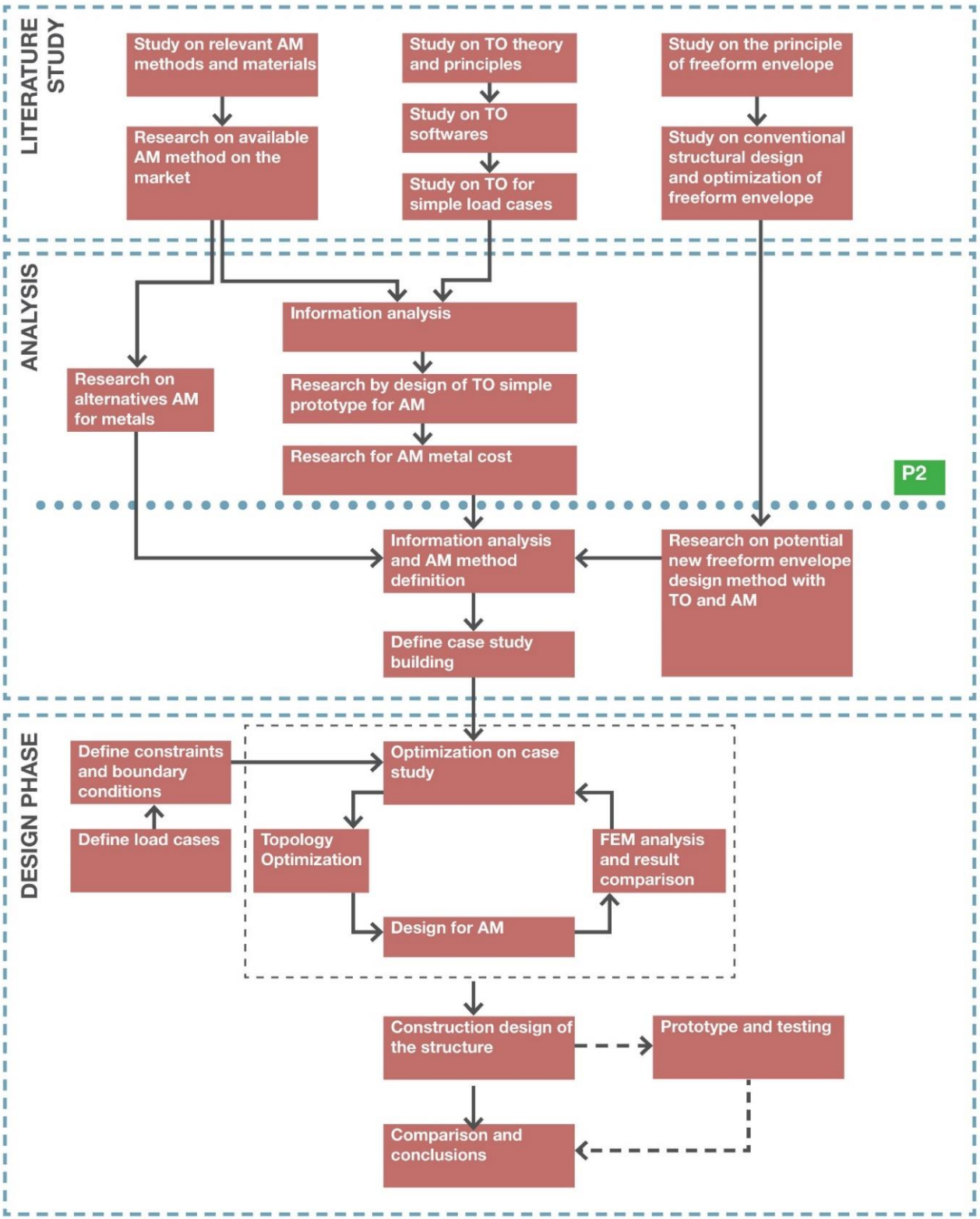

Figure 1-3 Thesis research scheme

1.6 References

Bendsoe, M., & Sigmund, O. (2003). *Topology optimization: Theory, methods, and applications*. Berlin: Springer.

Blaauwendraad, J., & Hoefakker, J. H. (2013). Structural shell analysis: Understanding and application (*Solid Mechanics and Its Applications, v.200*). Dordrecht: Springer. doi:10.1007/978-94-007-6701-0

Burns, M. (1993). *Automated fabrication: Improving productivity in manufacturing*. Englewood Cliffs, N.J.: PTR Prentice Hall.

Christensen, P. W., & Klarbring, A. (n.d.). An Introduction to Structural Optimization. *Solid Mechanics and Its Applications,* 1-7. doi:10.1007/978-1-4020-8666-3_1

Gibson, I., Rosen, D., & Stucker, B. (2015). *Additive manufacturing technologies: 3D printing, rapid prototyping, and direct digital manufacturing* (Second edition.). New York, NY: Springer. doi:10.1007/978-1-4939-2113-3

Knaack, U. (2007). *Facades: Principles of construction*. Ba: Birkha¨user. http://public.eblib.com/choice/publicfullrecord.aspx?p=336679

Langelaar, M., & Keulen, F. (2015). Topology optimization. A natural counterpart of additive manufacturing. *TU Delft Lecture Notes*.

Oxman, N., Laucks, J., Kayser, M., Tsai, E., & Firstenberg, M. (2013). *Freeform 3D Printing: Toward a Sustainable Approach to Additive Manufacturing. Green Design, Materials and Manufacturing Processes.*

Pawlyn, M. (2011). *Biomimicry in architecture*. London, UK: Riba Publishing.

Strauss, H., Knaack, U., & Techen H. (2013). *AM Envelope: The Potential of Additive Manufacturing for facade constructions*. TU Delft. http://resolver.tudelft.nl/uuid:3a69355a-51d7-4207-943f-57a03f855d04

Winslow, P. (2014). *Multi-criteria gridshell optimization. In Shell structures for architecture: Form finding and optimization*. London: Routledge/ Taylor & Francis Group.

SUMMARY

TO design method is the natural counterpart of AM (Langelaar & Keulen, 2015), many believes that the technology could revolutionize the way we manufacture our everyday products. However, the level of research for the application of the technology in the building industry is still far behind compared to other more advanced industry such as the aerospace or automotive. This research thesis explores the opportunities and the possibilities of using this relatively young technology in the building industry, by developing not only a new manufacturing process but also new design methodology for architecture projects.

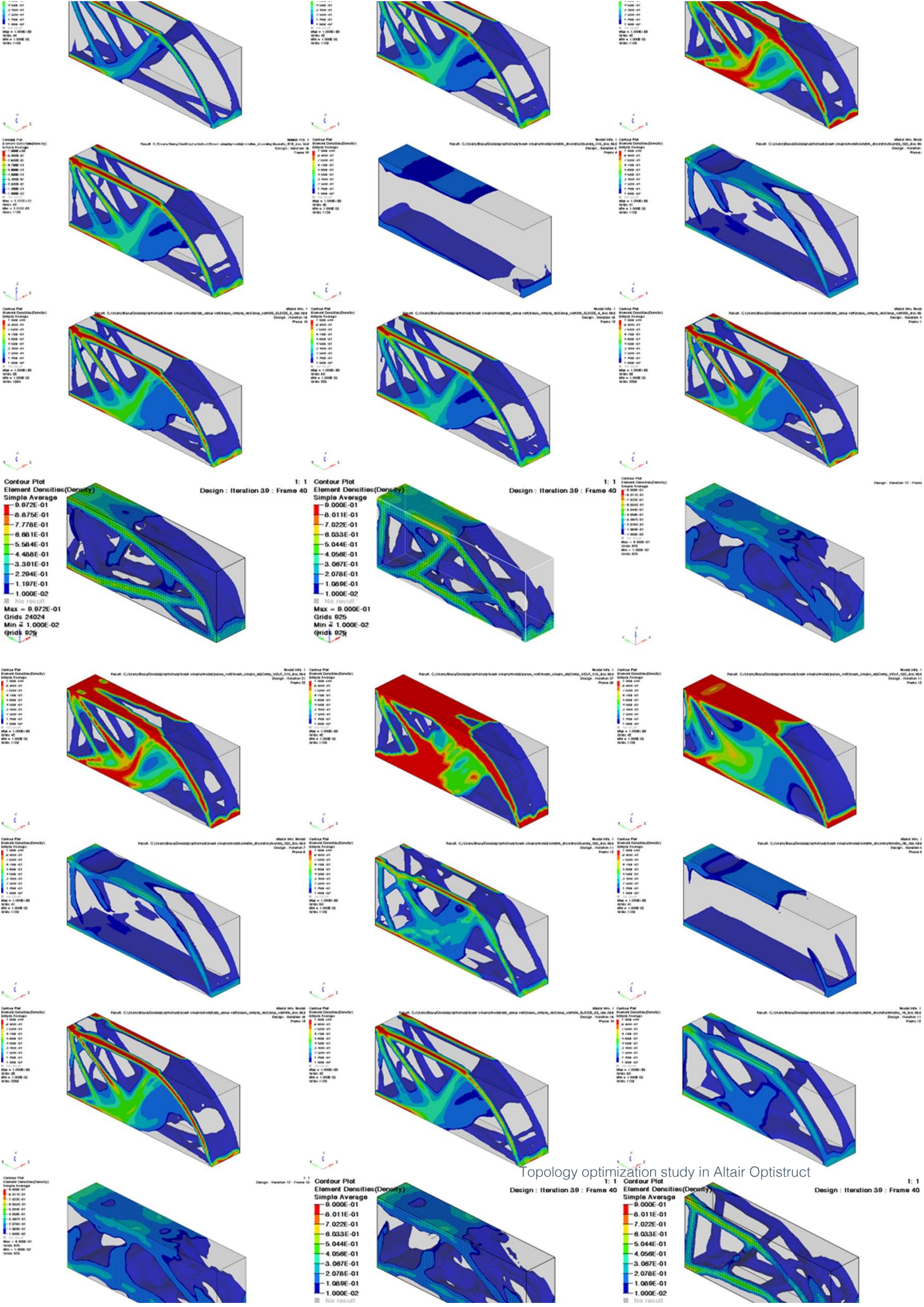
Contour Plot
Element Densities(Density)
Simple Average
9.972E-01
8.875E-01
7.778E-01
6.681E-01
5.584E-01
4.488E-01
3.391E-01
2.294E-01
1.197E-01
1.000E-02
No result
Max = 9.972E-01
Grids 24024
Min = 1.000E-02
Grids 925
1: 1
Design : Iteration 39 : Frame 40
Contour Plot
Element Densities(Density)
Simple Average
9.000E-01
8.011E-01
7.022E-01
6.033E-01
5.044E-01
4.056E-01
3.067E-01
2.078E-01
1.089E-01
1.000E-02
No result
Max = 9.000E-01
Grids 925
Min = 1.000E-02
Grids 925
1: 1
Design : Iteration 39 : Frame 40
Topology optimization study in Altair Optistruct

TOPOLOGY OPTIMIZATION

2

TOPOLOGY OPTIMIZATION

2.1 Structural optimization in general

Structural optimization is the subject of making an assemblage of materials to sustain loads in the best way (Christensen & Klarbring, 2009). Designers following certain predetermined constraints and conditions can define the term “best” subjectively. One can optimize a structure to be as light as possible or as stiff as possible. Designers can measures a number of structural performance as parameters, such as weight, stiffness, critical load, stress, displacement, and geometry. A structural optimization problem are formulated with a combination of these parameters as an objective function that should be maximized of minimized and using some other measures as constraints.

Figure 2-1 Multiple iteration steps of Topology Optimization of a chair. The solid material is gradually removed based on structural load of a person seating applied. (http://www.liftarchitects.com/)

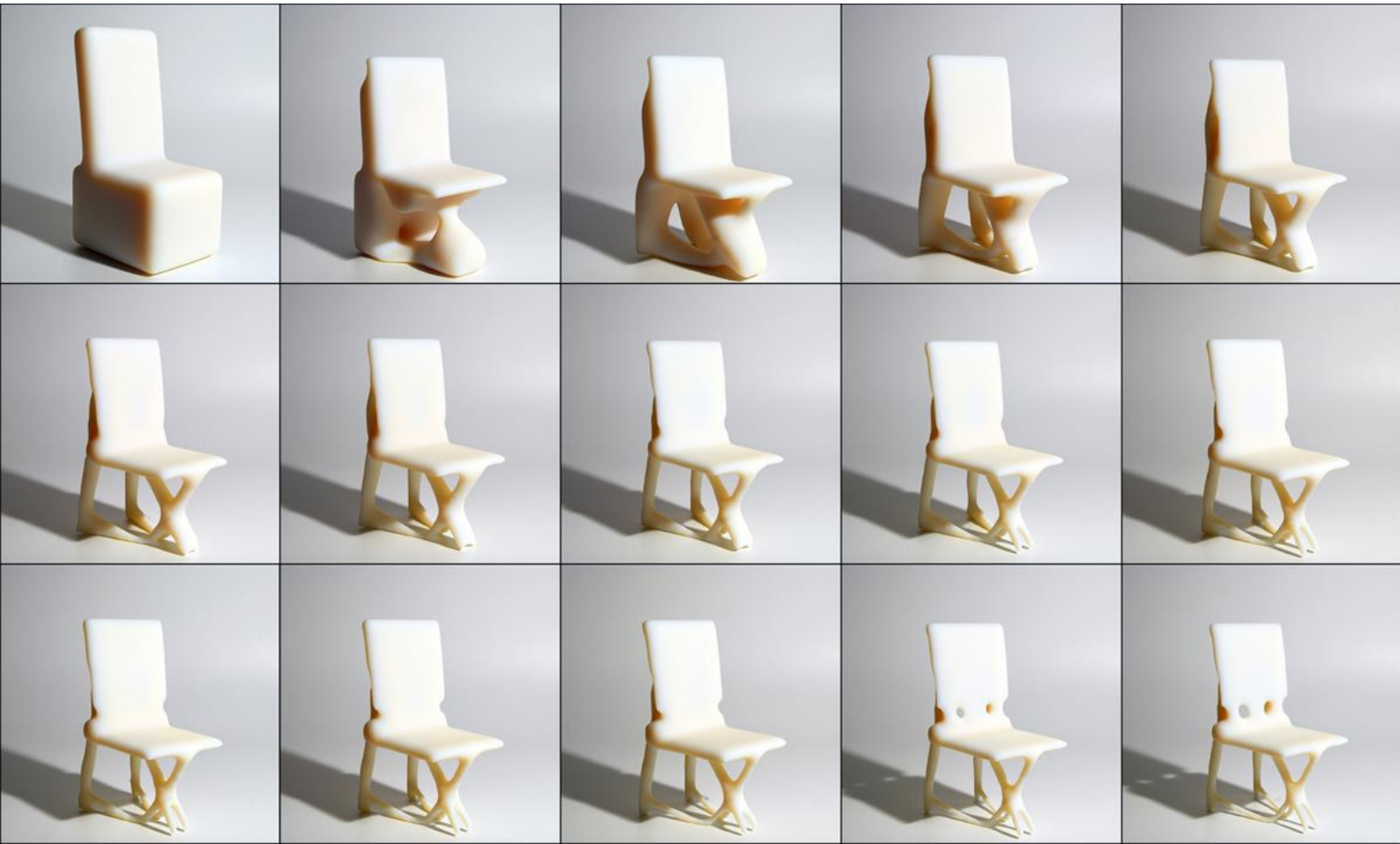

1. General mathematical form of a Structural Optimization problem.

In a structural optimization problem, there are three general function and variables that are always present (Christensen & Klarbring, 2009):

- *Objective function* (*f*): A function that is used to classify the design. For each possible design alternatives, *f* returns a number which indicates the performance of the design. Usually the optimization problem is defined as minimization problem, where the objective is to have a smaller value of *f*.
- *Design variable* (*x*): A function or vector that describes the design as a parameter which can be changed during optimization. It may represent geometry or material properties.
- *State variable* (*y*): For a given design *x*, *y* is a function or vector that represents the feedback of the structure. It may represent displacement, stress, strain, or force.

$$(\boldsymbol{SO})\begin{cases}\text{minimize } f\ (x\ , y) \text{ with respect to } x \text{ and } y \\ \text{subject to} \begin{cases}\text{behavorial constraint on } y \\ \text{design constraints on } x \\ \text{equilibrium constraint.}\end{cases}\end{cases}$$

A structural optimization problem can have more than one objective function, a multiple objective optimization problem:

$$\text{minimize } \big(f_1(x\ , y), f_2(x\ , y), \dots, f_l(x\ , y)\big),$$

where *l* is the number of objective functions, and the constraints are the same as for (SO). One should typically tries to achieve so-called *Pareto optimality:* a design is Pareto optimal if there is no other design alternatives that satisfies all of the objectives better.

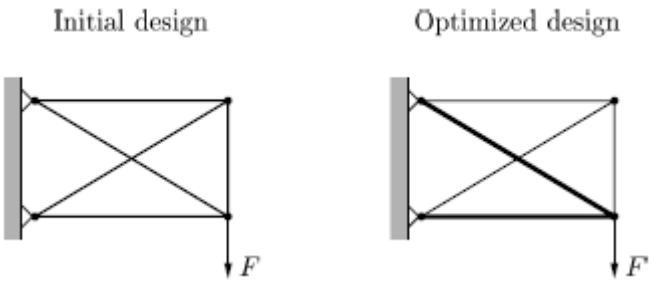

Figure 2-2 Sizing optimization

2. Three Types of Structural Optimization Problems

- Sizing optimization

An approach to optimal design with variable of structural thickness and dimension as design variable, i.e., cross-sectional dimensions of truss members or thickness distribution of a plate.

- Shape optimization

The design variable is the form of the boundary of the structural domain, while maintaining the boundary and the connectivity of the structure.

- Topology optimization

In this case, the process begins by discretization of the geometry of the design domain, and applying a value of 0 to 1 into these elements and taking away elements with low value. In short, topology optimization place the material only where they are useful to achieve a certain objective.

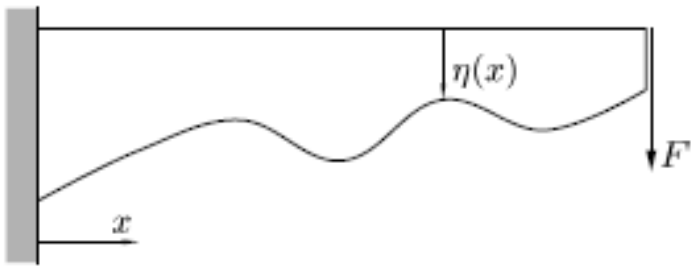

Figure 2-3 Shape optimization

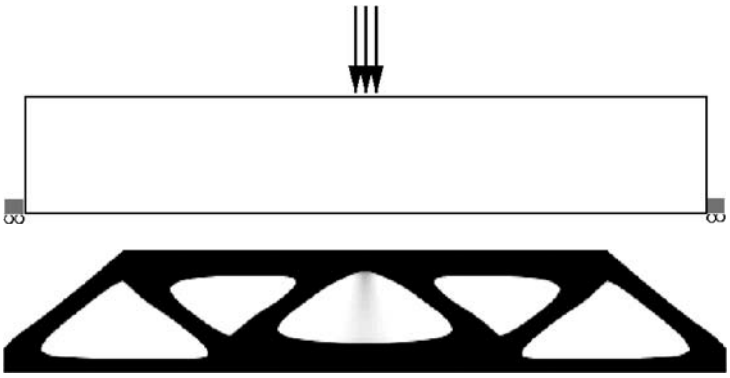

Figure 2-4 Two-Dimensional topology optimization

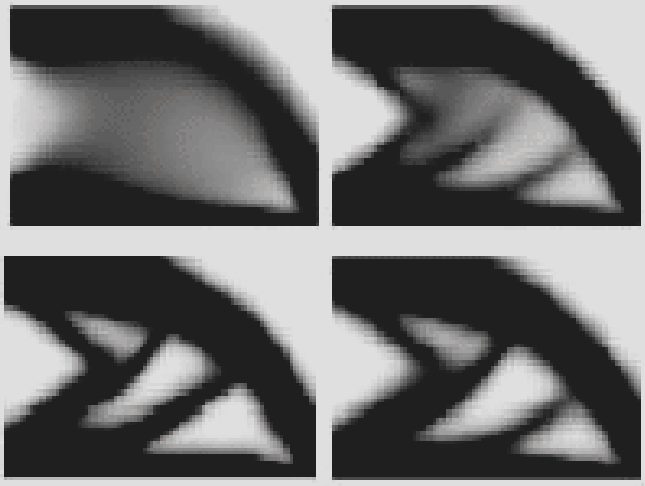

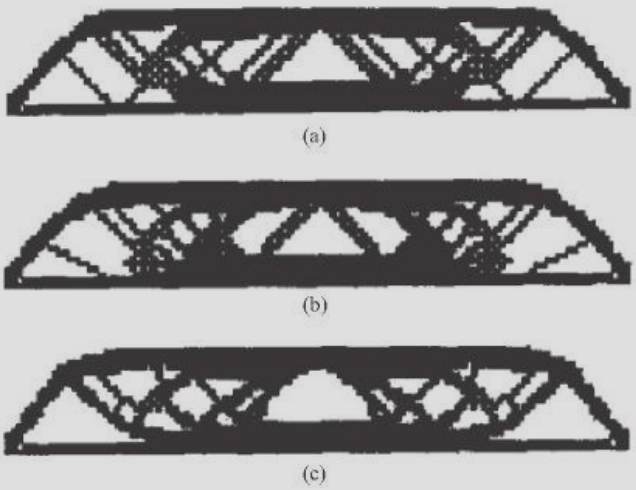

Figure 2-5 (Top) TO with SIMP method (Bendsoe & Sigmund, 2003)

Figure 2-6 (Top right) ESO topologies for a centrally loaded beam with different element removal ratio (err): (a) = 1%; (b) = 2%; (c) = 4%. (Huang & Xie, 2010)

Figure 2-7 (Right) BESO evolution history of 3d structural topology: (a) iteration 15; (b) iteration 30; (c) iteration 45; (d) iteration 60; (e) iteration 80; (f) iteration 87. (Huang & Xie, 2010)

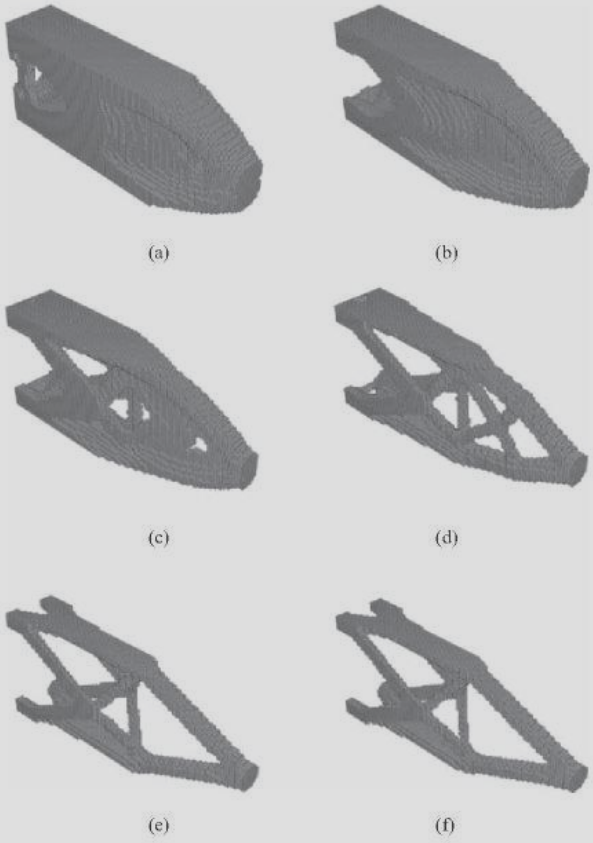

2.2 Method of Topology Optimization

Topology optimization is the most general type of structural optimization, it studies the topology of a structure. The method discretize a given design domain into finite element mesh with a state value, i.e. if it consists of material, void, or an intermediate. The take place with a predefined loads, boundary conditions, and additional design restrictions such as prescribed solid or void areas, e.g. holes for connections.

TO is used in the early conceptual design phase. The optimized topology found as a solution to a specific structural design problem, designers and engineers need to translate the result topology geometry for its design context and manufacturability. There are several method of TO process developed by researcher (Lundgren & Palmqvist, 2012):

1. Solid Isotropic Microstructure with Penalization (SIMP) method

   The SIMP method based on the assumption that each element contains an isotropic material with variable density. The elements are used to discretize the design domain where the design variables are the relative densities of the elements. The densities of each elements are visualized as a value between 0 to 1, or white, shades of grey, and white. Elements with zero density represented by white colour implies removal of the element. Then, a penalization occurs with the power-law interpolation scheme to penalize the intermediate densities to obtain solutions with nearly 0 and 1 material distribution. By varying the penalization parameter value one can define how much grey material are. A maximum penalization value will result a true black and white solution, which from engineering perspective is preferable. (Bendsoe & Sigmund, 2003)

2. Evolutionary Structural Optimization (ESO) method

   The ESO method is based on the simple concept of gradually removing inefficient material from a structure, with the low value of stress (or strain) as an indicator of inefficient use of material. Low-stressed material is assumed to be under-utilized and is therefore removed by deleting elements from the finite element model subsequently. The stress level of each element is determined by comparing, e.g. the von Mises stress of each element with the maximum von Mises stress of the whole structure. The cycle of finite element analysis and element removal is repeated until a steady state is reached and there are no more elements needed to be removed using the current rejection ratio. (Huang & Xie, 2010)

3. Bi-directional Evolutionary Structural Optimization (BESO) method

   The BESO method allows material to be removed and added simultaneously. The sensitivity numbers of the void elements are estimated through a linear extrapolation of the displacement field after the finite element analysis. Then, the solid elements with the lowest sensitivity value are removed and the void elements with the highest sensitivity value are changed to solid. The quantity of removed and added elements in each iteration are determined by rejection ratio (*RR*) and inclusion ratio (*IR*) respectively, where these two parameters are treated separately. (Huang & Xie, 2010)

4. Homogenization method

   An optimization problem with Homogenization method for generalized topology is defined by solving the optimal porosity of the elements identified from a design domain. The method uses infinitely discretization of micro scale voids forming a porous elements which creates a linearly elastic structure. If a portion of porous elements consists of only voids, material is not placed. Whereas, if there is no porosity on another portion, it defined as solid material. (Suzuki & Kikuchi, 1991)

5. Level set method.

   The Level set method combines the shape sensitivity analysis with the Hamilton—Jacobi equation for moving the level-set function, to find the topology design of structures. The method optimize the structure by modifying the boundaries of the design domain. Material is removed and added in regions of low stress and high stress respectively. The method utilize evolutionary process which can be characterized by the disappearance of holes which are initially positioned at the wrong places. (Wang, Wang, & Guo, 2003)

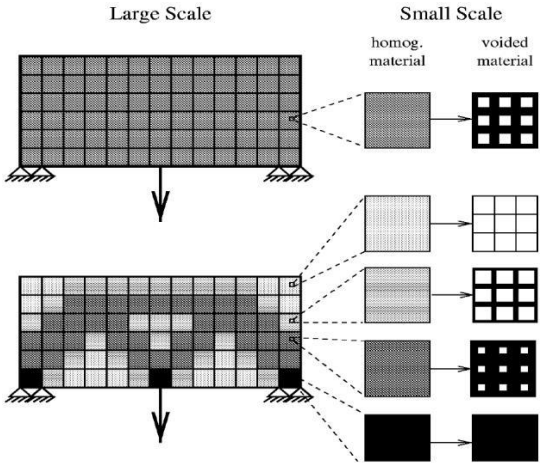

Figure 2-8 Porous material of homogenization method (Suzuki & Kikuchi, 1991)

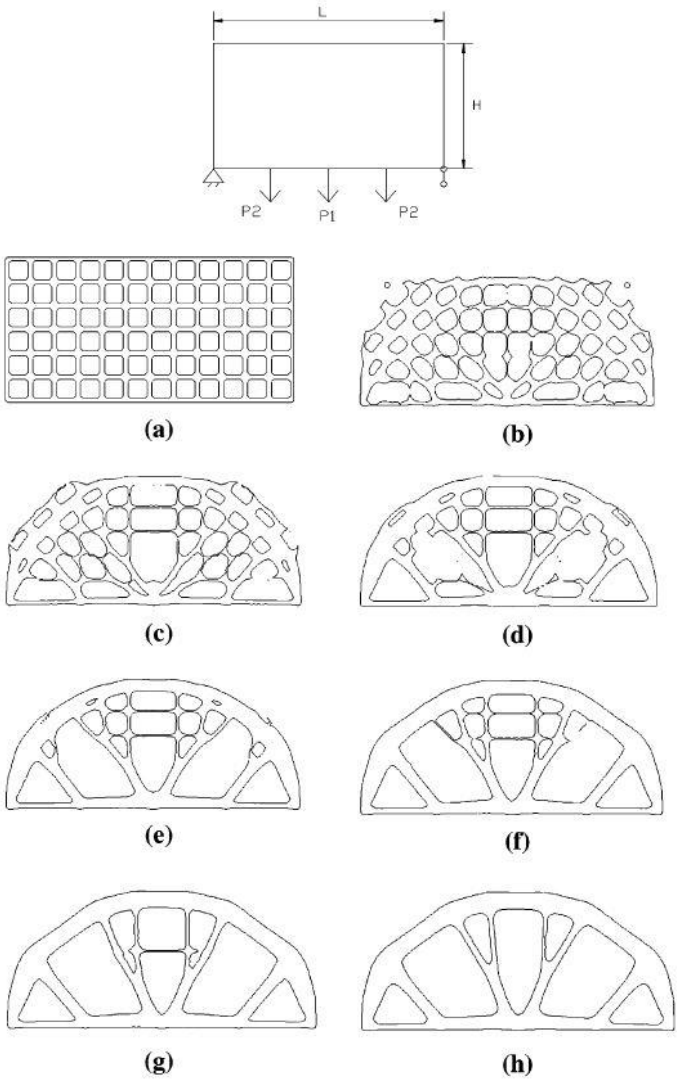

Figure 2-9 Level set method optimization of a beam: (a) initial design, (b-g) intermediate result, and (h) final solution (Wang, Wang, & Guo, 2003)

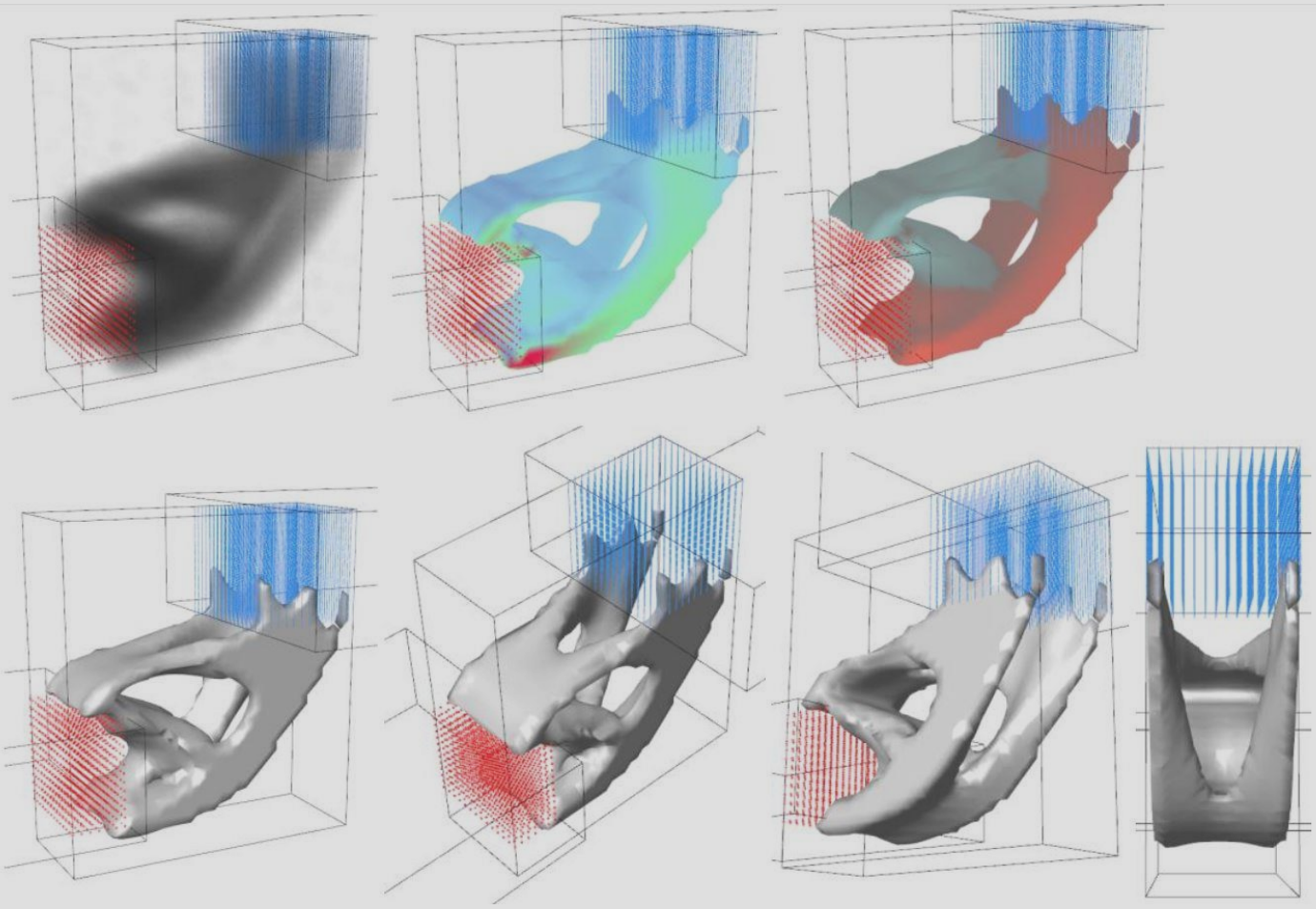

Figure 2-10 Basic three dimensional topology optimization with millipede (Kajima & Panagiotis, 2016)

2.3 Topology Optimization Softwares

1. Millipede

Millipede is a structural analysis and optimization of structures plug-in for Rhino-Grasshopper (a visual programming tool for parametric modelling). The components use a very fast structural analysis algorithms for linear elastic system. It contains its own optimization algorithms based on homogenization method of topology optimization but due to its speed it can be used in combination with Galapagos (evolutionary optimization algorithm tool for Grasshopper) for solving generic form finding problems. The tool is a free software for academics with non-commercial license. (Kajima & Panagiotis, 2016)

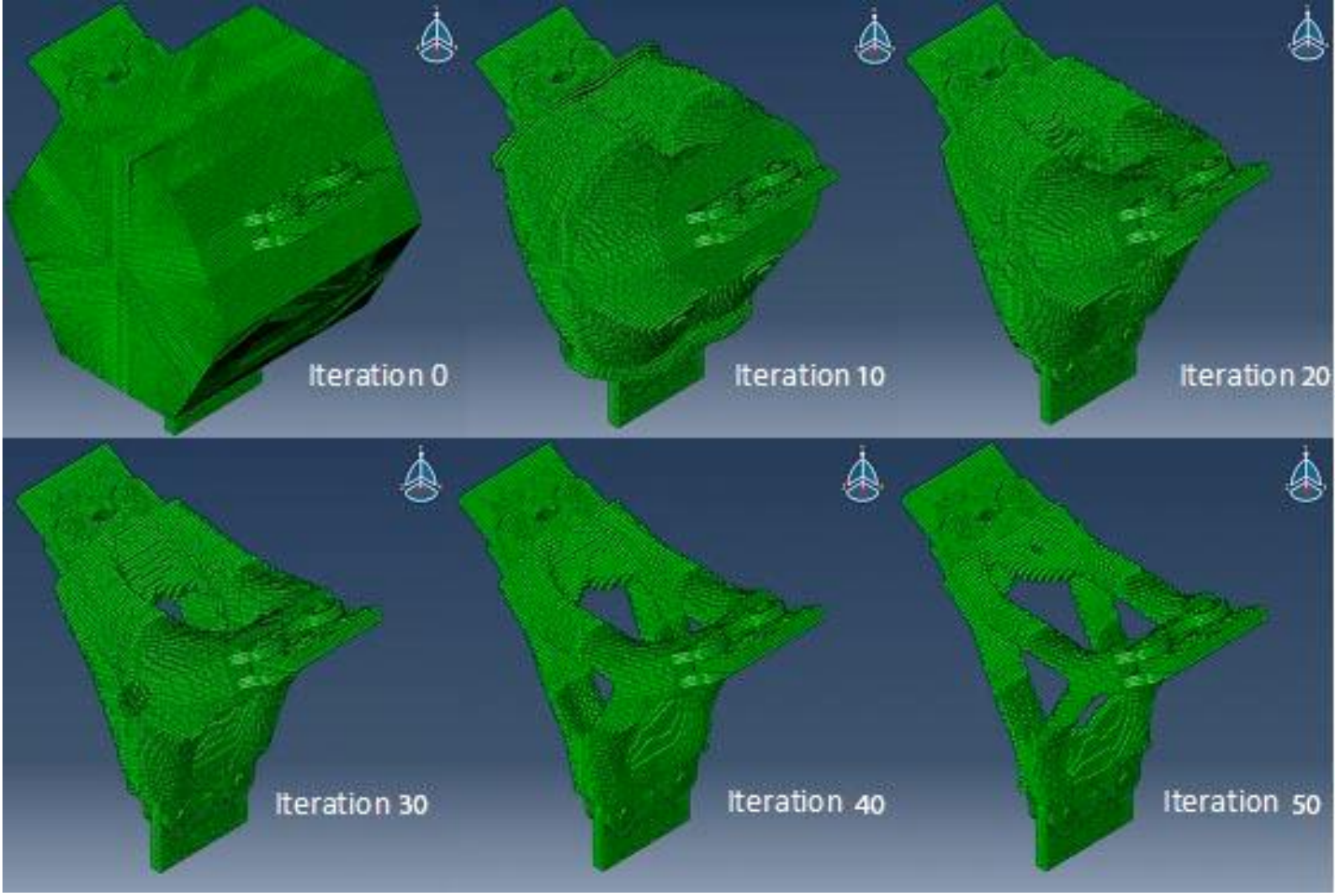

Figure 2-11 Iteration steps of TO process in BESO3D for structural nodes (Donnell, et al., 2015)

2. BESO3D

The tool based on BESO method for topology optimization for 2D and 3D structures developed by researcher of RMIT Australia (Huang & Xie, 2010). The software is free for academics with non-commercial license. The package contains a standalone BESO2D program, BESO3D plug-in for ABAQUS, BESO3D for Rhinoceros, BESO3D in python script, and Matlab code.

3. Altair OptiStruct

Altair OptiStruct is a structural analysis solver for linear and non-linear problems under static and dynamic loadings. OptiStruct is part of Altair HyperWorks engineering software package. The tool provides topology optimization with options of using SIMP method or Level set method. Moreover, OptiStruct offers other types of structural optimization such as lattice structures, shape optimization, and topography optimization. The software also enables manufacturing constraints to the optimized structure, e.g. extrusion constrains, pattern repetition, and symmetry constrains.

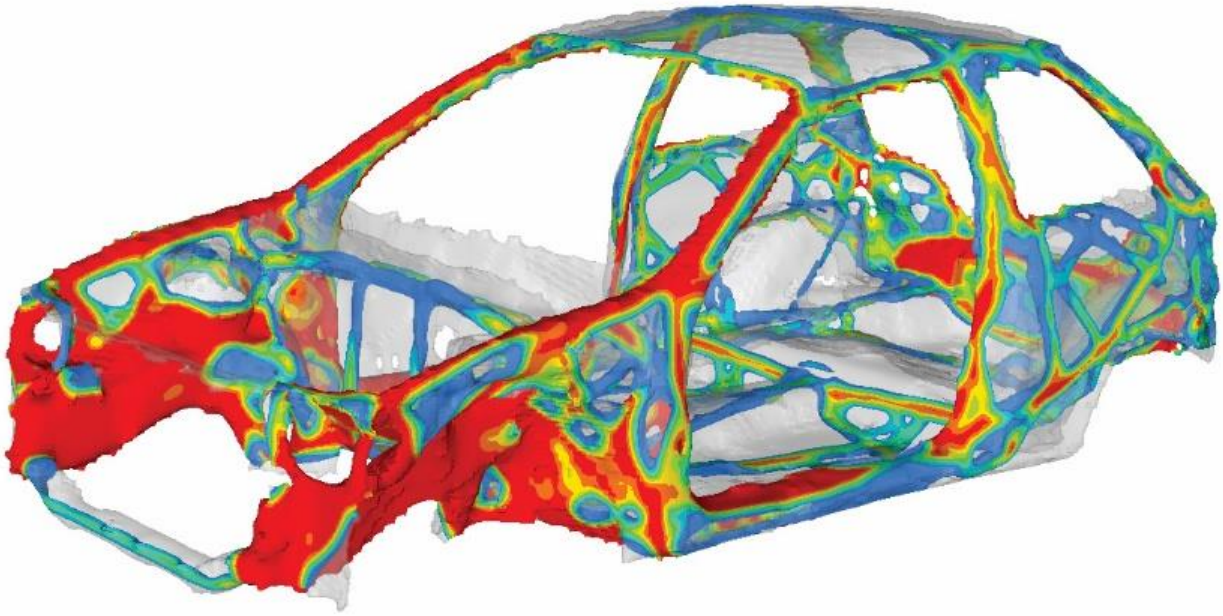

Figure 2-12 Topology optimization of a car chassis with OptiStruct (www.altair.com)

4. Solidthinking Inspire

Solidthinking Inspire was also developed by Altair, using similar technology of Optistruct. However, the software is targeted for designers to find a quick design solution with topology optimization. It has a very simple user interface and is easy to use for designers without experience in using FEM analysis tools. The software offers extended manufacturing constraints features similar to OptiStruct.

Figure 2-13 Bike frame assembly optimization in Inspire (www.solidthinking.com)

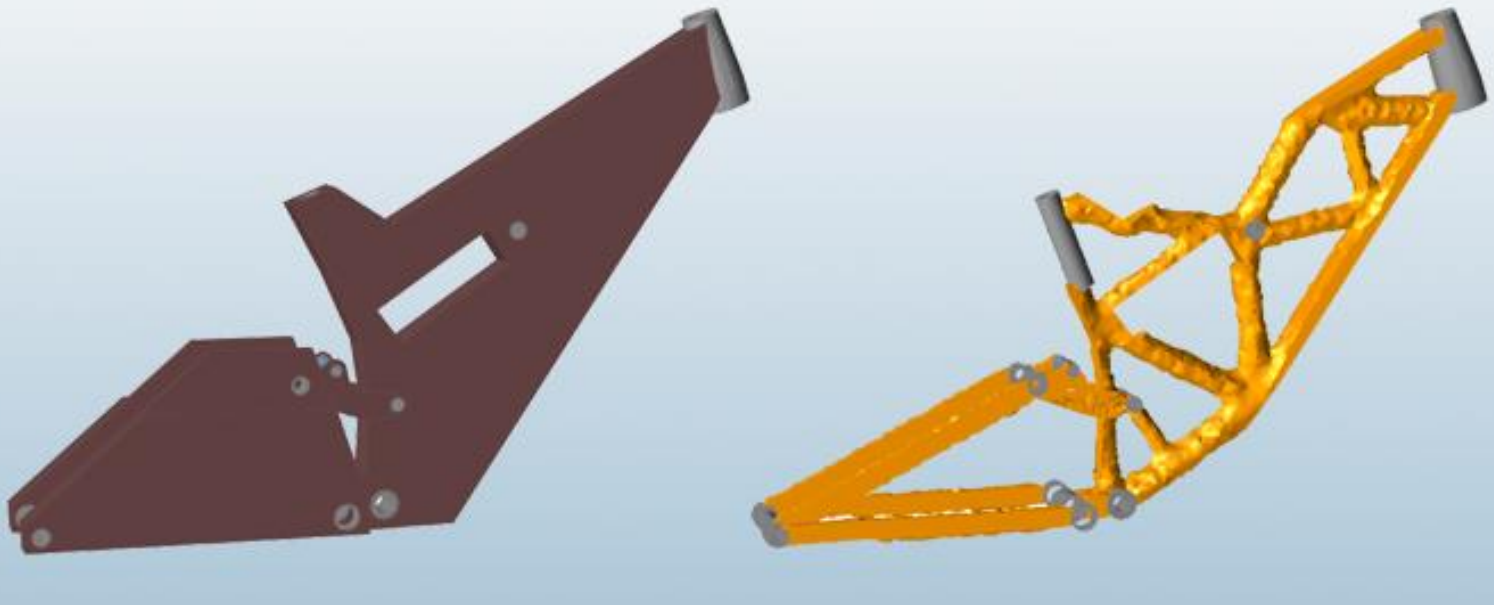

2.4 References

Altair. (2015). *Practical aspects of structural optimization, A study guide.* Altair University.

Altair. (n.d.). Altair Optistruct | Structural Analysis Solver for Linear & Nonlinear. Retrieved June 18, 2016, from http://www.altairhyperworks.com/product/OptiStruct

Bendsoe, M., & Sigmund, O. (2003). *Topology optimization: Theory, methods, and applications*. Berlin: Springer.

Christensen, P. W., & Klarbring, A. (n.d.). An Introduction to Structural Optimization. *Solid Mechanics and Its Applications,* 1-7. doi:10.1007/978-1-4020-8666-3_1

Huang, X., Xie, Y. M., & Wiley InterScience (Online service). (2010). *Evolutionary topology optimization of continuum structures: Methods and applications*.Chichester, West Sussex: Wiley.

Kajima, S., & Panagiotis, M. (n.d.). *Millipede*. Retrieved January 6, 2016, from http://www.sawapan.eu/

Lundgren, J; Palmqvist, C. (2012). *Structural Form Optimization Methods of Numerical Optimisation and Applications on Civil Engineering Structures.* Chalmers University of Technology.

Sigmund, O., & Maute, K. (2013). Topology optimization approaches. Struct Multidisc Optim Structural and Multidisciplinary Optimization, 48(6), 1031-1055. doi:10.1007/s00158-013-0978-6

Suzuki, K., & Kikuchi, N. (1991). A homogenization method for shape and topology optimization. Computer Methods In Applied Mechanics And Engineering, 93(3), 291-318.

Wang, M. Y., Wang, X., & Guo, D. (2003). A level set method for structural topology optimization. Computer Methods In Applied Mechanics And Engineering, 192(1-2), 227-246.

SUMMARY

Topology Optimization is a complex optimization algorithm based on a finite element method for mechanical analysis. There are many different methods and algorithms of TO developed by different researchers. However, they all have one similar purpose: to generate the most optimal shape and material distribution specific for the structural objective and constraints. This research focuses on implementing the available TO tools (software) and use them as a design tool and explore the possibilities to integrate TO method in a design working environment.

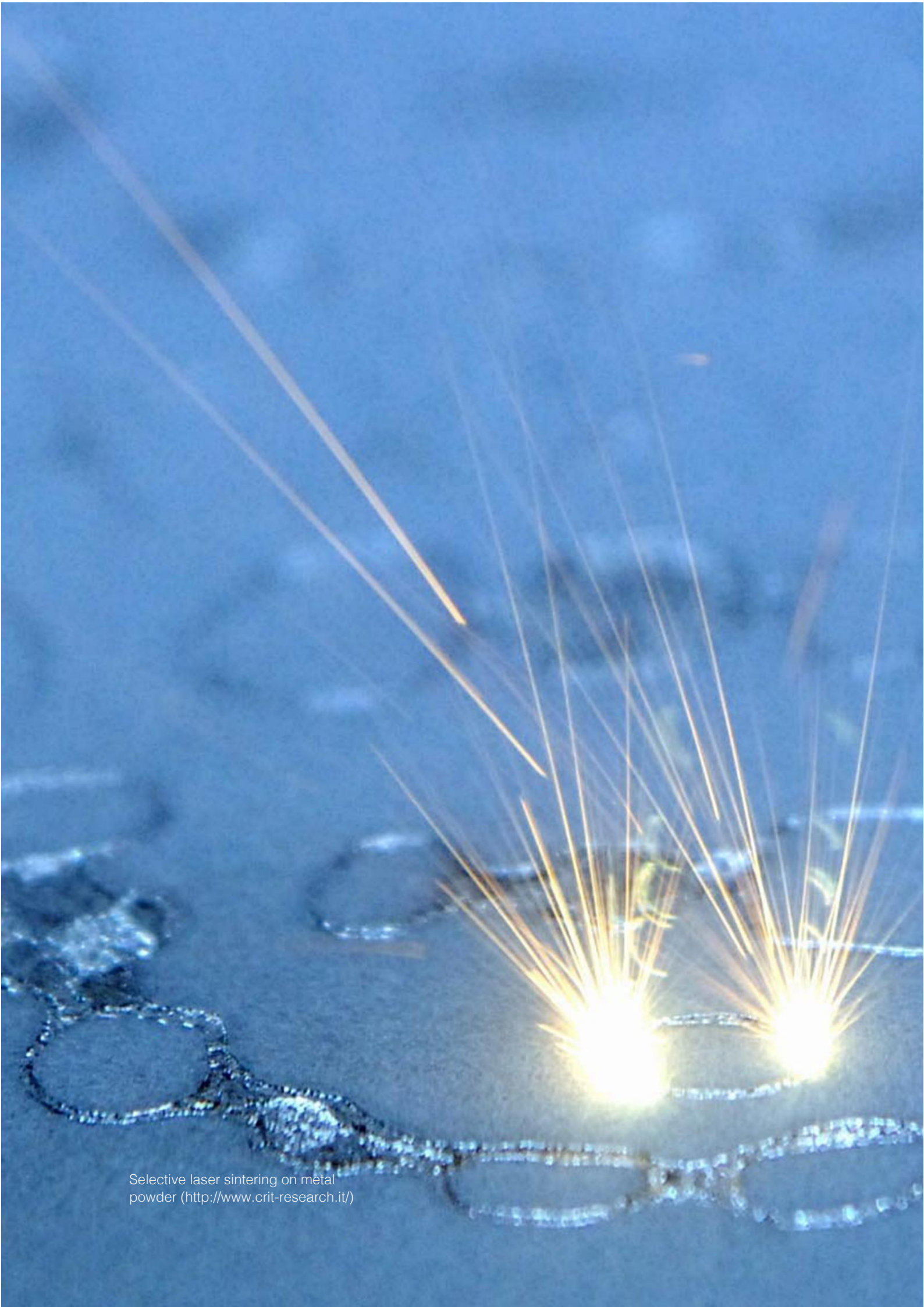

Selective laser sintering on metal powder (http://www.crit-research.it/)

ADDITIVE MANU FACTURING

3

ADDITIVE MANUFACTURING FOR STRUCTURE

Additive Manufacturing (AM) is a fabrication technology where in principle, a model which initially created using three-dimensional Computer Aided Design (3D CAD) system can be fabricated directly without the need of complicated process planning. Additive Manufacturing is the formalized term for what used to be called rapid prototyping and is popularly called 3D printing. AM can greatly reduce and simplify the process of producing complex 3D objects from digital data. The fabrication process of AM needs only basic dimensional details and a small amount of understanding as to how the AM machine works and the materials that are used to build the part. Although the process of AM in reality is not as simple as it first sound, it clearly simplifies fabrication process significantly especially for complex geometry from digital data. While the conventional manufacturing processes require careful and detail analysis and planning of fabrication, e.g. order of which different features of the part geometry can be fabricated, option and tools that must be used, and additional fixtures to complete the part.

Figure 3-1 Concept rendering of a 3D printed bridge in Amsterdam (www.mx3d.com/)

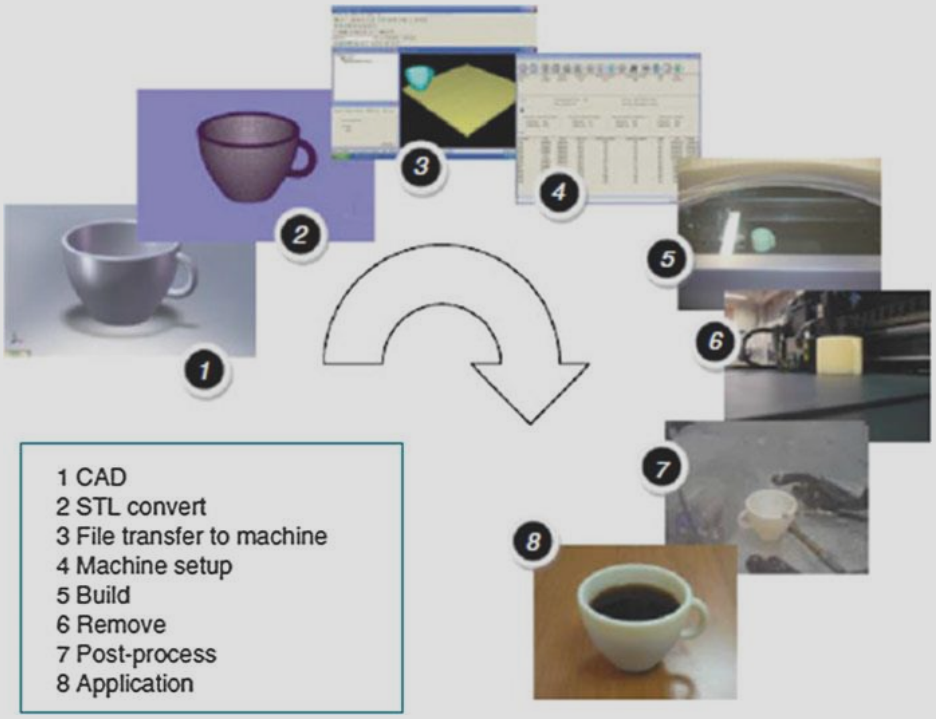

Figure 3-2 Generic 8-steps AM process (Gibson, Rosen, & Stucker, 2015)

3.1 Generic AM procedures

The process of AM involves a number of steps starting from the digital design environment in CAD until the physical production of the product. The process are not always similar depends on the complexity and the purpose of the design. Visualization prototype model could have a simple process while a more complex usable parts will need more detailed and greater engineering process steps. In general, AM processes can be divided into the following eight steps:

1. CAD

   The model has to be defined in a digital environment of CAD. This data could come from any CAD tools used by designer and engineer working on the design. The object must be a solid 3D model or surface representation either in NURBS or mesh geometry.

2. Conversion to AM recognizable format

   The current most accepted file format for AM process is STL format. It is basically triangular mesh geometry representing the object. The file format has been developed since 1993 and is used widely in digital prototyping until the present day (Burns, 1993). There is currently a development for a new fil format called 3MF, initiated by Microsoft with the ambition to replace the STL format in AM process. The 3MF format is promised to be a file format with a complete model information contained within a single archive: mesh, textures, materials, colours, and print ticket. 3MF provides a clear definition of manifoldness without ambiguity for model with self-intersections and have more interoperability with other format (3MF, 2016).

3. Data transfer to AM machine and working file manipulation

   For STL format, the file transferred to the AM with some necessary manipulation including the addition of support structures if required depending on the geometry of the model.

4. Machine setup

The AM machine must be properly set up with settings related to the build parameters of the object such as material constraints, layer thickness, print speed, etc.

5. Build

The building process is mainly computer-controlled phase with minimal supervision required, depends on the types of AM process and material use. All AM machine will have a similar sequence of layering process until the build is complete.

6. Removal and clean-up

Most of the case, the output from the AM machine is not ready for use yet. The part must be separated from the build platform and removal of support structure and excess build material must be dealt with. There is often a significant amount of manual work on the clean-up phase especially in metal AM process, where another equipment may be needed by a skilled operator to prevent damage on the part.

7. Post-processing

If necessary, some manual process of finishing may be needed before the application of the object takes place. This may involve abrasive finishing such as polishing, sandpapering, and application of coatings.

8. Application

The finished parts are finally ready to use, whether as a final product or part of a larger assembly. It should be noted that parts that made from AM process are most of the time have a different material properties compare to those made by other manufacturing process using the same material. Designers should be aware of these differences and take them into account in the early design stage.

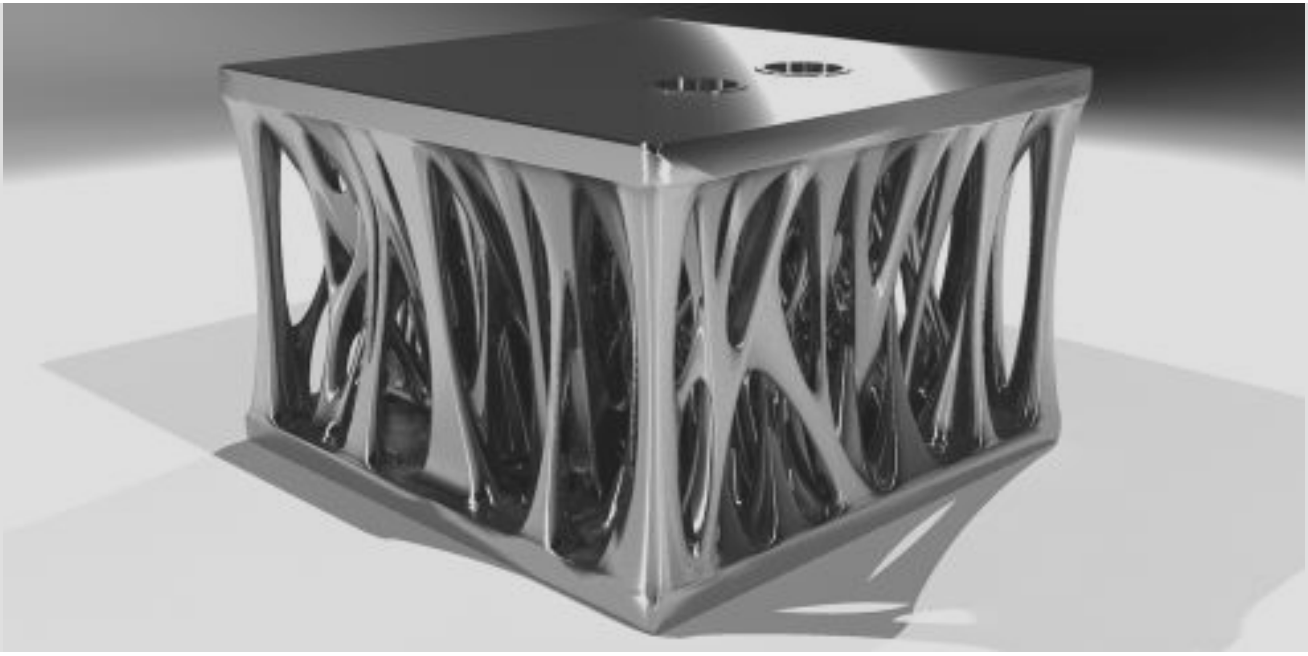

Figure 3-3 Liquid lattice structures produced with EOS additive manufacturing technology (http://www.eos.info/automotive)

3.2 AM for Metal

The operation of AM process for metal is conceptually similar to polymer systems. However, there some points worth considering (Gibson, Rosen, & Stucker, 2015):

1. **The use of substrates**
   Most of the AM metal system uses base platform or substrate where parts are built and later removed using machining. If the built parts were not rigidly attached to a solid platform, there would be a tendency for the part to wrap as it cools, caused by high-temperature difference between the temporarily molten material and its surroundings, resulting in large residual stress.

2. **Energy density**
   The energy required to melt metals is obviously much larger than for melting polymers. This also may requires more heat shielding, insulation, temperature control, and atmospheric control at much more advanced level than for polymer system.

3. **Weight**
   The AM machine must be capable to handle the mass of the material powder, especially when it needs to process high-density tool steel powder. Mechanical power requirements for positioning and handling equipment must be quite substantial to deal with the tasks.

4. **Accuracy**
   AM for metals system generally as accurate as polymer powder system. The character of the surface is rough and grainy but the part accuracy is excellent. Most of the case, key connection part for assembly requires smoothing with surface machining or grinding. The part density is generally over 99%, although some voids may still be seen.

5. **Speed**
   The requirements to handle heavy materials and large amount energy to melt the powder results a lower build speed compare to the polymer system. The laser power required usually double the amount of power required in polymer system. While slowing the process, it ensures enough energy is delivered to the powder.

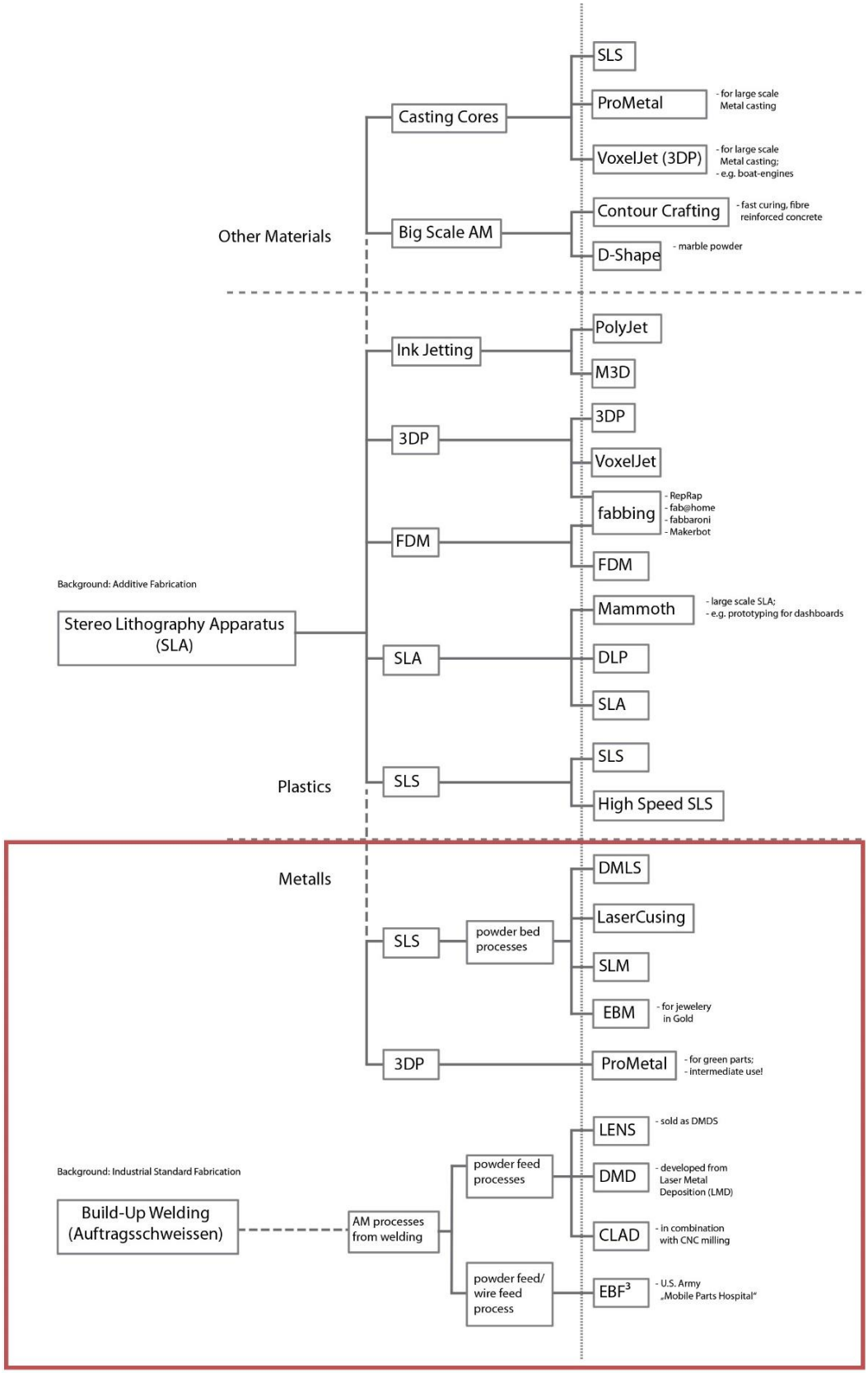

Figure 3-4 Family tree of AM process (Strauss, Knaack, & Techen, 2012)

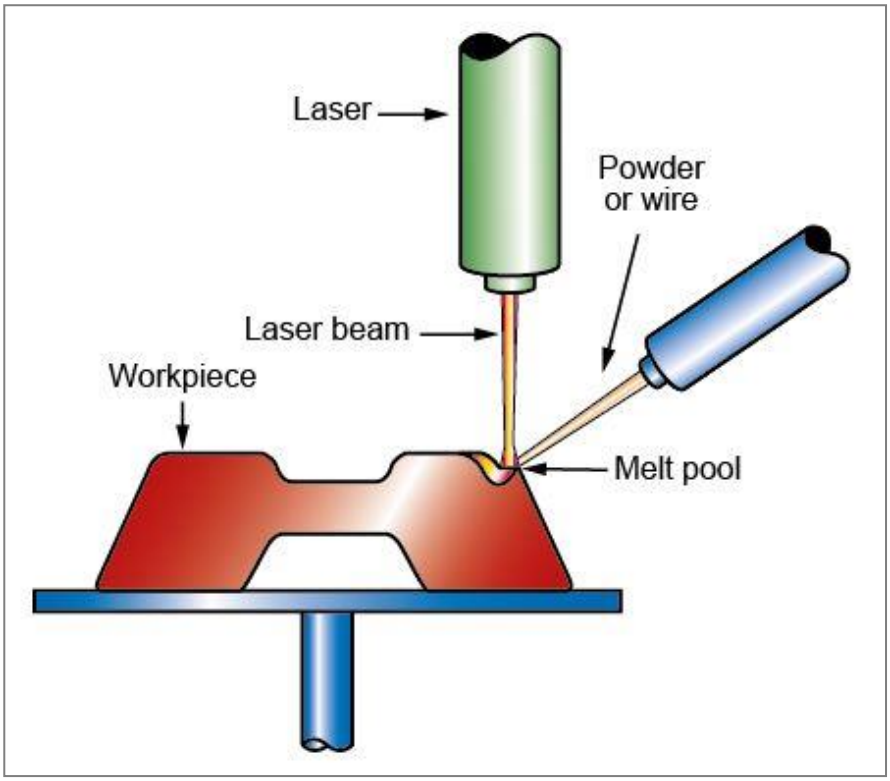

Figure 3-6 Generic diagram of powder feed process (CES Edupack 2015)

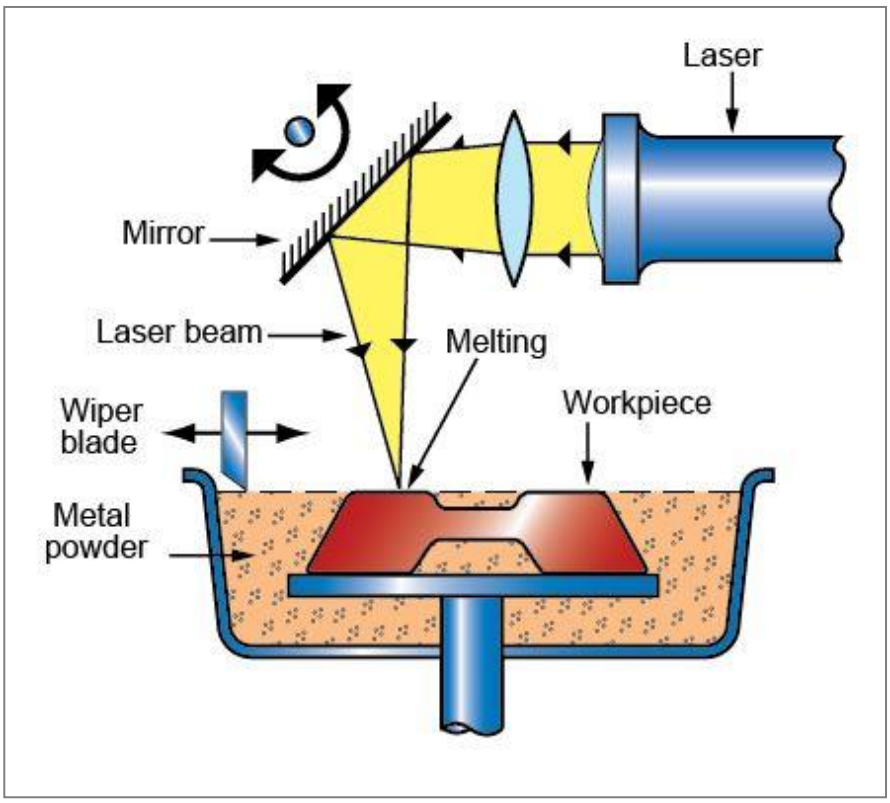

Figure 3-5 Generic diagram of powder bed process (CES Edupack 2015)

The AM process for metal powder in general can be differentiated into two principles:

1. Powder feed process

Also called Fused Metal Deposition method, an energy source (laser or electron beam) generates melting bath on the surface of the model while metal powder is then blown into the melting bath through nozzles. The process offers the possibilities to use different materials in one part. The process mostly used for repairing worn-out region in parts. All components that need to be accurately true to size must be reworked, the powder feed process is a questionable method for complex parts. The advantage of tool-less manufacturing is therefore annihilated (Strauss, Knaack, & Techen, 2012).

- Laser Engineered Net Shaping (LENS)

One of the first DMF technology, it is mainly used for repairs. The print head consist a central nozzle directing the energy beam and surrounded radially by material nozzle delivering the metal powders.

Figure 3-7 Optomec LENS 850R printhead (3dprintingindustry.com)

- Direct Metal Deposition (DMD)

Also known as Laser Metal Deposition (LMD). Pure metal powder as the source material is sprayed into the CO2 laser melting bath in particle form, it deposits metal onto existing tools and components in layers. The laser tip is mounted on a five-axis CNC robot, allowing metal layers to be deposited three dimensionally.

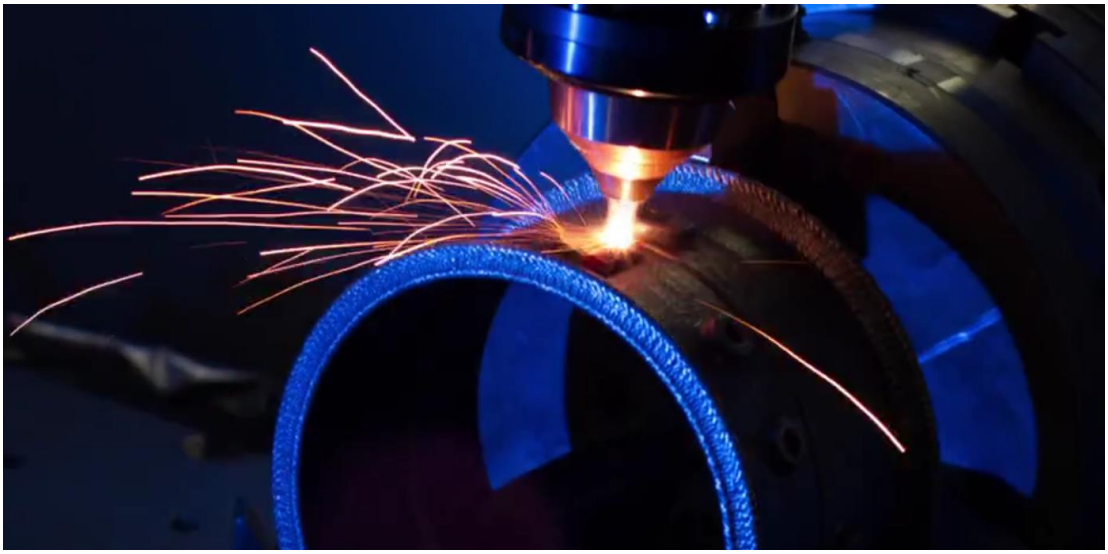

Figure 3-8 DMD process in POM Group (http://www.pomgroup.com/)

- Electron Beam Free Form Fabrication (EBF3)

Also called Electron Beam Additive Manufacturing (EBAM), EBF3 combines various elements of the previous described method into one laser based deposition process with a firm metal wire for material supply instead of metal powder. A vacuum is applied in the chamber during processing and components must be reworked with subtractive process.

Figure 3-9 EBAM system from Sciaky (http://www.sciaky.com/)

- Construction Laser Additive Directe (CLAD)

The system uses a powder feed process, combined with specialised software and a three to five axial CNC system to move the print head makes it possible to create components with complexity of geometry.

Figure 3-10 CLAD system in Irepa Laser (http://www.irepa-laser.com/)

2. Powder bed process

The parts model is generated from a powder bed of metal powder which includes transferring the process heat into a base substrate via the model contours and support structures. The process currently limits only one powder type to be processed at a time. In contrast to plastic powders, there is no tiring of the powder caused by heating, Therefore the powder can be reused without adding new material (Strauss, Knaack, & Techen, 2012).

- Selective Laser Melting (SLM)

The SLM system has developed where it can also process reactive metal powders such as aluminium and titanium using inert gas to generate a protective atmosphere in the chamber. SLM is still the cutting-edge amongst the metal powder processes.

Figure 3-11 SLM 500 machine by SLM Solutions (http://www.stage.slm-solutions.com/)

- LaserCusing

The powder in LaserCusing system is laser-melted at a density of 100% without adding any other substances. All the unused powder can be used for further processing without compromising quality. The system allows hybrid fabrication of CNC milled as the mounting system of the substrate plate always delivers defined reference points for the parts.

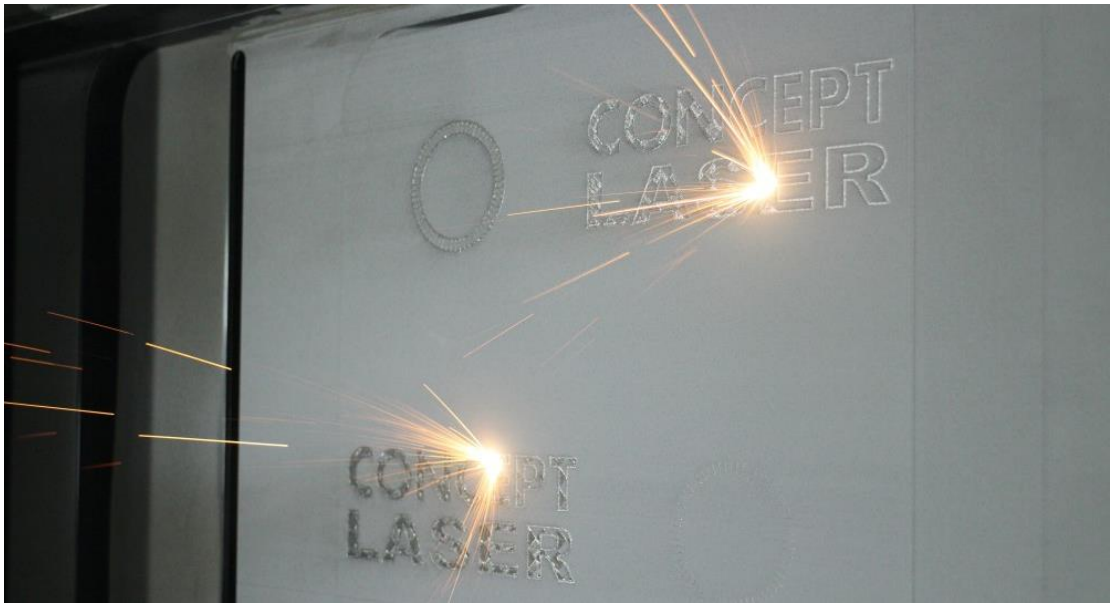

Figure 3-12 LaserCusing process by Concept Laser (www.concept-laser.de/en/home.html)

- Electron Beam Melting (EBM)

EBM is basically resembles the laser sintering method, while instead of using laser, it employs an electron beam. The process is done under vacuum at an operating temperature of approximately 1000°C. The parts show a higher level of melting-through than laser sintered parts.

Figure 3-13 Parts made by EBM process (http://pencerw.com)

- Direct Metal Laser Sintering (DMLS)

DMLS is a direct development of polymer SLS, where instead of plastic powder, it uses metal powder in the process chamber. The DMLS method is used to produce components for tools or machines as well as end use products.

Figure 3-14 Sample Application from the Dental Industry on a EOS M 100 Building Platform (http://www.eos.info/dental)

Overview

Compared to the research by Strauss in 2013, the obvious development we can see in today latest AM metal machine is that in average, the build chamber has nearly double the size. The biggest build chamber for powder bed process metal AM is currently available on 3d systems' machine ProX 400, although the machine is just announced and is not available in the market yet by the time this report is written. Other than the machines produced by big leading manufacturer in Europe, 2015 also marks the year where the development of AM metal machine start to reach to low-cost consumer product market. Some of these promising new AM metal machines are:

- Aororalabs (http://auroralabs3d.com/)
- MatterFAb (http://matterfab.com/)
- Michigan Tech Open-Source 3D metal printer (http://www.appropedia.org/Open-source_metal_3-D_printer)
- ITRI Metal Printer (https://www.itri.org.tw/eng/)

Although most of the new low-cost metal AM machine are currently not available in the market yet, the development is expected to go really fast in the next few years.

Process group	AM Process	Manufacturer	Machine	Build Chamber (mm)	Min layer thickness
Powder bed process	SLM	SLM Solutions	SLM 500 HL	500 x 280 x 325	0.02
		Renishaw	RenAM 500M	250 x 250 x 350	-
		Realizer	SLM 300	300 x 300 x 300	0.02
		3d systems	ProX 400*	500 x 500 x 500	0.01
	LaserCusing	Concept Laser	M3 Linear	300 x 350 x 300	0.02
	EBM	Arcam	A2XX	350 x 350 x 380	0.13
	DMLS	EOS	EOSINT M 400	400 x 400 x 400	0.09
	unspecified	TRUMPF	TruPrint 3000 LMF*	300 x 300 x 400	-
		Farsoon	FS271M	275 x 275 x 320	0.02
Powder feed process	LENS	Optomec	LENS 850-R	900 x 1500 x 900	0.025
	DMD	POM Group	66R	robot arm	-
	EBF3	Sciaky	EBAM 300	5791 x 1219 x 1219	-
	CLAD	Irepa Laser	EasyClad Magic	1500 x 800 x 800	0.1

Table 1 Overview of currently available AM metal process

3.3 Materials

1. Metals

Special material mixes are offered to manufacture metal parts. Similar to AM process for plastics, parts coming from AM metal materials have differences in properties and characteristic compared to the product of conventional manufacturing using the same material. For instance, most of the AM materials will have an isotropic properties where the strength in Z direction build is often weaker than in its other direction, this is the result of layering process of AM fabrication.

Currently available metal materials for AM are titanium, aluminium, stainless steel, tool steel, cobalt chromate, and various alloys of these materials. Similar to conventional metal processing methods, different material properties can be achieved with hardening and annealing. The table below showing a list of different metal materials produced by EOS in Germany (EOS, 2016).

Figure 3-15 3d printed node of a tensegrity structure designed by ARUP

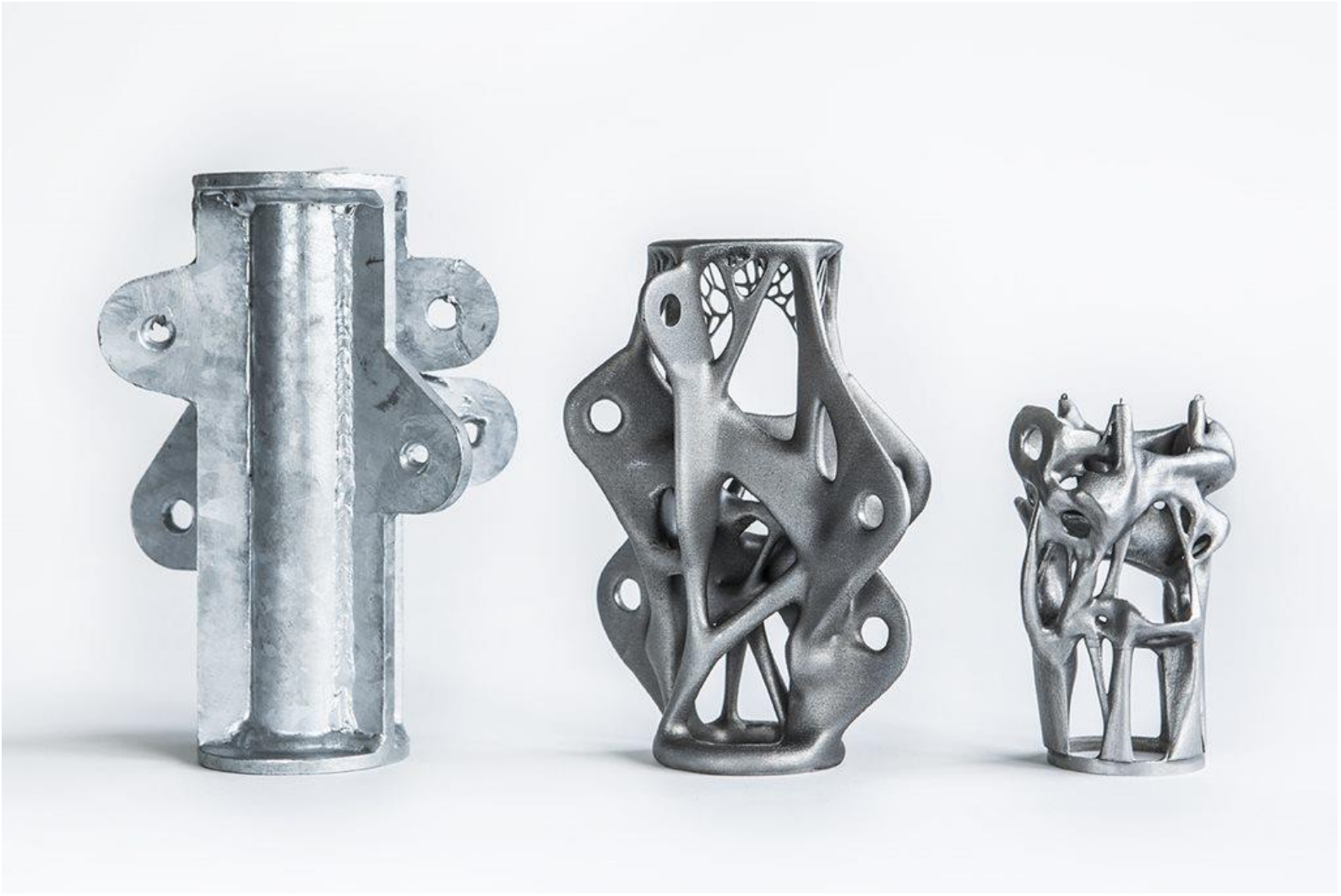

Product class	Product name	Material type*	Typical applications
Maraging steel	**EOS MaragingSteel MS1**	18 Mar 300 / 1.2709	Series injection molding tools; mechanical parts
Stainless steel	**EOS StainlessSteel GP1**	Stainless steel 17-4 / 1.4542	Functional prototypes and series-production parts; mechanical engineering and medical technology
	EOS StainlessSteel PH1	Hardenable stainless steel 15-5 / 1.4540	Functional prototypes and series-production parts; mechanical engineering and medical technology
	EOS stainlessSteel 316L	1.4404 / UNS S31673	Lifestyle: jewellery, functional elements in yachts, spectacle frames, etc. Aerospace: supports, brackets, etc. Medical: functional prototypes and series-production parts in e.g. endoscopy and orthopedics
	EOS StainlessSteel CX	Tooling grade steel	Manufacturing of injection moulding tools for medical products or products from corrosive plastics
Nickel alloy	**EOS NickelAlloy IN718**	Inconel™ 718, UNS N07718, AMS 5662, mat. # 2.4668	Functional prototypes and series-production parts; high-temperature turbine components
	EOS NickelAlloy IN625	Inconel™ 625, UNS N06625, AMS 5666F, mat. # 2.4856 etc.	Functional prototypes and series-production parts; high-temperature turbine components
	EOS NickelAlloy HX	UNS N06002	Components with severe thermal conditions and high risk of oxidation, e.g. combustion chambers, burner components, fans, roller hearths and support members in industrial furnaces
Cobalt chrome	**EOS CobaltChrome MP1**	CoCrMo super alloy, UNS R31538, ASTM F75	Functional prototypes, series-production parts, mechanical engineering, medical technology, dental
	EOS CobaltChrome SP2	CoCrMo super alloy	Dental restorations (series-production)
	EOS CobaltChrome RPD	CoCrMo super alloy	Removable partial dentures
Titanium	**EOS Titanium Ti64**	Ti6Al4V light metal	Functional prototypes and series-production parts; aerospace, motorsports etc.
	EOS Titanium Ti64ELI	Ti6Al4V ELI	Functional prototypes and series-production parts in medical technology
Aluminium	**EOS Aluminium AlSi10Mg**	AlSi10Mg light metal	Functional prototypes and series-production parts; mechanical engineering, motorsports etc.

Table 2 AM Metal materials manufactured by EOS Germany

3.4 Alternatives for Metals

1. High Performance Polymers

Plastic – polymers are the most common material used in general AM process because of the original intention of AM for prototype manufacturing. Groups of plastic materials such as PLA, ABS, acrylate, photopolymer, nylon, epoxy, polycarbonate, and acryl glass are commonly used for prototyping. There are a number of material mixes specially designed for defined applications. Polyamide was modified as incombustible and could therefore be used for aerospace industry. For instance, PEEK is a special material with a higher mechanical properties for applications in the automotive industry.

Manufacturer		Material name	material	process	UTS		Yield S		E Modulus GPA	
					x-y	z	x-y	z	x-y	z
stratasys	GER	ULTEM 1010	PEI	FDM	81	42	64	37	2.7	2.2
		ULTEM 9085	PEI	FDM	69	42	47	33	2.2	2.1
Arevolabs	US	PEEK	PEEK	FDM	95	-	-	-	4.4	-
		PEEK - CF	PEEK CF	FDM	145	-	-	-	20	-
Indmatec	GER	PEEK 450G	PEEK	FDM	98	-	-	-	3.8	-
EOS	GER	EOS PEEK HP3	PEEK	SLS	90	-	-	-	4.2	-

Table 3 Overview of high performance polymer for AM

Figure 3-16 Parts made of PEEK with SLS process
(http://www.3dprinterworld.com/article/solid-conceptsoffering-peek-material-sls-projects)

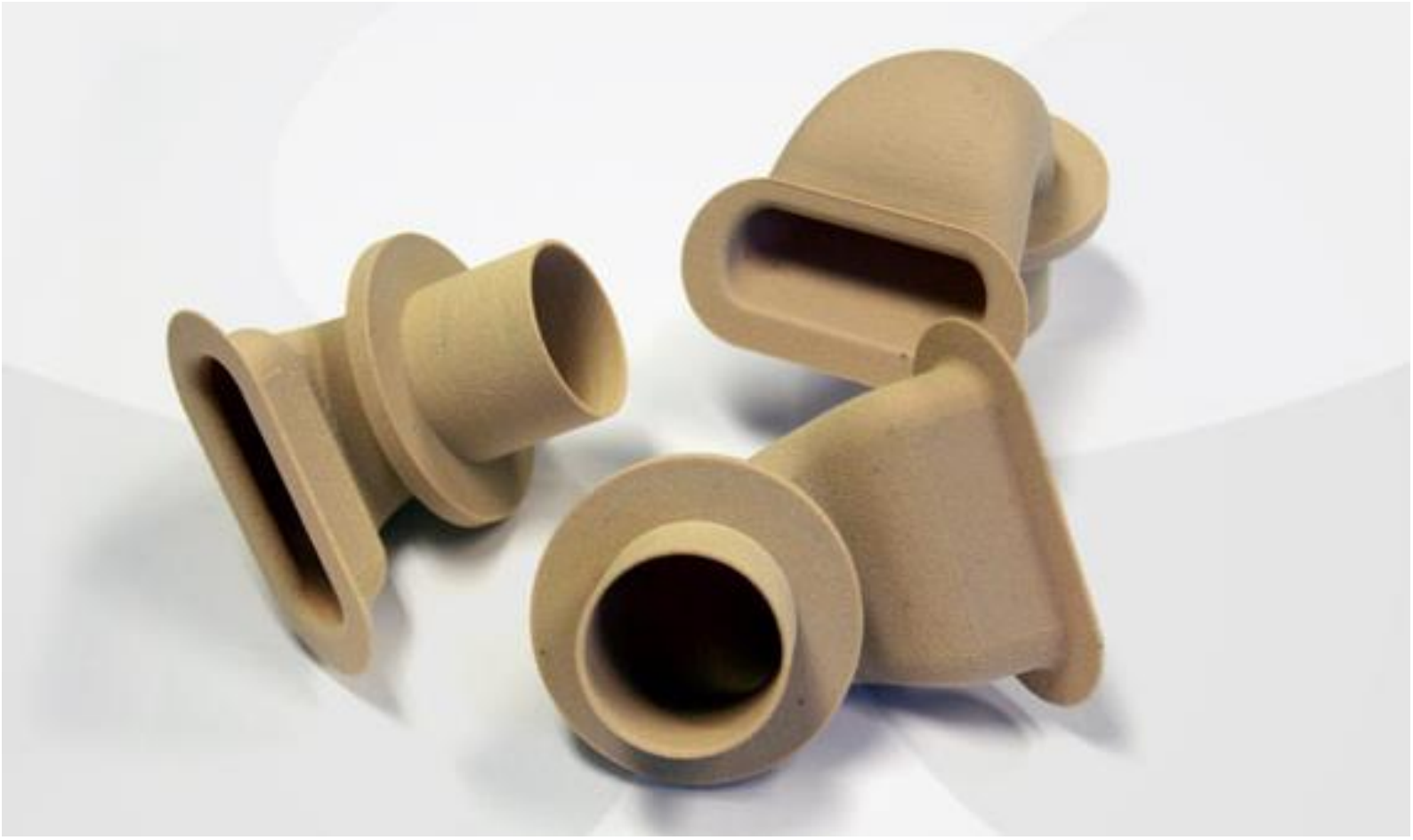

Figure 3-17 3D printed bike crank with embedded continuous carbon fiber (https://markforged.com/)

2. Composites

Another modification of plastic material is to reinforce the plastic with embedded fibres and therefore improve the mechanical properties of the AM products. Carbon Fibre is a common composite material with excellent strength for a lightweight structure. The development of AM materials with fibre reinforcement is relatively new. However, most of the manufacturer believed the materials is relevant in terms of being an alternatives for metal in AM production with its advantages in much lower cost and more simple production process.

Manufacturer		Material name	material	process	UTS		Yield S		E Modulus GPA	
					x-y	z	x-y	z	x-y	z
Windform	IT	windform xt 2	PA - CF	SLS	83	-	-	-	8.9	-
Markforged	US	CFF Carbon Fiber	Nylon CF	FDM	700	-	-	-	-	-
		CFF Fibreglass	Nylon FG	FDM	610	-	-	-	-	-
		CFF Kevlar	Nylon KV	FDM	590	-	-	-	-	-
EOS	GER	CarbonMide	PA - CF	SLS	72	25	-	-	6.1	2.2

Table 4 Overview of composite material for AM

3.5 References

3MF. (n.d.). 3MF | Supporting innovation in 3D printing. Retrieved June 18, 2016, from http://3mf.io/

Burns, M. (1993). *Automated fabrication: Improving productivity in manufacturing*. Englewood Cliffs, NJ: PTR Prentice Hall.

EOS Additive Manufacturing Systems. (n.d.). Retrieved June 18, 2016, from http://www.eos.info/en

Galjaard, S. (n.d.). Resources / Embrace new tools for design freedom. Retrieved June 18, 2016, from http://thoughts.arup.com/post/details/462/embrace-new-tools-for-design-freedom

Guido A. O. Adam Detmar Zimmer , (2015),"On design for additive manufacturing: evaluating geometrical limitations", Rapid

Prototyping Journal, Vol. 21 Iss 6 pp. 662 - 670Gibson, I., Rosen, D., & Stucker, B. (2015). *Additive manufacturing technologies: 3D printing, rapid prototyping, and direct digital manufacturing* (Second edition.). New York, NY: Springer. doi:10.1007/978-1-4939-2113-3

Strauss, H., Knaack, U., & Techen H. (2013). *AM Envelope: The Potential of Additive Manufacturing for facade constructions*. TU Delft. http://resolver.tudelft.nl/uuid:3a69355a-51d7-4207-943f-57a03f855d04

SUMMARY

AM is a fabrication technology where in principle, a model which initially created using three-dimensional CAD system can be fabricated directly without the need of complicated process planning. AM is often associated with the term 'complexity for free' where shape complexity is not necessarily an issue in the process, unlike the conventional fabrication method. Although the industry is currently have not reach most of the mainstream product manufacturing AM-machine today is able to fabricate a fully functional products which can completely replace the traditional manufacturing method. For instance, the jet engine fuel nozzle manufactured by GE with direct metal AM.

Courtyard roof of Smithsonian Art Museum. Design by Norman Foster and Buro Happold (www.burohappold.com)

FREEFORM ENVELOPE

4

FREEFORM ENVELOPE

4.1 The Architecture of freeform envelope

The main function of building envelope is to separate usable interior space form the outside world. It defines the architectural appearance of the building, provides views and lights to the inside and outside, carrying wind loads, self-weight, and other building components. Building envelope or façade could allow sunlight to penetrate while giving protection from the sun at the same time. It must protect the building interior from rain water and has to handle humidity from within and without. It also provides insulation against heat, cold, and noise and sometimes facilitates energy production. (Knaack, 2007)

The shapes of a freeform surface are not described by closed mathematical relations or by geometrical principle. They are described in a numerical manner, using complex mathematical procedures (NURBS-surface), which are implemented in many CAD-tools. (Schober, 2015)

Figure 4-1 Facade functions (Knaack, 2007)

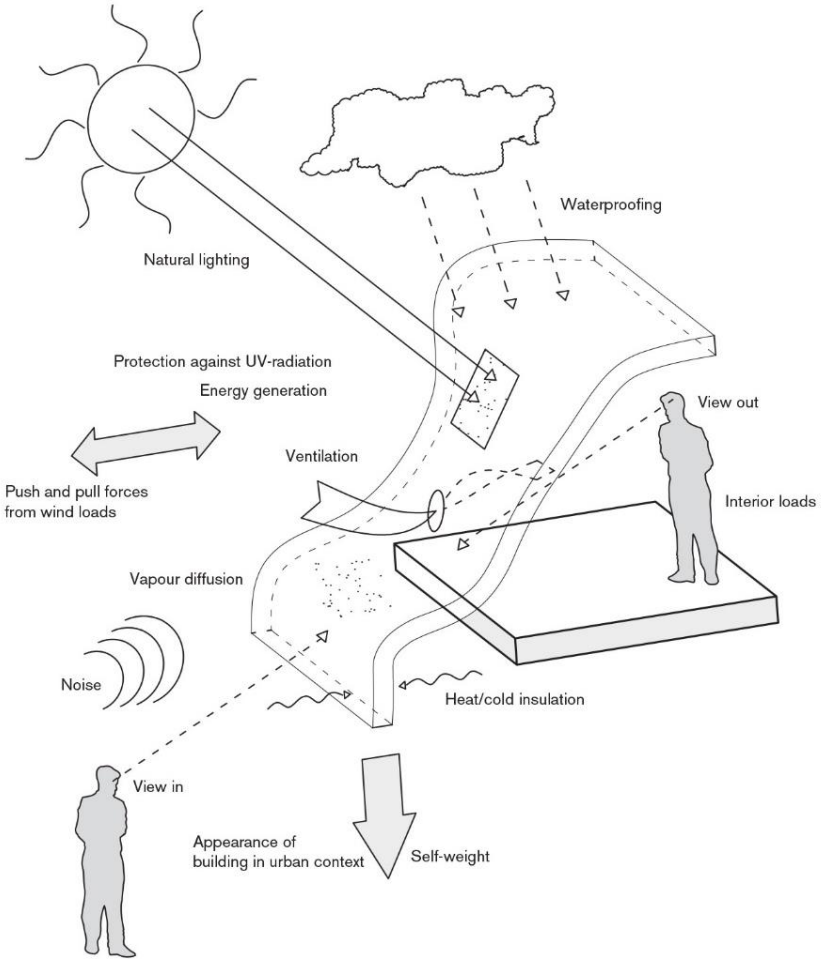

Figure 4-2 Freeform roof of westfield shopping center, London (www.benoy.com)

Free-form geometries are very popular in the present architecture. It is not only designed for aesthetic purpose, free-form geometry sometimes is the ideal design solution to answers architectural problems in terms of spatial quality, indoor climate and building physics performance and also structural performance. Computer Aided Design (CAD) helps architects and designers realized freeform geometry from digital representation into fabrication.

Gridshells are often used as a structural system from freeform envelope. It is closely related to shell structure which consist of a continuous surface carrying the structural loads. On the other hand, gridshells consist of discreet members connected in nodal points which assembled together representing an imaginary shell structure. Unlike shell structure, gridshells structure offers flexibility of having different types of façade functions assembled into the structure. For instance, the roof of Westfield shopping centre carries glass panels giving transparency to the architecture and solid panels with different function such as insulation (Knippers & Helbig, 2009).

4.2 Structural principle of freeform geometry

The structural principle of freeform geometry correspond to the structural principles of plane shells. It carries the load with axial forces (membrane behaviour) instead of with bending moments.

Shell theory

Shell is a generalization term of an isotropic homogenous plate. The dimension of shells are in two direction much larger than in third dimension (thickness). It is defined by their middle plane, thickness and material properties. In freeform envelope, the middle plane of the structure is the reference freeform geometry. The curvature of a double curved freeform shells make it possible to carry out-of-plane loads by in-plane forces which is not possible for plates. This behaviour is described as *membrane theory.*

Bending moments occurs where the equilibrium and deformation requirements cannot be met by membrane solution. Thus, it is preferred to avoid bending moments as they could lead to large deformations on shells. The analysis of bending moment behaviour is called *bending theory.* The membrane theory combined with the bending theory creates the *shell theory* (Blaauwendraad & Hoefakker, 2013).

Figure 4-3 Membrane and bending conditions in shells (Blaauwendraad & Hoefakker, 2013)

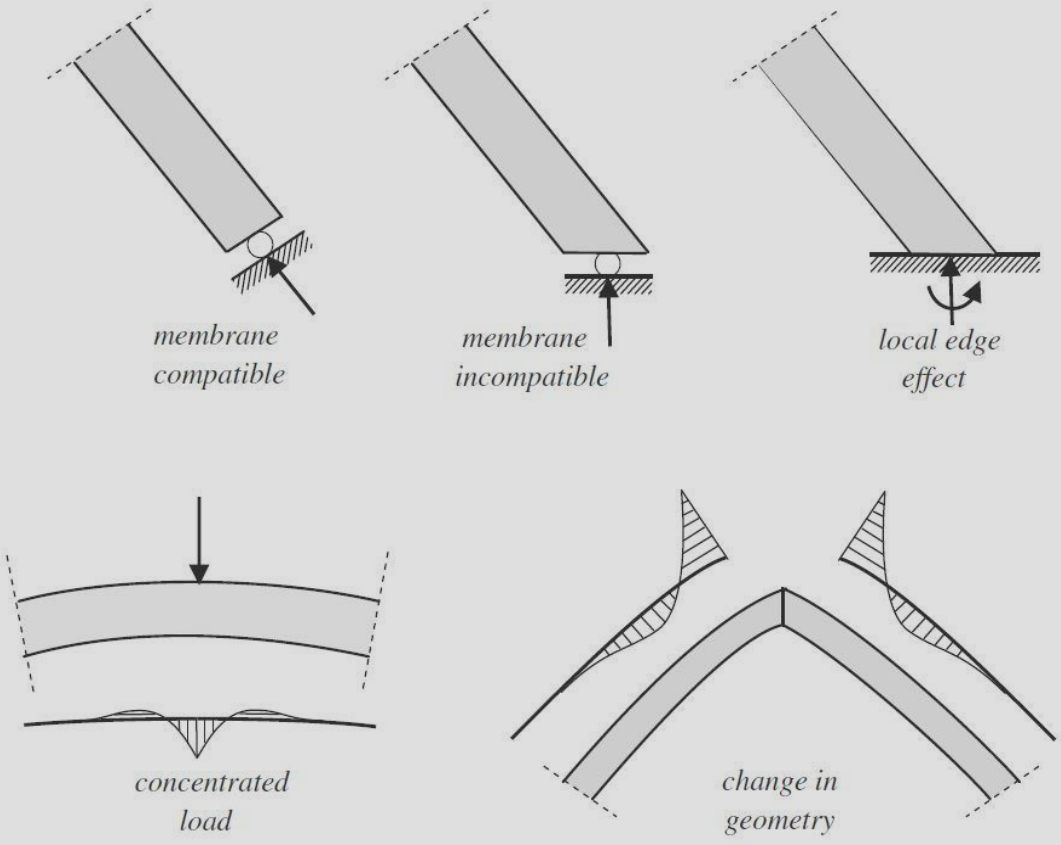

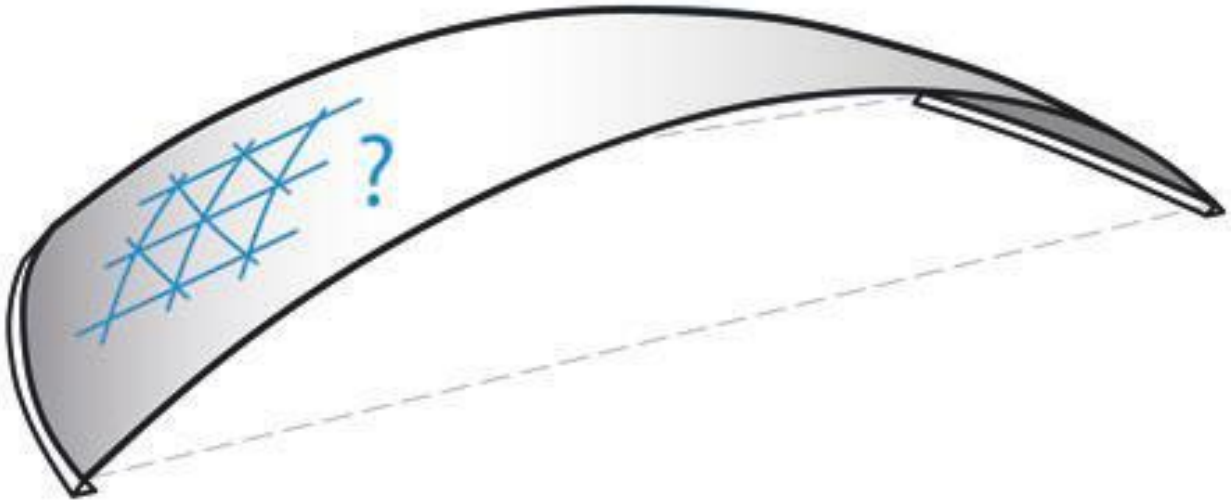

Figure 4-4 Mapping of grid layout on a given surface

4.3 Translation of freeform surface to gridshell

The availability of NURBS modelling software currently allows designers and architects to create complex surface forms. However, it is not always clear how to create an efficient gridshell structure to support a given freeform shape. There are many challenges in competing requirements and performance objectives, such as buckling, deflection, multiple load cases, envelope cladding, constructability, and aesthetics.

The conventional approach in designing a freeform surface is to break down the problem into three stages: (Winslow, 2014)

1. Surface form – conceptual shape by the designer.
2. Grid layout – defining member layout on a given surface.
3. Member size – section sizes are chosen once geometry is defined.

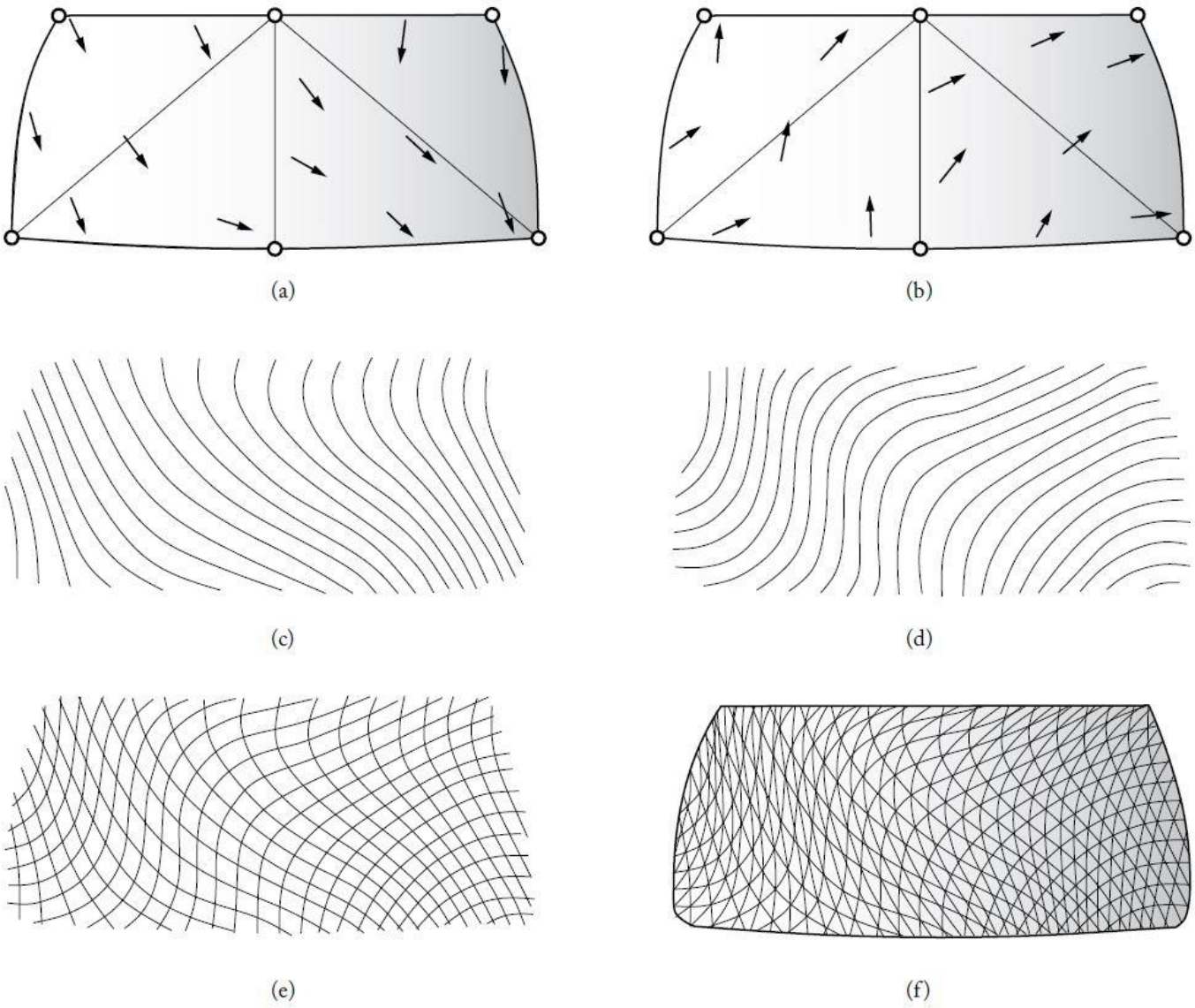

Figure 4-5 Optimized grid layout following structural forces directions (Winslow, 2014)

Triangulation is the most common discretization of freeform surface as it gives advantages as a simple solution. In terms of geometrical properties, triangle is always a planar surface. In terms of structural properties, triangular is a rigid geometry, and one might imagine that a triangulated grid is relatively isotropic. While it is true for the case of equilateral triangle, the stiffness of a triangle from different direction is not the same, depends on the angle of each corner of the triangle. Therefore, optimization on a macroscopic scale in defining the layout of freeform grid is considered a significant approach to improve the structural performance of a freeform structure.

Figure 4-6 British museum great courtyard roof
(www.fosterand partners.com)

4.4 Case studies of freeform gridshells

1. British Museum Great Courtyard, London

Architect	: Foster and Partners
Structural Engineer	: Buro Happold
Roof area	: 6,000 m2
Completion	: 2000

The British Museum is one of the main tourist attractions of London. With its archaeological and ethnological collections from all over the world, the museum attracts more than five million visitors a year. With the refurbishment of the courtyard, Foster and Partners added a freeform glass roof that created a generous circulation zone where visitors have easy access to the various galleries. The spectacular glass roof covered the central space providing areas for shops, cafes, and other central functions.

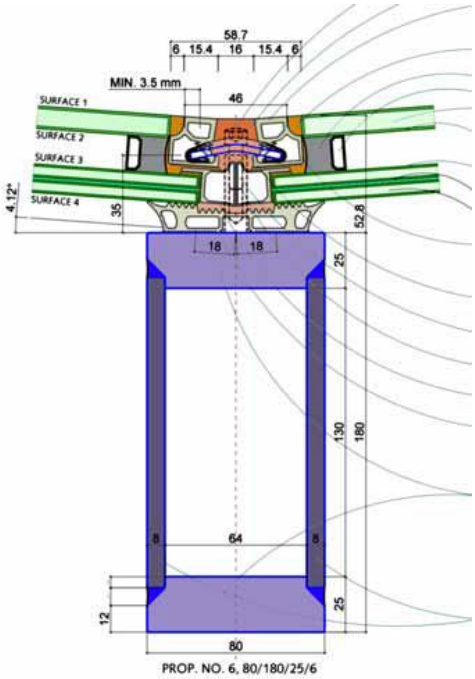

Figure 4-7 Detail of the structural members (Sischka & Biro, 2008)

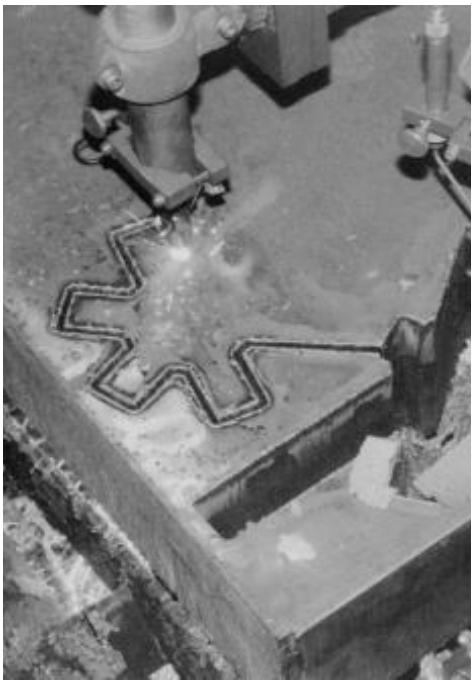

Figure 4-8 Cutting of nodes out of steel plate 180 mm with CNC machine

The new roof has a complex geometry – a torus stretched to a rectangular form. The roof has an average radius of about 50 m and becomes flatter towards the corners. The elements of the roof structures were welded in the workshop and hoisted by cranes over the museum building.

The roof is covered with 3,312 triangular panels of double-glazing, which every one of them has a different form. There are 4,878 welded hollow sections and 1,566 connecting nodes (Sischka & Biro, 2008).

Figure 4-9 Geometry of the node generated parametrically by computer model

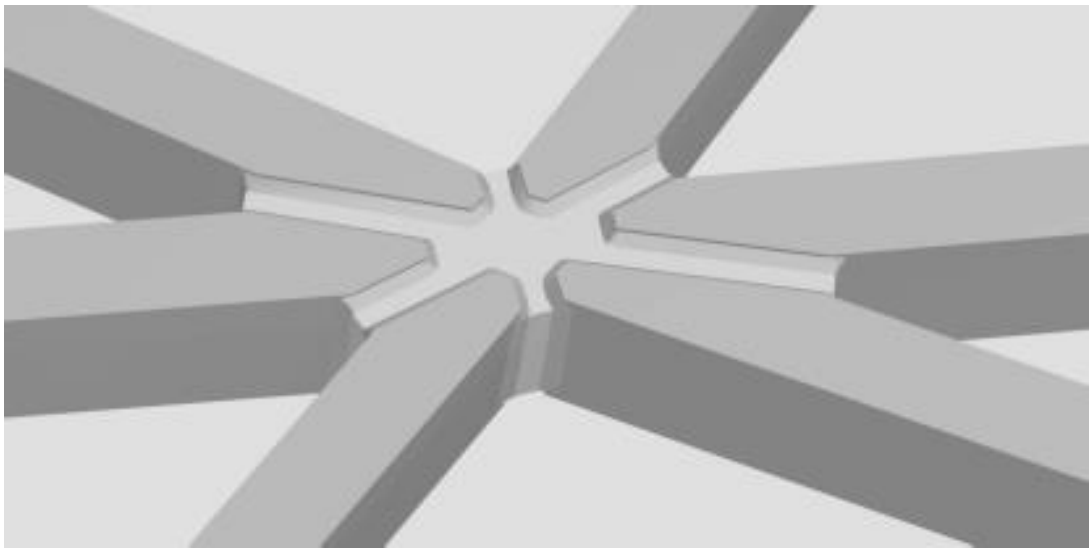

Figure 4-10 Interior view of Westfield shopping center (http://www.waagner-biro.com/)

2. Westfield shopping center, London

Architect	: Benoy
Structural Engineer	: Knippers Helbig Advanced Engineering
Roof area	: 17,000 m2
Completion	: 2007

The free formed gridshell roof covering a shopping mall consists of two parts with rectangular span of 24 m and a total surface of 17,000 m^2. It has 8,500 steel members consist of welded hollow box sections with size of 160 x 65 mm and average length of 2.3 m. A bolted connection was proposed by the contractor, which connects the members by vertical face plates. The hollow box nodes were welded, each of them has a different geometry and consists of 26 different plates.

Figure 4-11 Exploded view of the node elements and connection to beams (Knippers & Helbig, 2009)

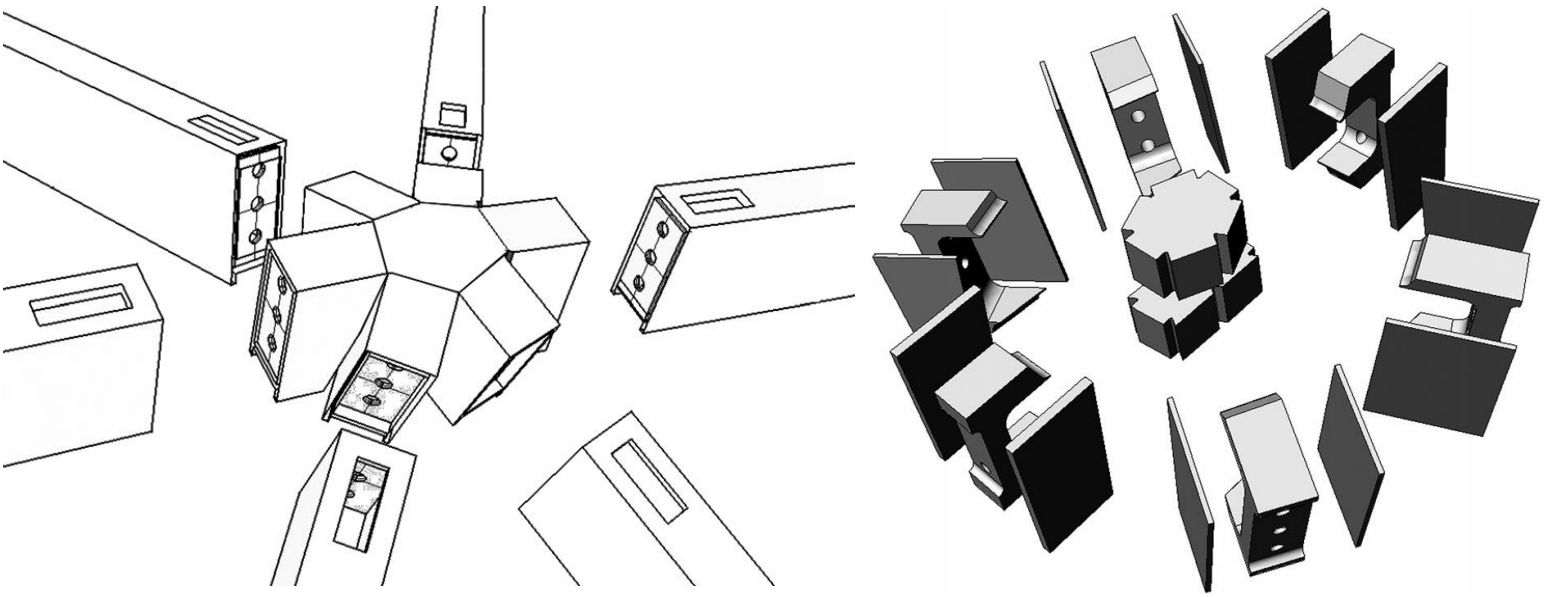

Final adjustment to the exact geometry was achieved by machining the face plates. The nodes were bolted to the straight members on site without any option for adjustment of the geometry. The high degree of prefabrication, the accuracy of the bolted connectors and a shop-made corrosion protection allowed for a rapid installation regardless of weather conditions.

Figure 4-12 Machining of nodes for final accuracy (Knippers & Helbig, 2009)

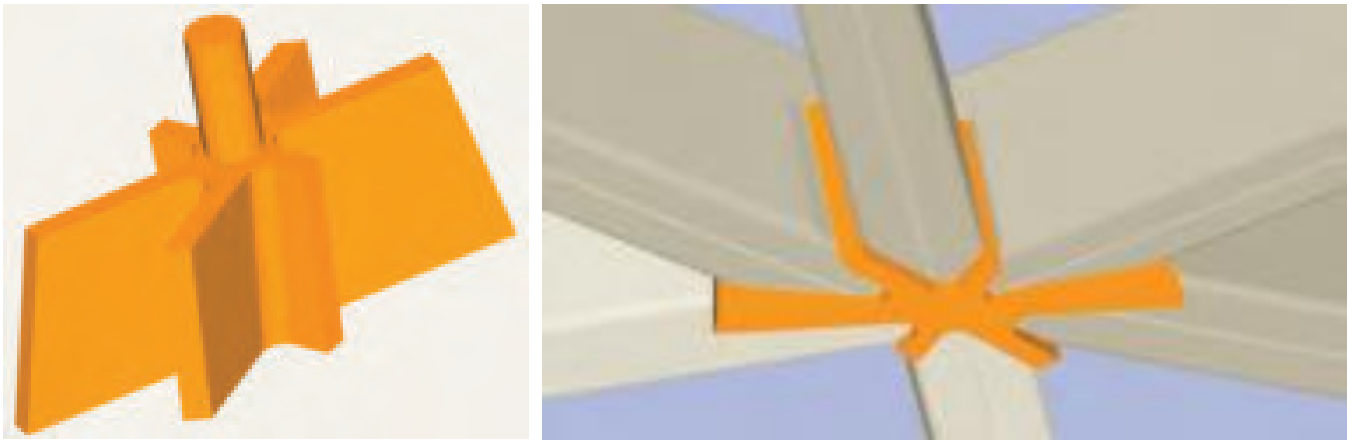

Figure 4-13 Node geometry
(Anderson & Czajewski, 2008)

3. Zlote Tarasy mixed use development, Warsaw

Architect	: The Jerde Partnership
Structural Engineer	: ARUP
Roof area	: 10,200 m2
Completion	: 2007

The project contains office space, an entertainment center, a shopping complex, and public spaces that make it a center for urban activity in the city. The roof consist of a triangulated mesh of steel rectangular hollow sections, is supported by a large end beam and intermediate branching tree columns.

The roof has a total weight of 1400 tons and average weight of 130 kg/m2. The structural members and joints of the roof was made using similar design and fabrication methodology with the British Museum design. Digital fabrication was utilized extensively to effectively produce joints with non-repeating angles and shapes (Anderson & Czajewski, 2008).

Figure 4-14 Interior view of
Zlote Tarasy atrium roof
(Anderson & Czajewski, 2008)

4.5 Quad paneling for freeform structure

Triangulated paneling is usually the preferred options for freeform envelope tessellation layout, it can describe any freeform surface with planar triangular surface. However, employed in construction they are economically less advantageous than equivalent surface structures built of quad panel: Quadrangular mesh constructions require fewer machining operations on the glass, and fewer mullions (as they eliminate the diagonal mullion from one side of the triangle). However, this achieved economy of scale can only be maintained if the quadrilateral facets of the surface structure are maintained planar: the cost of single- or double-curved glass facets would immediately void the premise for a quadrilateral solution.

The challenge in quad panel freeform structures is not only in the development of a geometric strategy for generating quad planar panels but also maintaining the design intent, which is the freeform surface created initially by the designers.

One of the simple method in creating a planar quad paneling freeform surface is using the principle of translation surface. The principle is that two spatial, parallel vectors are always defining a planar quad surface. The vectors and the connection between their points of origin and end points make up the edge of the quadrangular surface. Translating any spatial curve (*generatrix*) against another random spatial curve (*directrix*) will create a spatial surface consisting solely of planar quadrangular mesh. Parallel vectors are the longitudinal *and* lateral edges. Subdividing the directrix and the generatrix equally results in a grid with constant bar length and planar mesh. (Glymph, et al. 2004).

Figure 4-15 Geometric principle of translation surface (Glymph, et al. 2004).

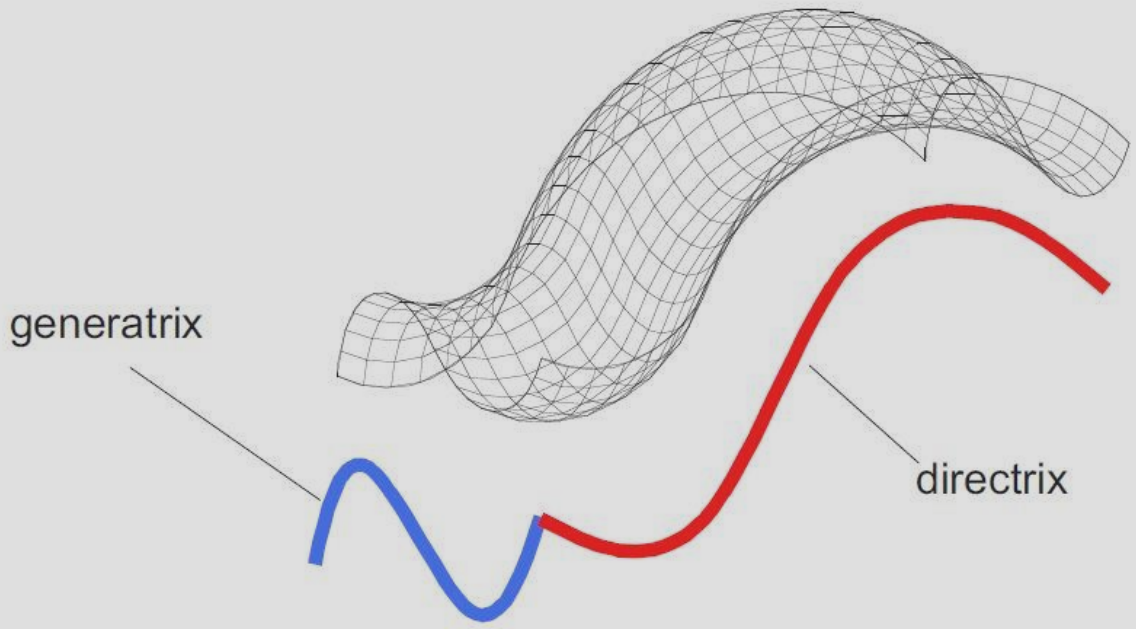

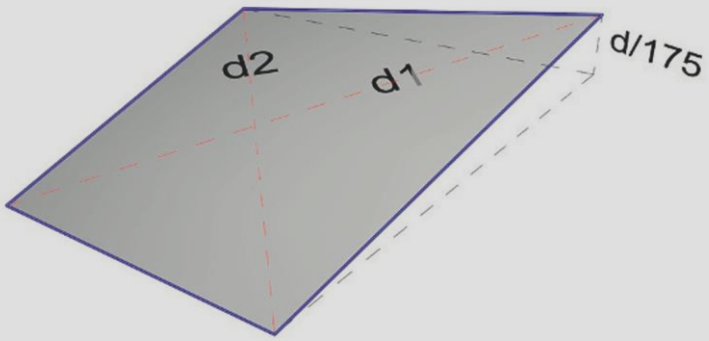

Figure 4-16 The limit of planar quad panel warping according to Schober (2015)

4.6 Freeform gridshell with warped quad panels

Another method in the construction of freeform structure with fully planar quad paneling is by allowing certain deviation of the planar panels to the intended surface geometry. According to Schober in his book 'Transparent Gridshells' (2015) The permissible warping of insulation glass panel can be specified:

$w < d/175$

where d is the average length of the diagonals d1, d2. The critical point is not ensuing tension in the glass panes, but the stress on the edge bond, resulting in a risk of leaks. The permissible value for warping is to be further clarified and agreed with the glass manufacturer. (Schober, 2015)

Figure 4-17 Example project with warped planar quad glass panes on the inner courtyard of the Portrait Gallery roof, Washington DC (Foster and partners)

Figure 4-18 The stepped flat insulating glass system on the courtyard roof.

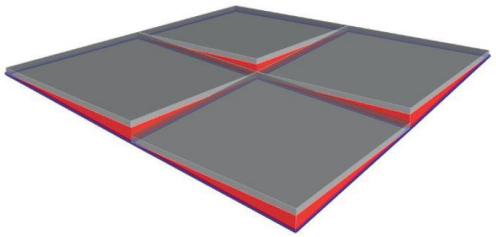

Example project using this type of construction is the inner courtyard canopy roof at the Portrait Gallery in Washington DC by Foster and partners. The roof is a diagonally directed structure of warped quad grids. At the edges each glass pane had to be held on the load-bearing profiles by two wedge-shaped spacers, and the stepping of the glass panels had to be covered by wedge-shaped metal strips. (Schober, 2015)

Figure 4-19 Detail drawing showing the construction of the stepped glass panes.

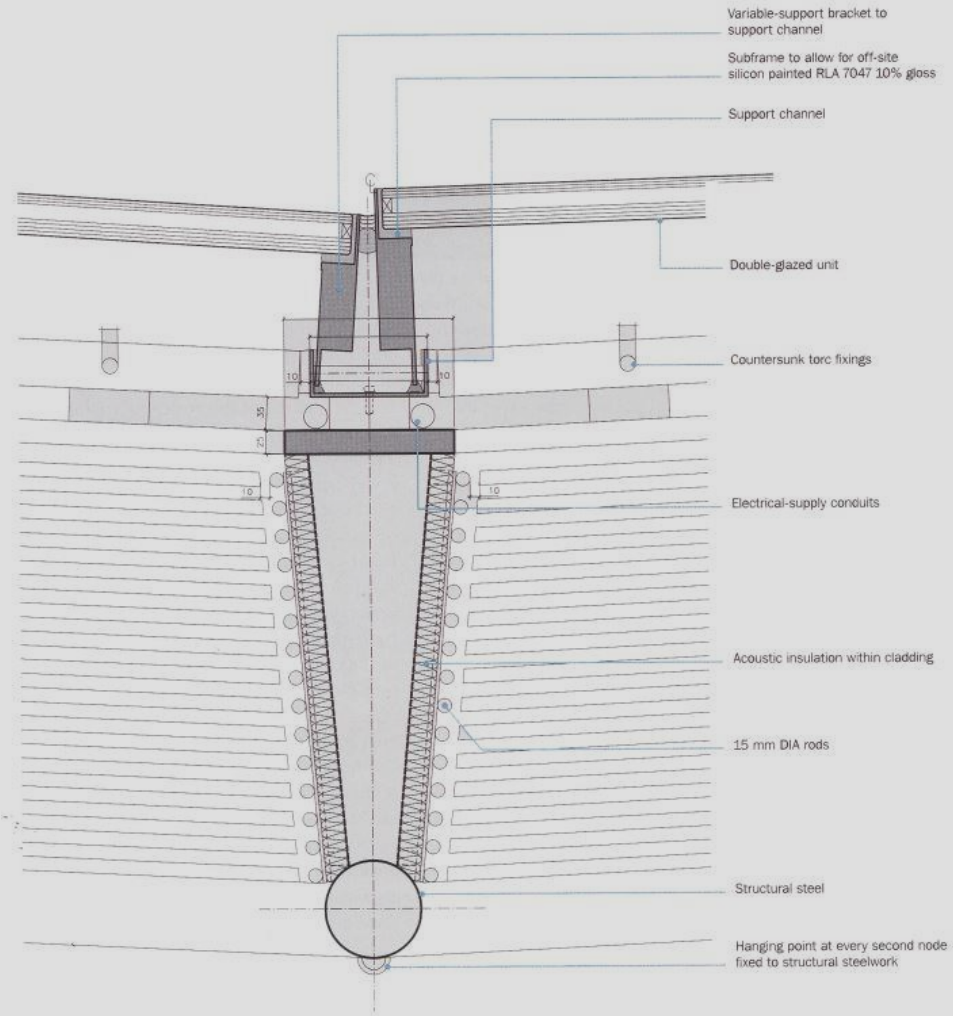

4.7 References

Anderson, Z. D; Czajewski, S. (2008). Zlote Tarasy, Warsaw , Poland. *Arup Journal, vol 1*

Blaauwendraad, J., & Hoefakker, J. H. (2013). *Structural shell analysis: Understanding and application*(Solid Mechanics and Its Applications, v. 200; Solid mechanics and its applications, v. 200). Dordrecht: Springer.

Glymph, J., Shelden, D., Ceccato, C., Mussel, J., & Schober, H. (2004). A parametric strategy for free-form glass structures using quadrilateral planar facets. *Automation in Construction, 13*(2), 187-202.

Knaack, U. (2007). *Facades: Principles of construction*. Ba: Birkha¨user. http://public.eblib.com/choice/publicfullrecord.aspx?p=336679

Knippers, J., & Helbig, T. (2009). Recent Developments in the Design of Glazed Grid Shells. International Journal Of Space Structures, 24(2), 111-126.

Schober, H., & Schaffert, C. (2015). *Transparent shells: Form, topology, structure*. Wiley.

Sischka, J; Biro, Wagner. (2008). Mesh match: Stories of seminal skins - Case study: The British Museum, London. *The Journal of the Society of Façade Engineering, 4.*

Winslow, P. (2014). Multi-criteria gridshell optimization. In *Shell structures for architecture: Form finding and optimization.* London: Routledge/ Taylor & Francis Group.

SUMMARY

Subjectively speaking, freeform gridshell not only a beautiful piece of architecture, but also an efficient structure. They allow double-curved form which transfer loads without bending. The important challenge is solving the construction system, how freeform surface broken down into elements of beams and panels. Although triangulated panels is the common way of gridshell system, the approach of using quad panels has more potential in terms of efficiency and architectural spatial quality since it requires less structural beam elements while having more surface are of the glass panels.

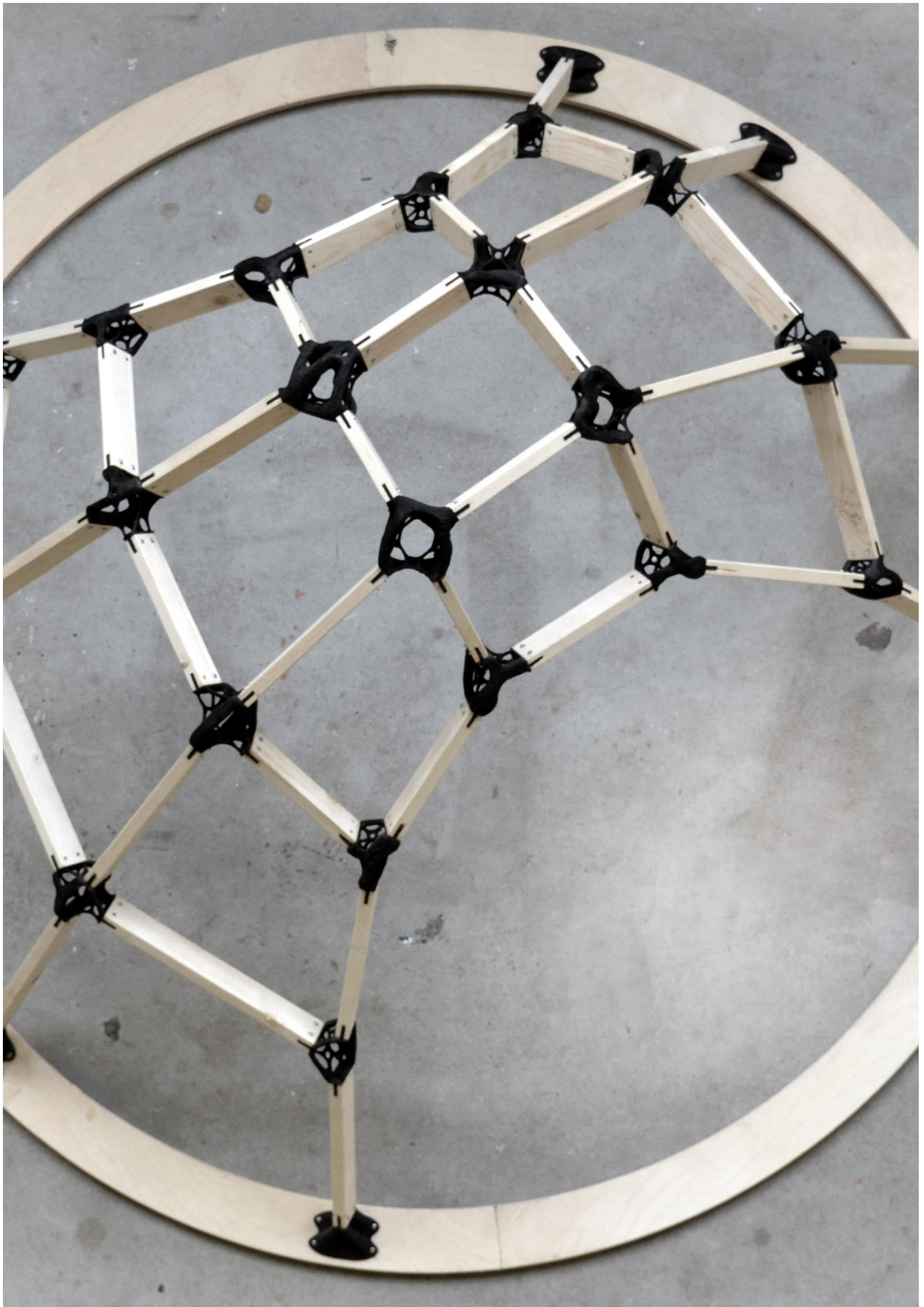

DESIGN RESEARCH: PROTOTYPE STRUCTURE

5

DESIGN RESEARCH - PROTOTYPE STRUCTURE

Before taking the concept of the research study into a real application in architecture, the system is first executed on a small scale pavilion-like prototype structure. The design of the prototype structure is built in a manageable scale in the scope of this research. Design exploration of the structure is meant to study and explore all the potential of new design and fabrication technology using TO and AM. Moreover, the specific constraints in building the prototype structure, such as cost, availability of 3d printer machine, the capability to build and the amount of time available are becoming the parameters in terms of shaping the final result of the prototype structure.

5.1 Schematic design and structural requirements

The purpose of the prototype structure is not only as a proof of concept for the TO and AM design concept in free-form gridshell, but also as a platform to create the complete design workflow from schematic design to fabrication to be implemented in the architecture scale.

Specification of the prototype structure:

* Solid wood as gridshell beams
* The optimized node is fabricated using FDM method
* The material chosen is a carbon fiber reinforced polyester filament

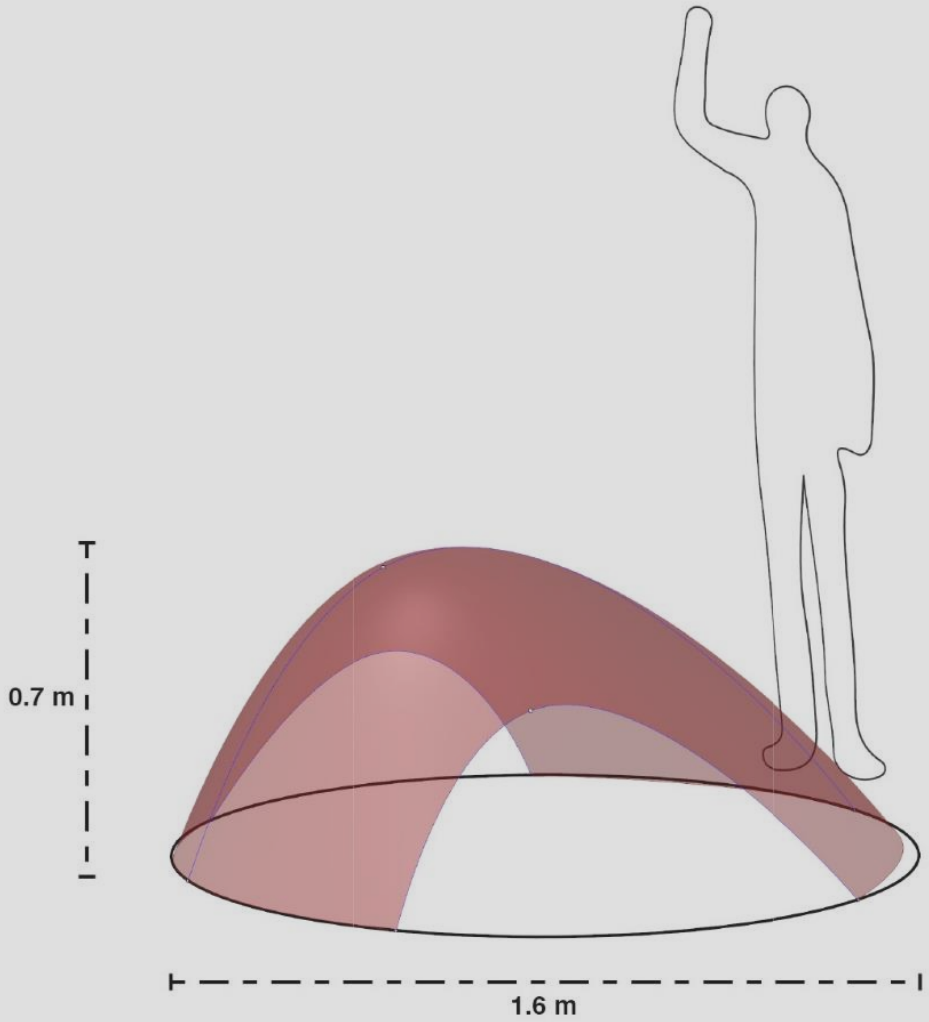

Figure 5-1 The intended scale and general geometry of the prototype structure

To showcase its structural capabilities, the structure must be able to hold an adult with 70 kg weight standing on top of it, a safety factor of 1.5 is applied to the optimization calculation. Considering that the structure will be built by only one person with limited tools available at the Faculty of Architecture TU Delft, the size of the structure is limited to around 2 x 2 meters with around 1 meter height. The geometry based on a dome-like structure. The structure will have a tension ring as a base to omit the need of anchoring the structure to the ground. The schematic geometry is a single surface, generated from loft of three curves on the surface's cross section.

5.2 Design and manufacturing strategy

The grid layout of the prototype structure is a quadrangular gridshell configuration. Although the quad layout optimization with panels' planarization are part of this research, it does not make sense to attempt the planarization on such a small scale structure. The proportion of the structure to the size of the beam and node elements making it almost impossible to do the quad planar optimization.

1. Material

The material chosen for the optimized node will be Colorfabb XT-CF20. It is a 20% carbon fiber reinforced polyester filament. The material properties which come from the manufacturer's material data sheet are:

Density	: 1.53 g/cm3
Max tensile strength	: 76 MPa
Elongation at break	: 7.5 %
Flexural strength	: 110 MPa
Flexural modulus	: 6.2 GPa

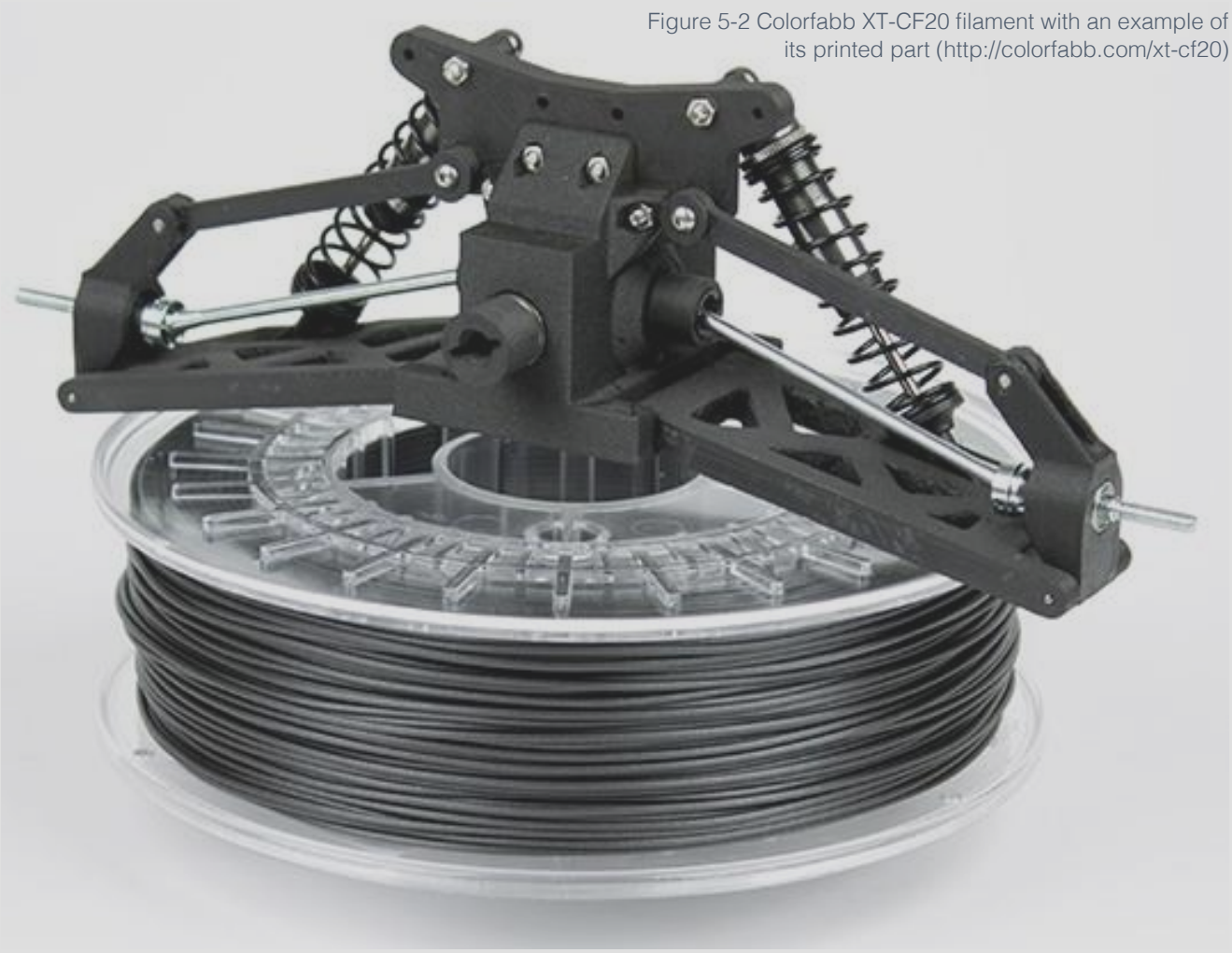

Figure 5-2 Colorfabb XT-CF20 filament with an example of its printed part (http://colorfabb.com/xt-cf20)

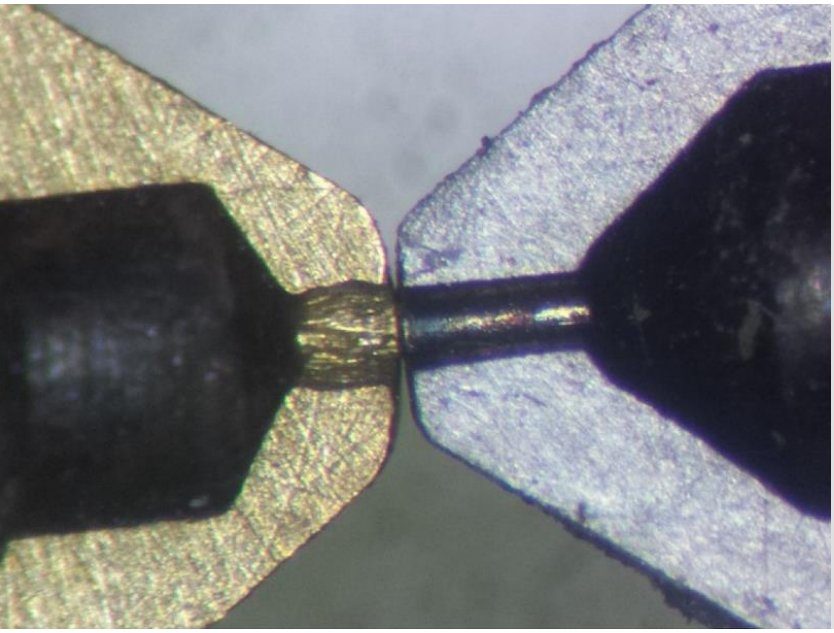

Figure 5-3 Comparison of how the carbon fibre wears the brass nozzle on the left compared to the nozzle made out of stainless steel

Figure 5-4 E3D v6 Hotend which able to withstand up to 400 degree Celcius

The material properties data from the manufacturer was tested on a raw specimen of the material. In practice, the strength of the material highly depends on the 3D printer machine and also the print setting of the 3D printing software. Further material test was done to find the detailed material properties, especially the orthotropic material behavior of the printed parts to use for the topology optimization process.

The carbon fiber node will be connected to the wooden beam with two standard size bolts. The beam consist of three planks of wood which glued together into a single beam, for the purpose of easier fabrication process. The face of the beams facing the node are designed to be always perpendicular to the axis of the beam. This makes the cutting process of the beam much simpler. Since the dimension of the beam's cross section are always identical, the only parameter needed to manufacture the wooden beam is its length.

2. FDM 3D printer

The 3d printer used for the project is a custom made RepRap Leeuwenhoek (http://dymensional.nl/) 3d printer designed by a student in Faculty of Architecture TU Delft, Aaron Bislip. The machine has a build volume of 230 x 130 x 100 mm, it is designed as a lightweight and portable 3d printer which is easy to carry around. Due to the special requirement of the carbon fiber material, some modification were needed for the original design of the printer. A special point of attention is the abrasive nature of the carbon fibers. In general these fibers will accelerate the nozzle-wear of brass nozzles, much faster than unfilled filaments. Therefore, the original brass nozzle was replaced with a stainless steel nozzle. Another modification was to replace the original hotend of the printer which can only withstand the temperature up to 245 degree Celsius, because the carbon fiber infused filament recommended print temperature is at least 250 degree Celcius. The new hotend used was the E3D v6 (http://e3d-online.com/) hotend which is able to withstand up to 400 degree Celcius.

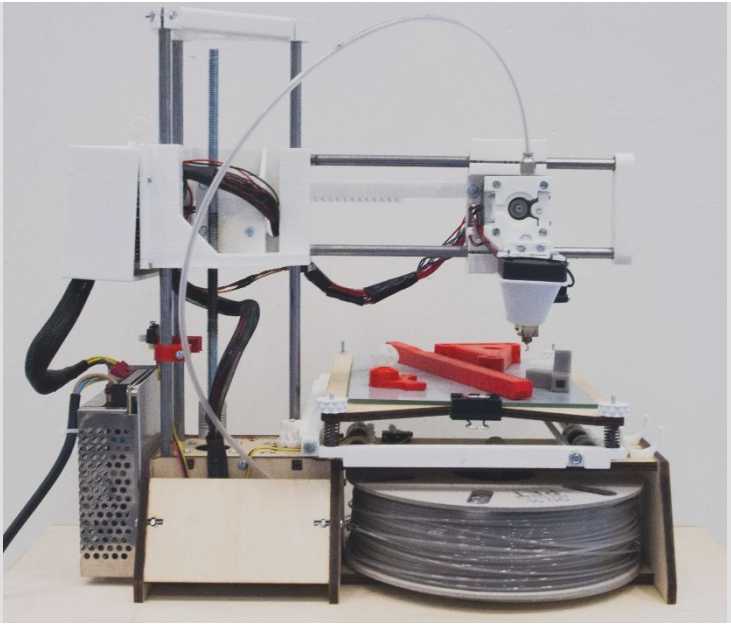

Figure 5-5 Leeuwenhoek portable 3D printer by Aaron Bislip (http://dymensional.nl/)

3. First prototype

The first prototype to test out the concept is a part structure consist of 6 nodes and 7 beams. The nodes were printed in standard PLA plastic. The first prototype shows different strategies for the topology optimized geometry design and also connection to the wooden beams. In this case the beam is made from attaching 3 planks of mdf wood glued together. The nodes were calculated with global optimization calculation and combined with different types of additional node design which will be explained in the next part of this chapter.

Figure 5-6 Connection detail strategy for the optimized nodes of the structure

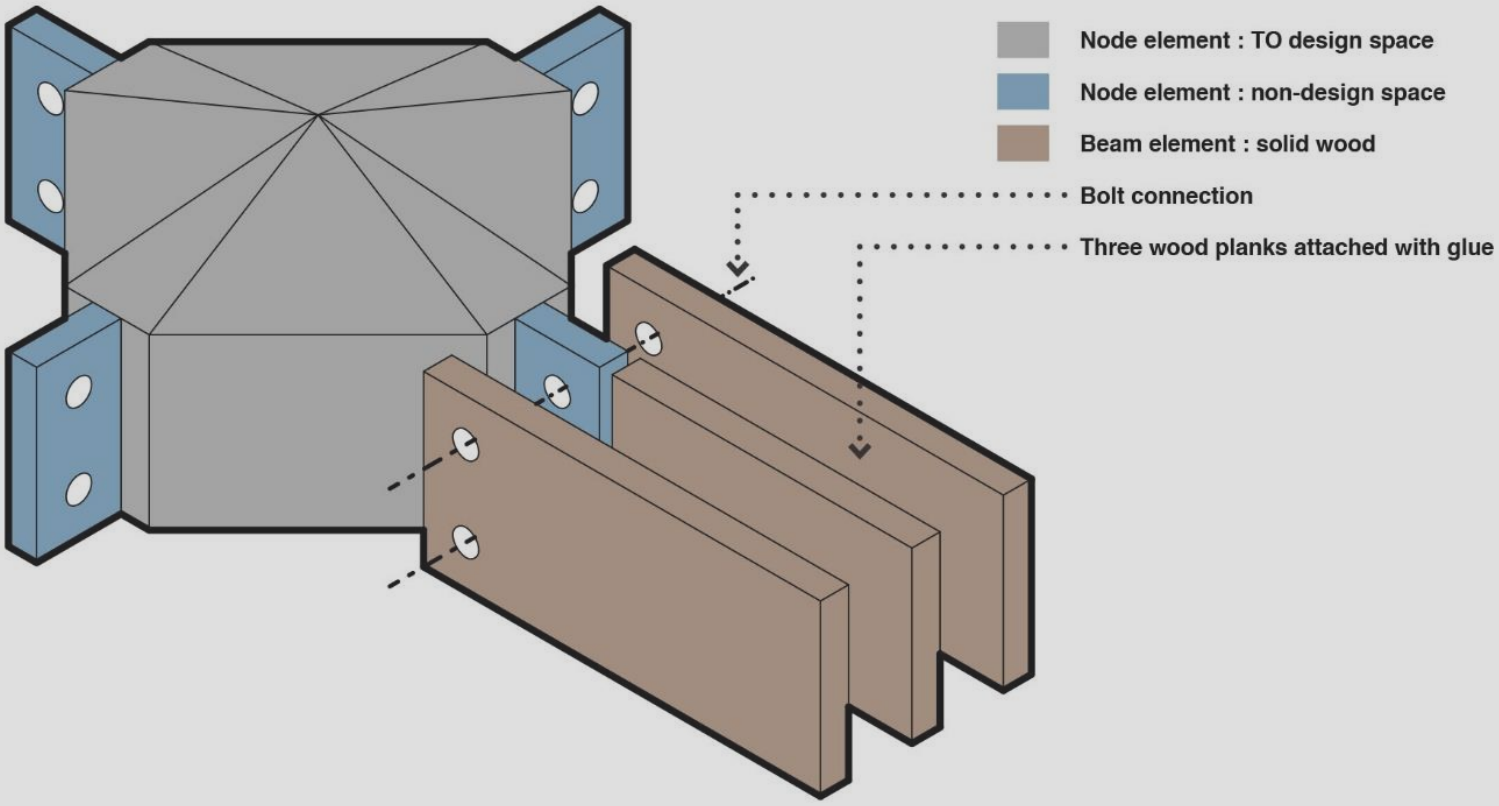

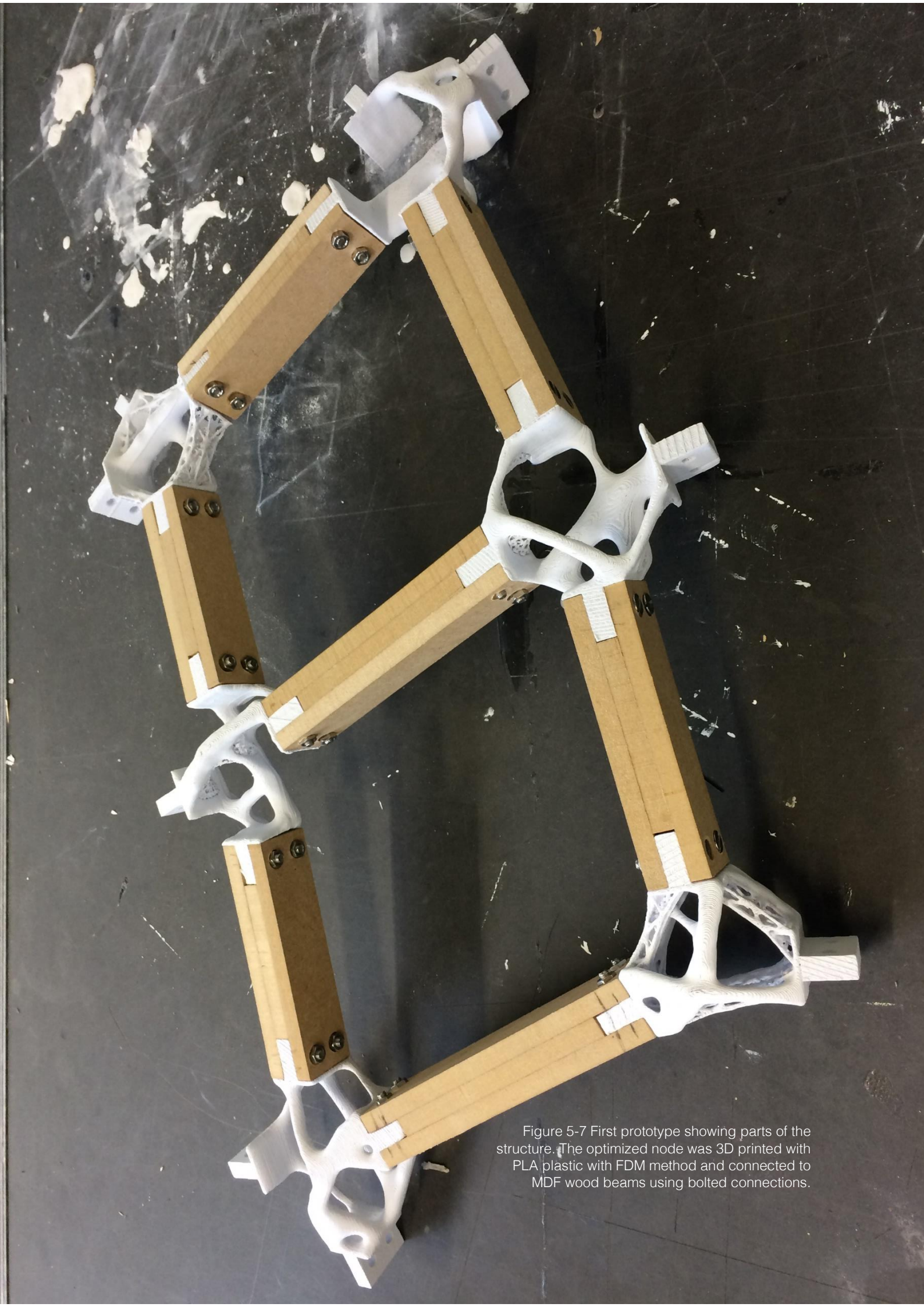

Figure 5-7 First prototype showing parts of the structure. The optimized node was 3D printed with PLA plastic with FDM method and connected to MDF wood beams using bolted connections.

5.3 Design development and parametric modeling

The surface geometry of the conceptual design of the structure was purely a designer's input which could be generated from any kind of modeling tools. An general parametric model need to be created to turn the schematic geometry into a working detailed model which can be used as functional structural solid model for FEM calculation and topology optimization. The parametric model was created on Rhino-Grasshopper with the following step-by-step process:

1. Quadrangular grid layout generation

For the purpose of making the work simpler, the initial surface was designed as a simple 4-sided untrimmed brep surface. This makes the quad-paneling process as just a simple division of the surface based on the surface's UV coordinates.

Figure 5-8 UV division of the initial design surface with 40 panels in total

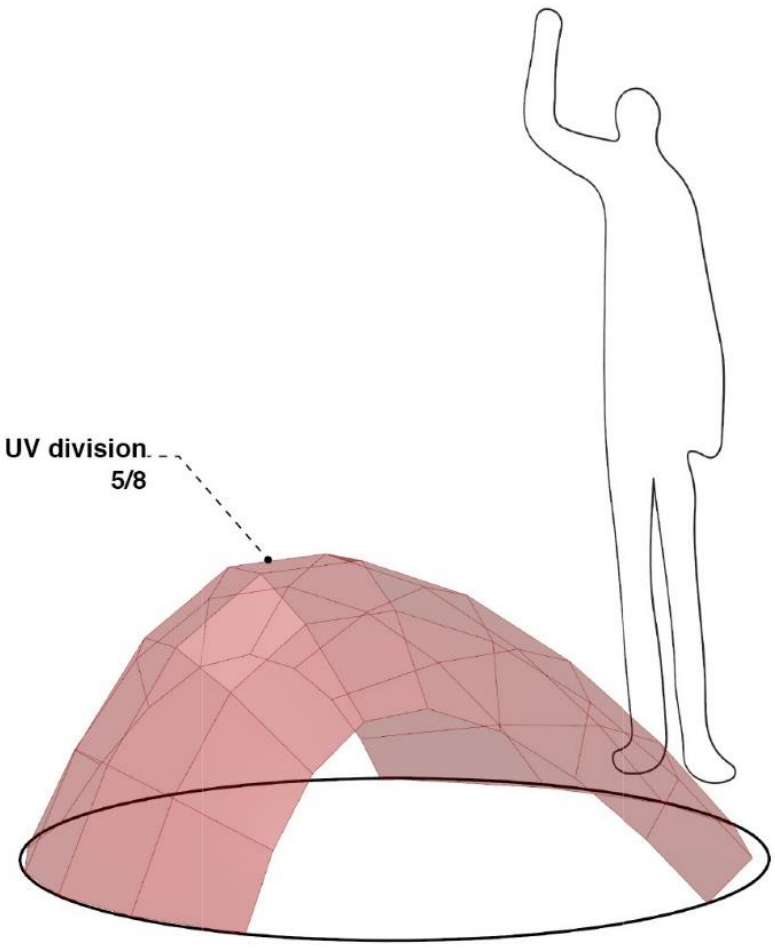

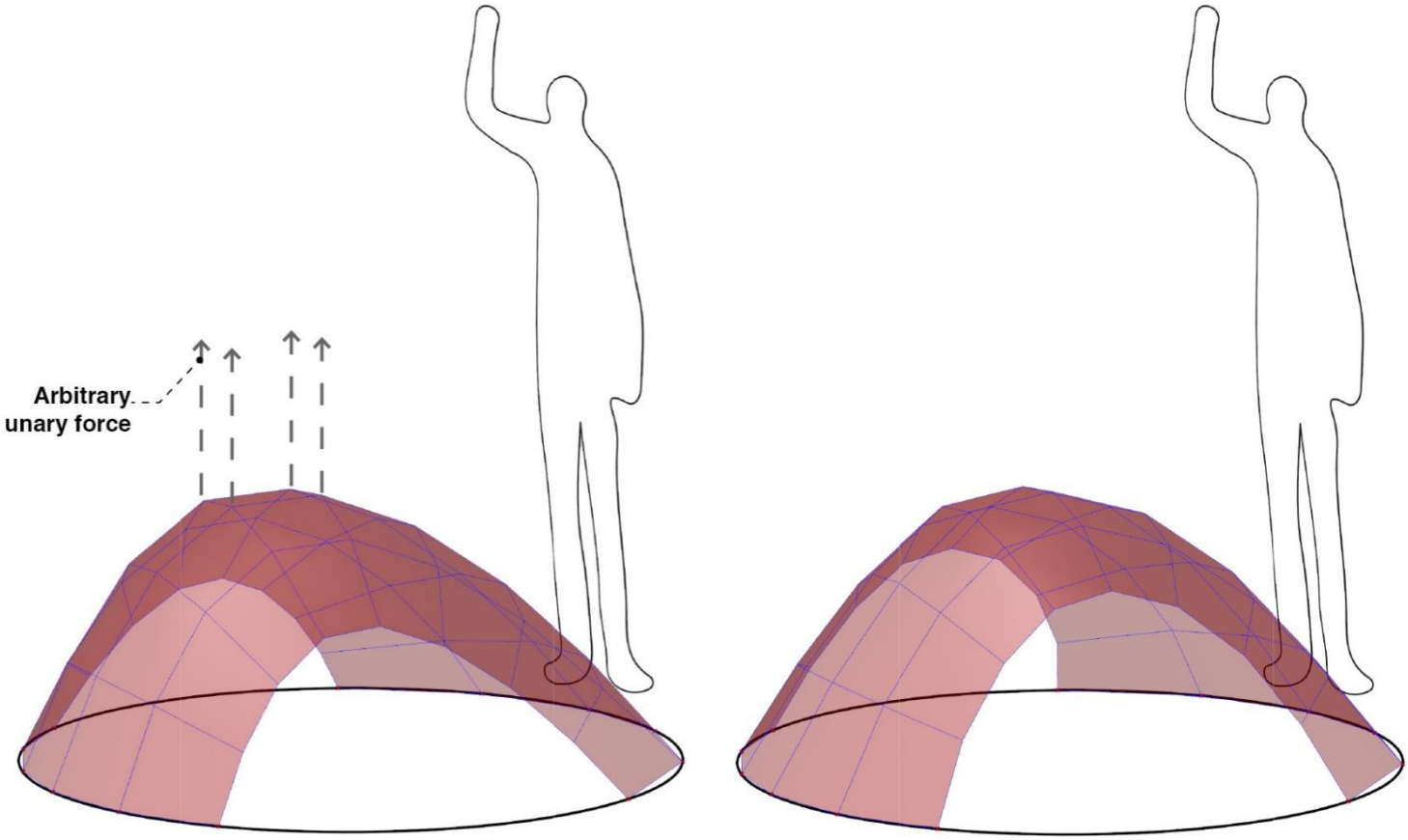

Figure 5-9 Forces applied to the geometry for shape optimization form-finding (left), and the optimized shaped after several iteration (right)

2. Shape optimization and form-finding

Even though the geometry of the structure is relatively simple, a general shape optimization executed to optimize the shape for the desired structural loads. In this step the conceptual structural model was defined. The tension ring base was not necessary at this point, thus the support of the structure was created as a fix support to the ground. Four point load was defined on the top nodes. The edges of the mesh were defined as a spring element with its stiffness as a variable parameter. Since it is a form-finding process, the value of the loads and the stiffness of the springs are defined as arbitrary numerical units which will be adjusted manually until the desired optimized shape is generated. The parametric form-finding process is carried out with Kangaroo, a physical simulation tools in Grasshopper.

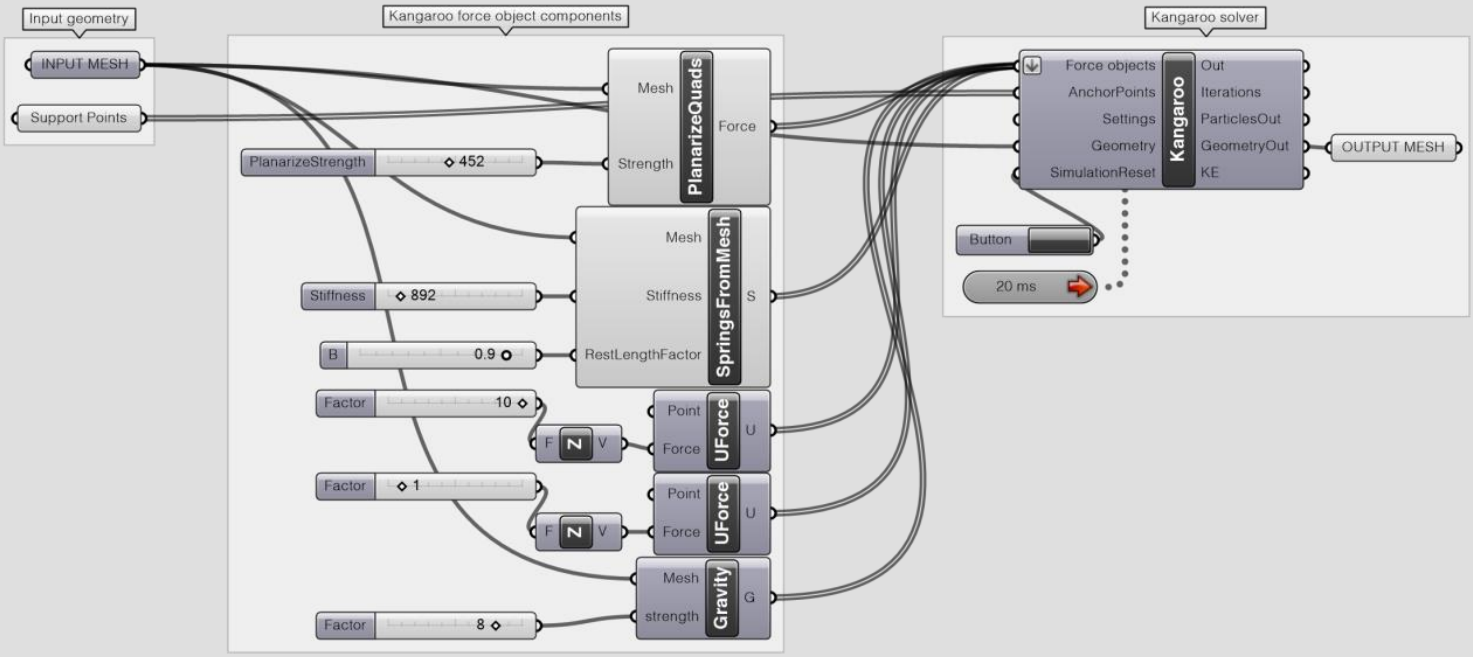

Figure 5-10 Grasshopper script for the initial 'hanging model' form-finding of the structure.

3. Conceptual structural analysis and beam size optimization

The next step is to turn the mesh geometry into a grid-shell structure. This is done by giving a sectional properties on each of the edges and applying all the load cases and boundary condition of the structure as a conceptual frame model structural analysis. Although there are no glass or panel cladding on top of the structure, the beam orientation are optimized to fit the quad panel geometry. The beam oriented to align with the normal vector of the mesh surface at the midpoint of each mesh edges.

For constructing beam structure, the wood material available at local hardware store are classified as spruce wood. The mechanical properties of the beam are gathered from a database software CES EduPack as an average of multiple types of wood within the spruce family.

Young's modulus	: 10 GPa
Shear modulus	: 0.8 GPa
Density	: 430 kg/m3
Yield strength	: 40 MPa

On this conceptual structural calculation phase, the base of the structure are assumed as a ground-fixed support neglecting the tension ring. The parametric model was created in a structural analysis tools within Grasshopper called Karamba. Since the parameters of the beam size were limited by the availability of the wood products, there are only a few numbers of combination of parameters. Therefore, a manual adjustment was enough to find the optimal beam size by considering maximum displacement as the constraint.

Figure 5-11 Grasshopper script with Karamba plugin to schematically analyse the structural behaviour

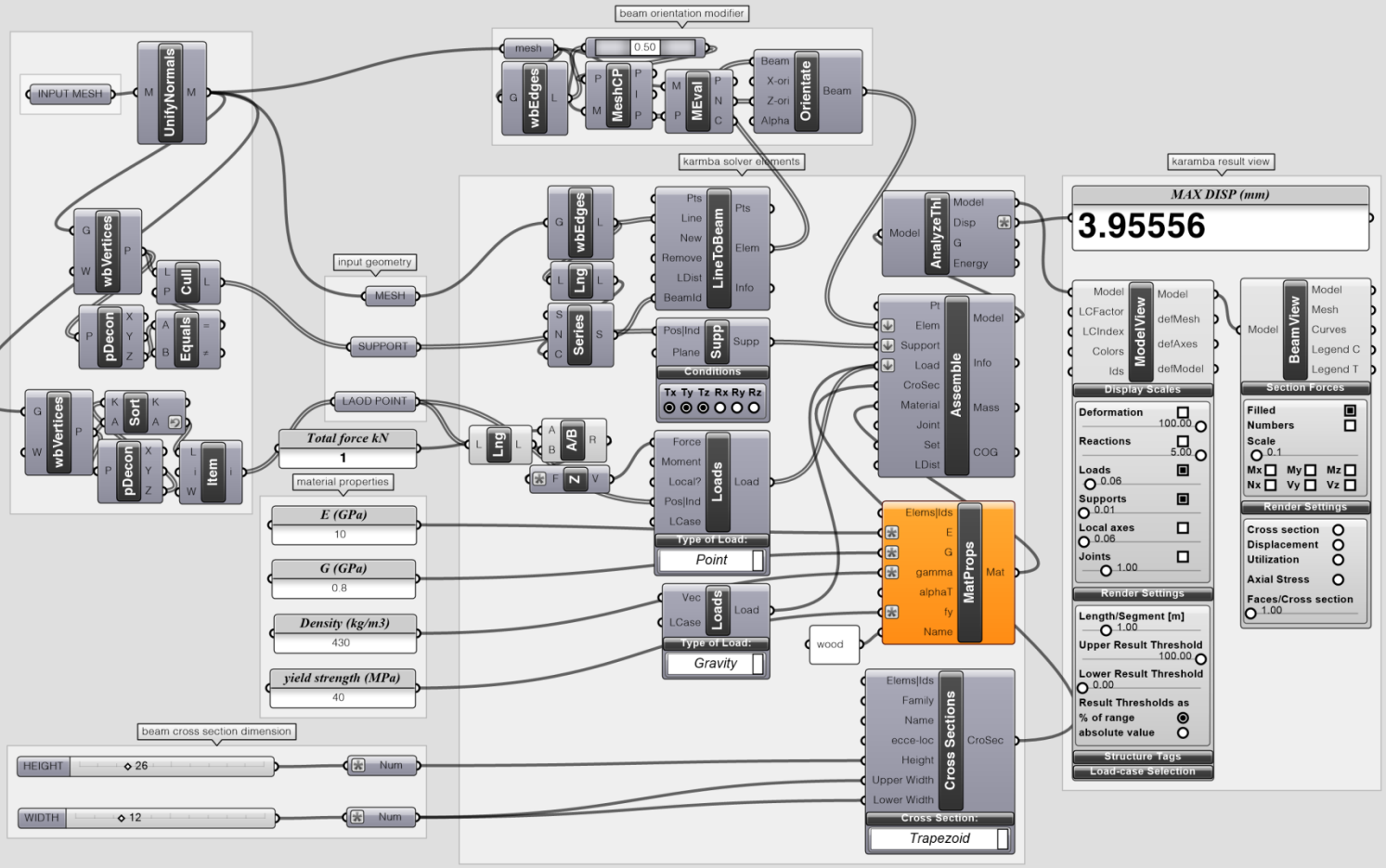

After the dimension of the beam was chosen, the resultant forces that take place on each beams were documented as numerical values. There are 6 type of forces that can be displayed on Karamba's beam analysis view:

Mx : Torsional moment on beam's local X-axis
My : Bending moment on beam's local Y-axis (out of plane bending)
Mz : Bending moment on beam's local Z-axis (in plane bending)
Nx : Normal (axial) forces on beam's local X-direction
Vy : Shear forces on beam's local Y-direction (in plane shear)
Vz : Shear forces on beam's local Z-direction (out of plane shear)

Figure 5-12 The orientation of each beams follows the normal vector on midpoint of each mesh edges, the optimized nodes geometry will follow the orientation of each beam's end surface.

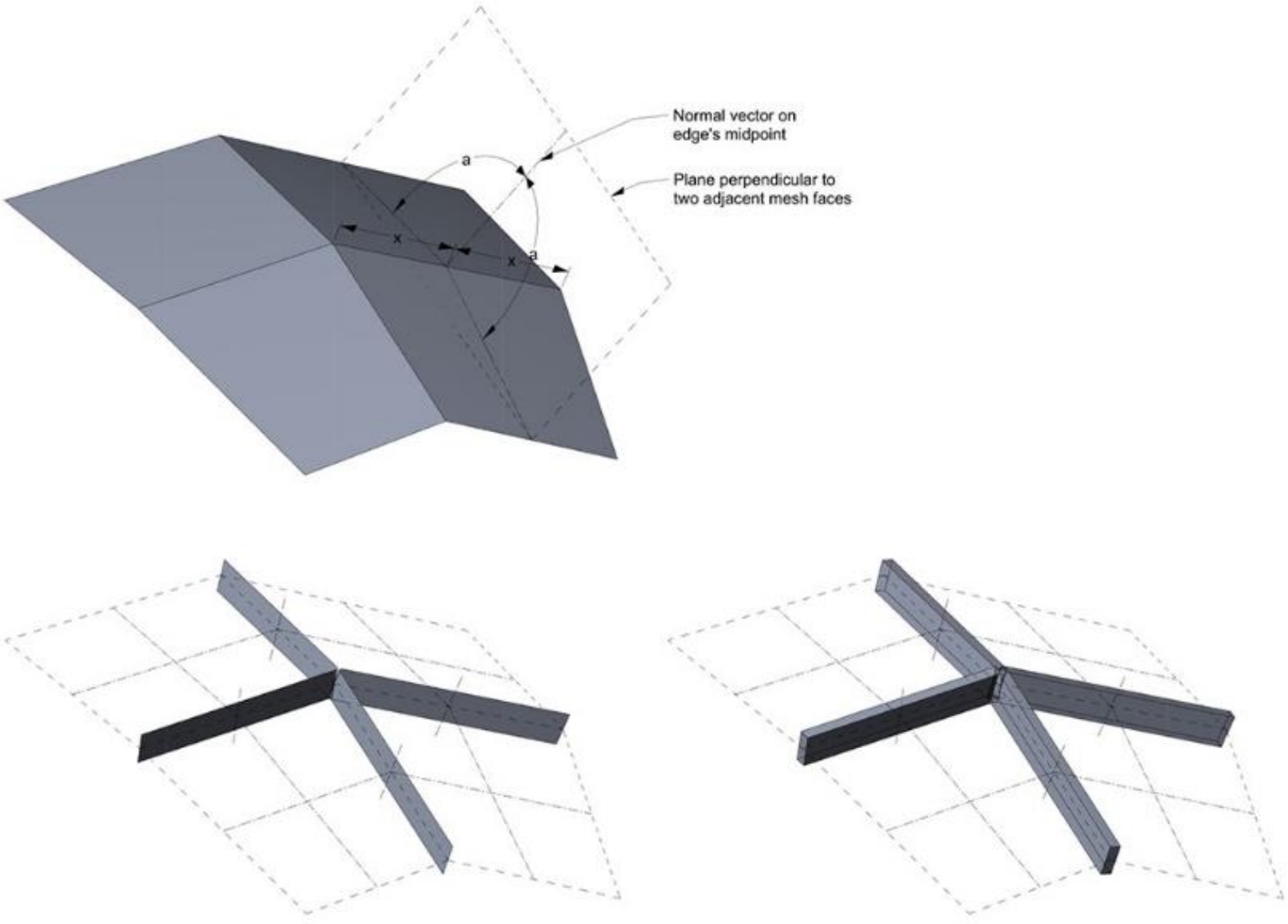

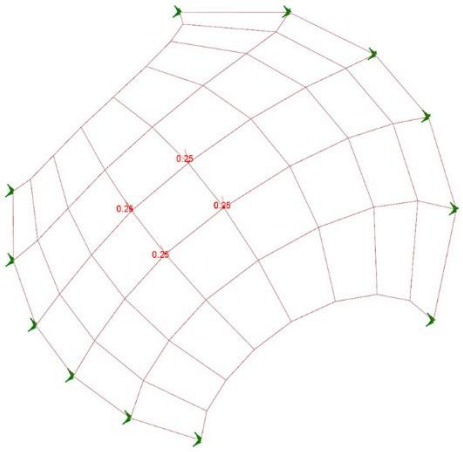

Loadcase and boundary conditions

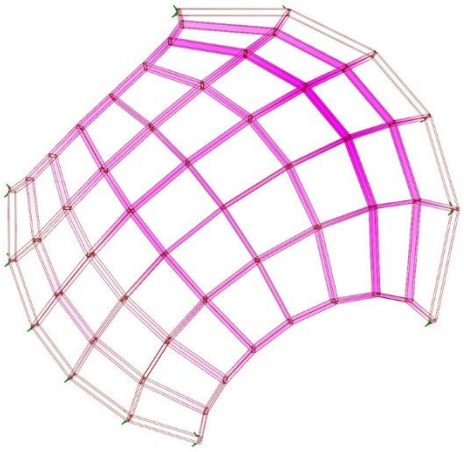

DIsplacement diagram

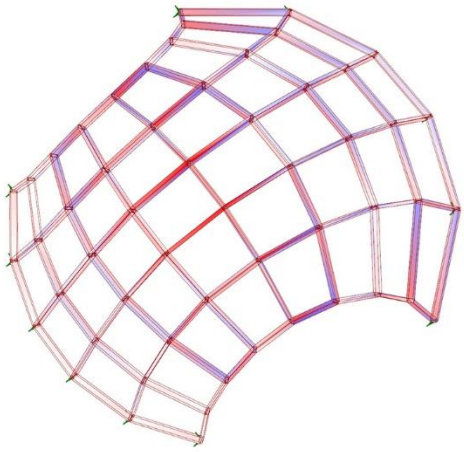

Beams utilization. Red: compression, Blue: tension

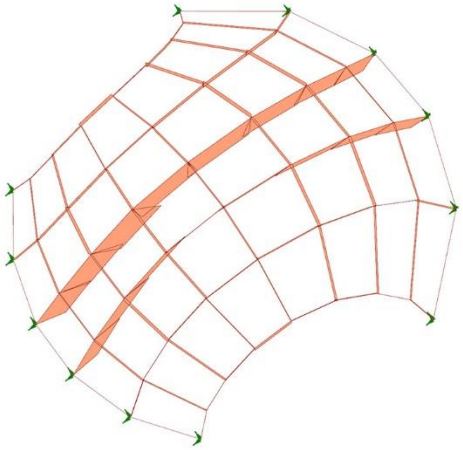

Nx: Normal (axial) forces on beam's local X-direction

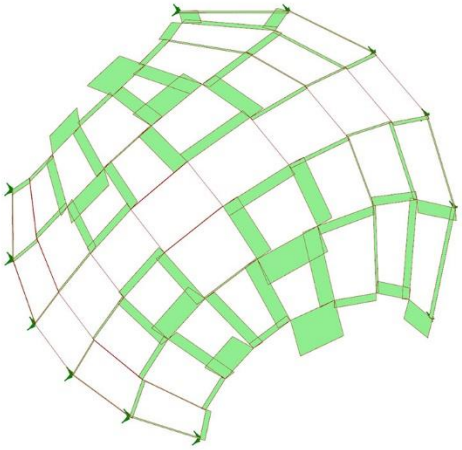

Vy: Shear forces on beam's local Y-direction (in plane shear)

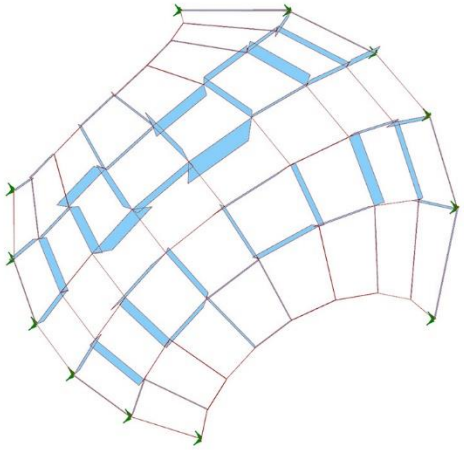

Vz: Shear forces on beam's local Z-direction (out of plane shear)

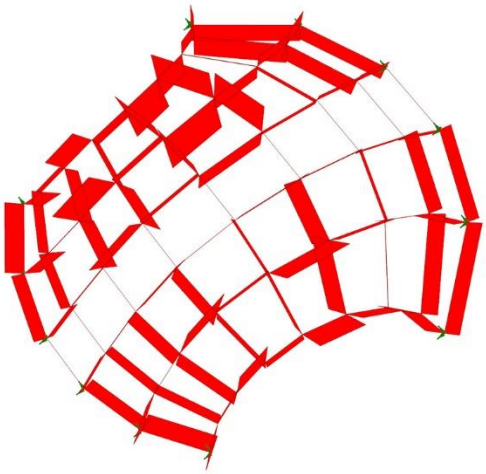

Mx: Torsional moment on beam's local X-axis

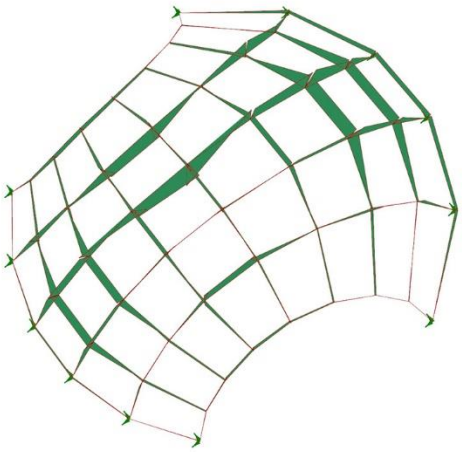

My: Bending moment on beam's local Y-axis (out of plane bending)

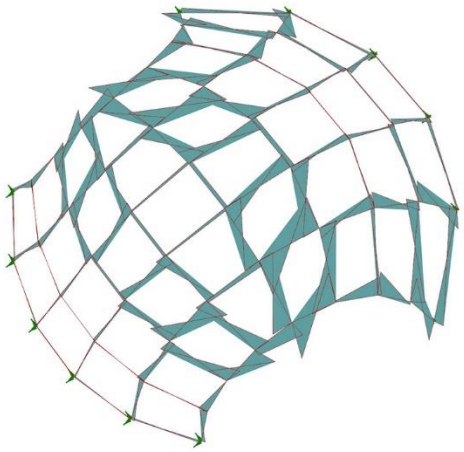

Mz: Bending moment on beam's local Z-axis (in plane bending)

4. Node design space parametric model

All the forces that take place on each nodes were compiled into a single numerical value which determined the size of the node. Beams with higher bending and shear forces will be shorter, thus these forces will ideally take place more on the nodes. On this step, the first AM constraints is applied. The maximum size of the nodes is determined by the size of the building chamber of the AM machine.

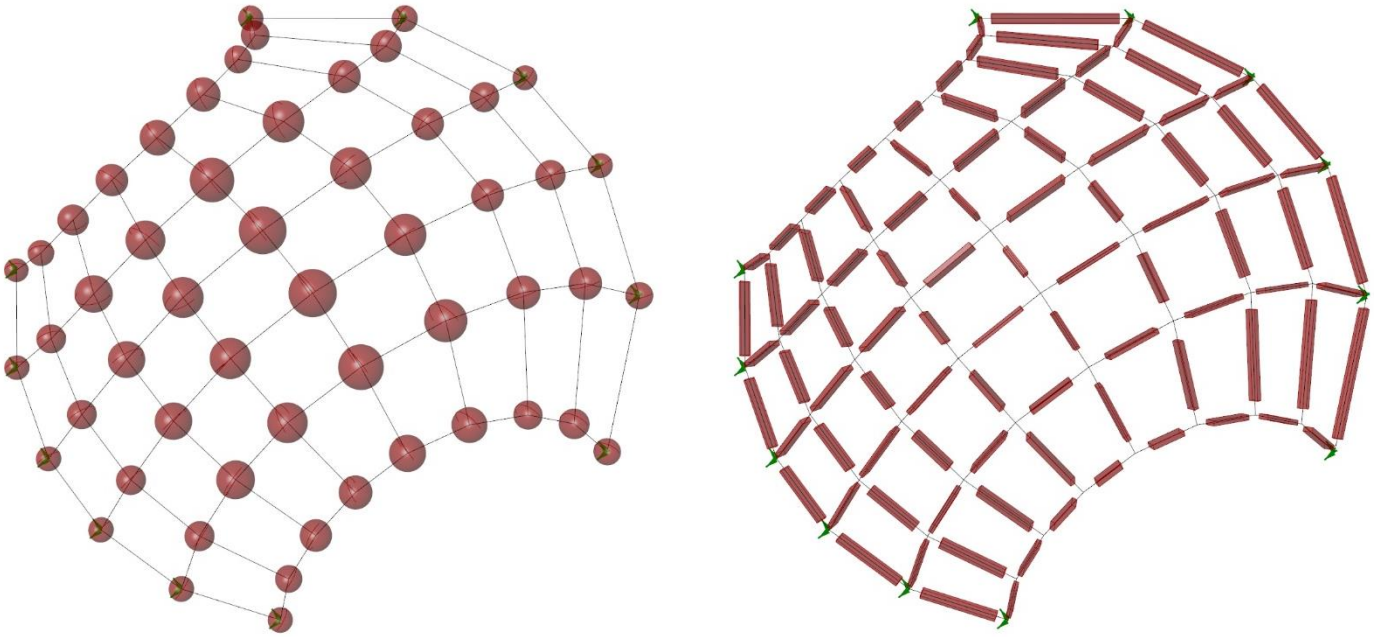

Figure 5-13 Simple visual representation of the nodes size based on the value of forces individually (left), and the different length of beams after the dimension of each node were determined (right).

The design space geometry is generated from 4 sides of the beams connected to each nodes. Another design input needed is the height of the node in the node's normal axis. The height is determined by separate value of top and bottom offset. On this prototype structure, there are no constraints of envelope paneling, thus the node height could go higher than the height of the beam.

Figure 5-14 Node's local z axis and geometry setting out

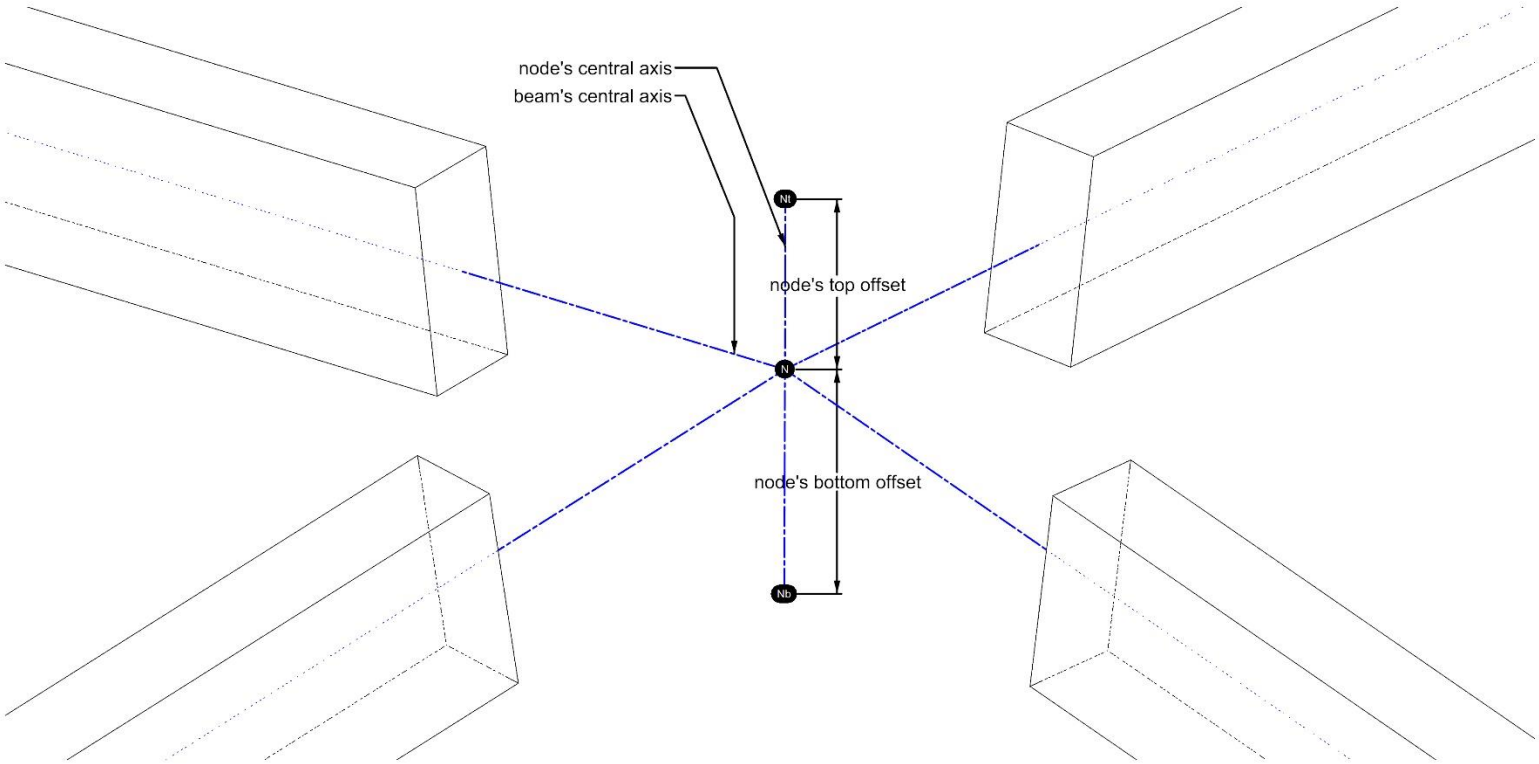

Figure 5-15 Completed node's design space for TO parametrically generated from its own context

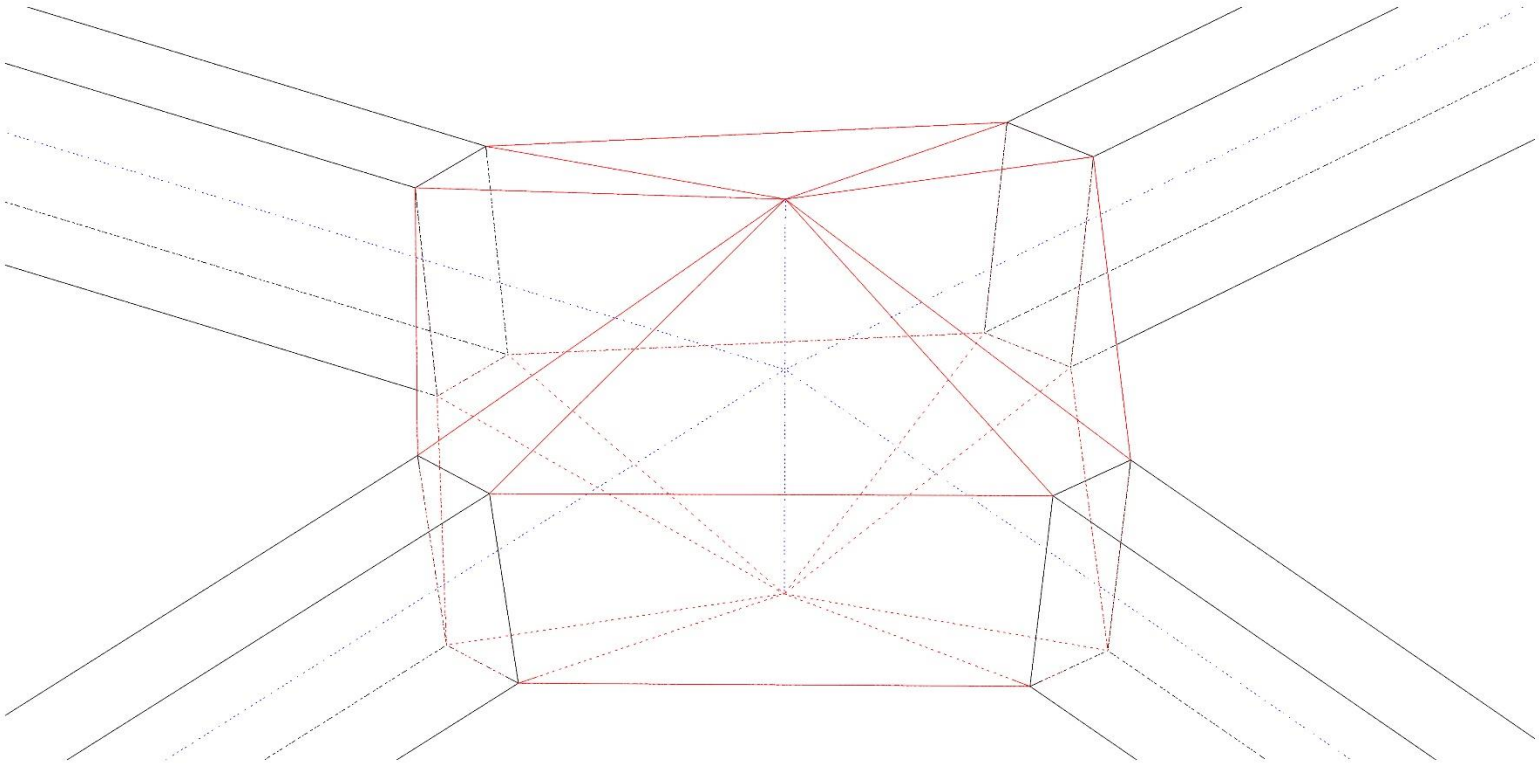

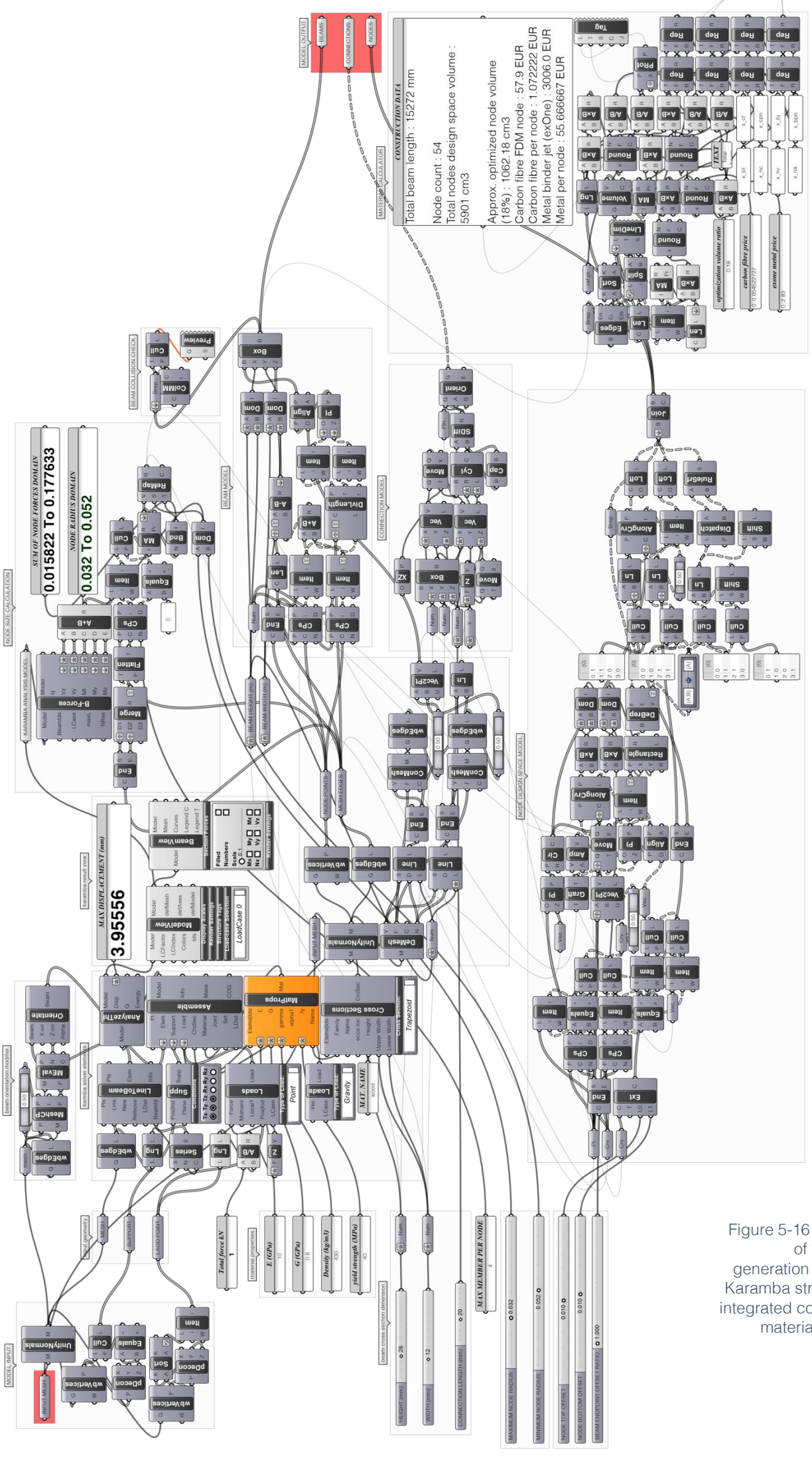

Figure 5-16 The complete script of the parametric node generation model based on the Karamba structural analysis with integrated connection model and material amount calculation

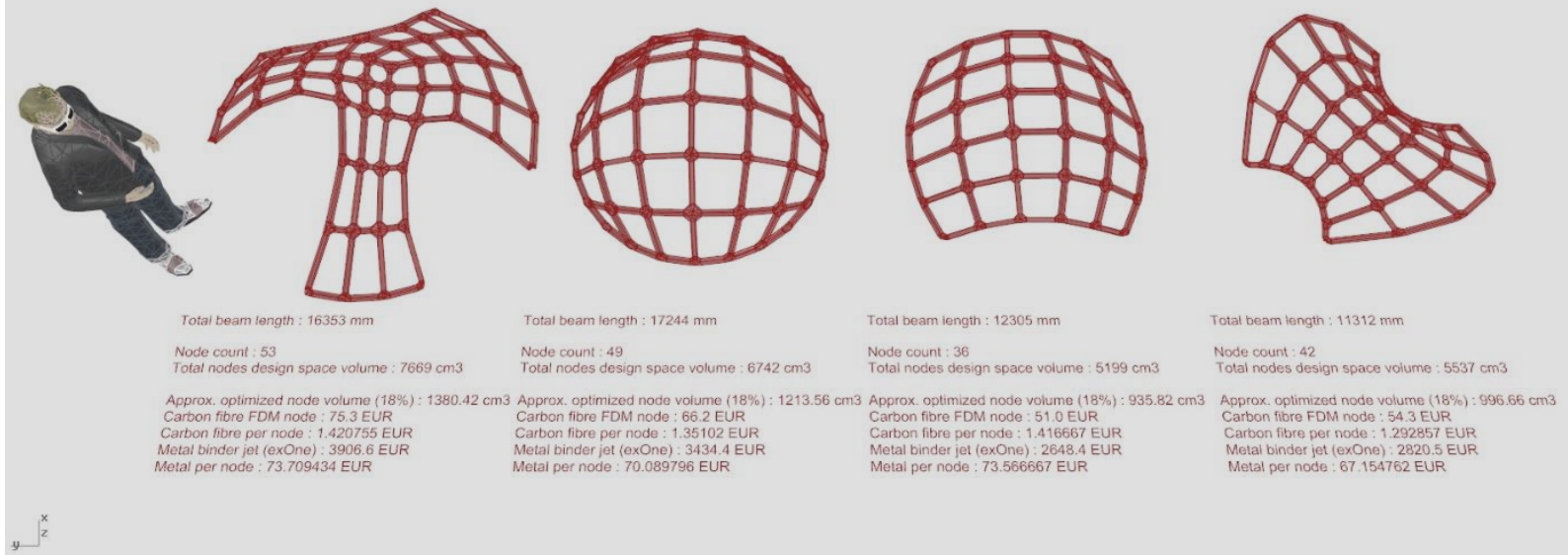

Figure 5-17 Design alternatives with parametric analysis of material amount and cost

5. Final prototype design

The final prototype design was chosen mainly based on the buildability and the amount of material needed which was restricted by the budget. The parametric model is able to give the accurate information of several design option in terms of quantitative comparison. The quantitative parameters that were generated was the total amount of the wooden beam, bolt and nuts for connection, and the number of nodes which need to be printed, which leads to an approximate calculation of the optimized volume to the price of the material needed.

The final design has 28 3D printed nodes, including 8 nodes connecting the base structure, 45 wooden beam with 44 x 18 mm profile, and base ring structure with diameter of 1.6 meters.

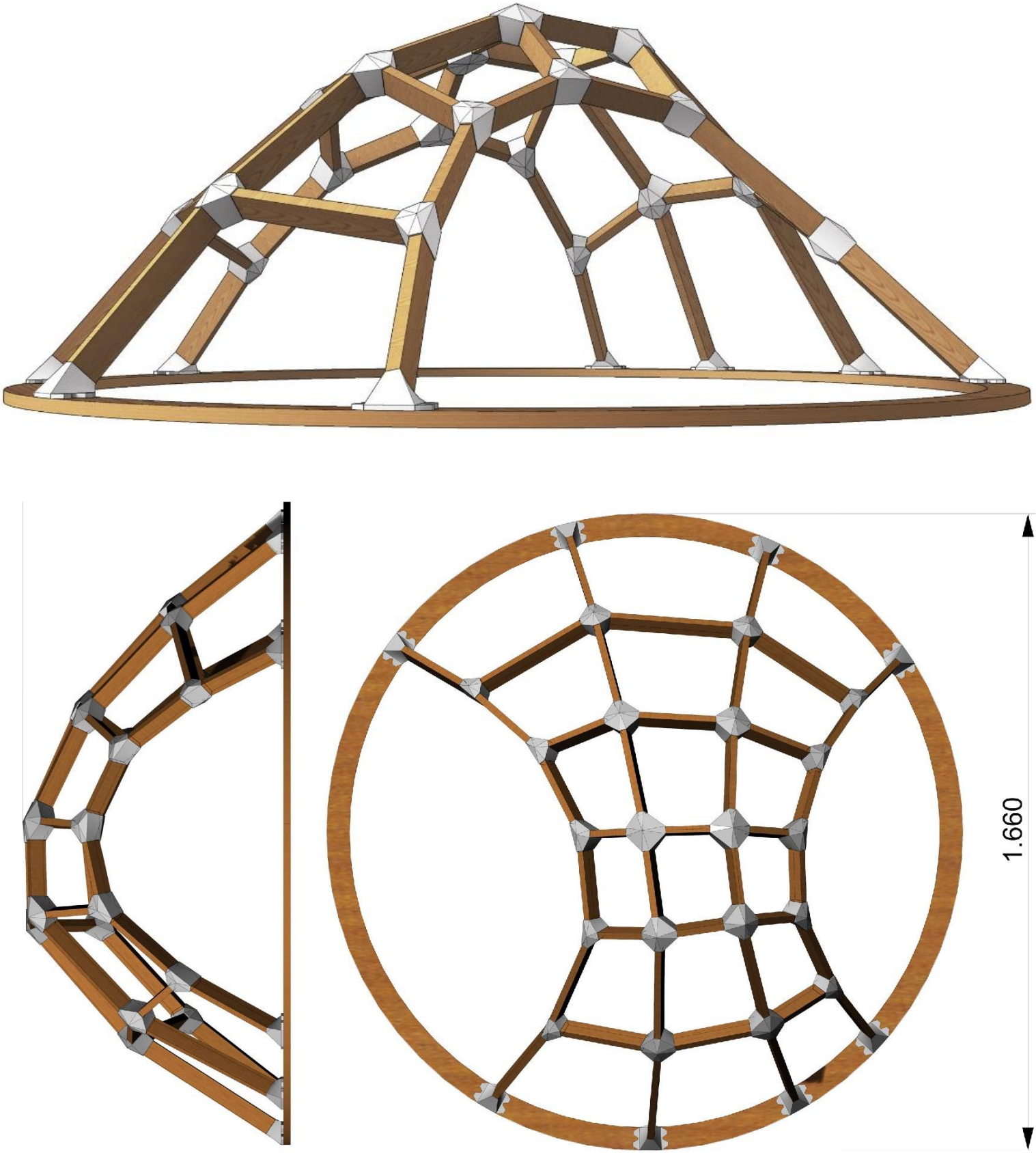

Figure 5-18 Drawings of the prototype final design

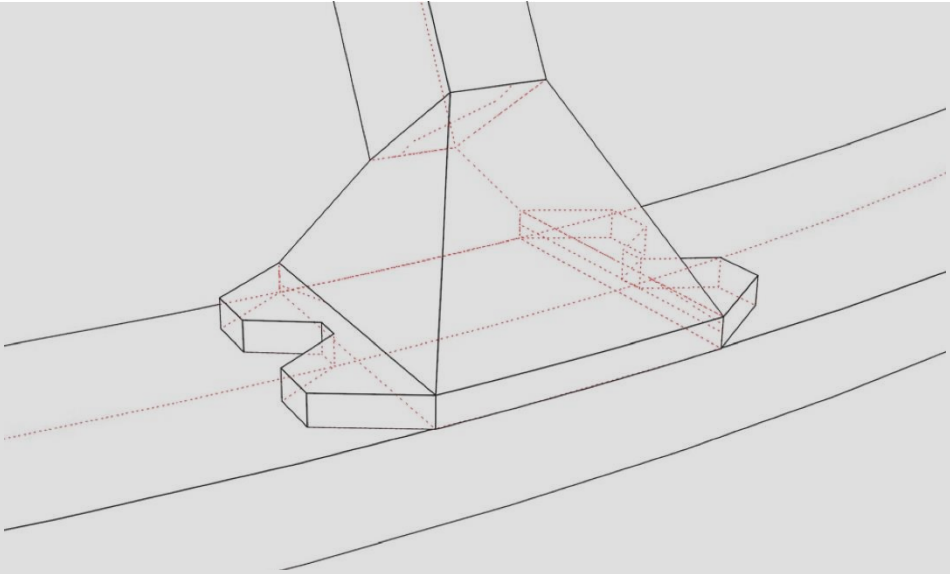

Figure 5-19 Base footing design space

6. Base footing nodes

The base footing nodes has a special treatment in terms of design space for topology optimization and connection detailing. The design space shape looks like a trapezoid pyramid with a flat surface touching the ring beam and connected with 4 bolts.

7. Connection detail

The 3D printed nodes are connected to the beams using simple 2 bolt and nut connection. Parts of the nodes element are extruded inside the beam's to provide the connection material. Since all the cross section dimension of the beams are equal, the connector part of the node were modeled separately which then oriented to each beam's direction.

Figure 5-20 Connection details
are standardized for all the nodes

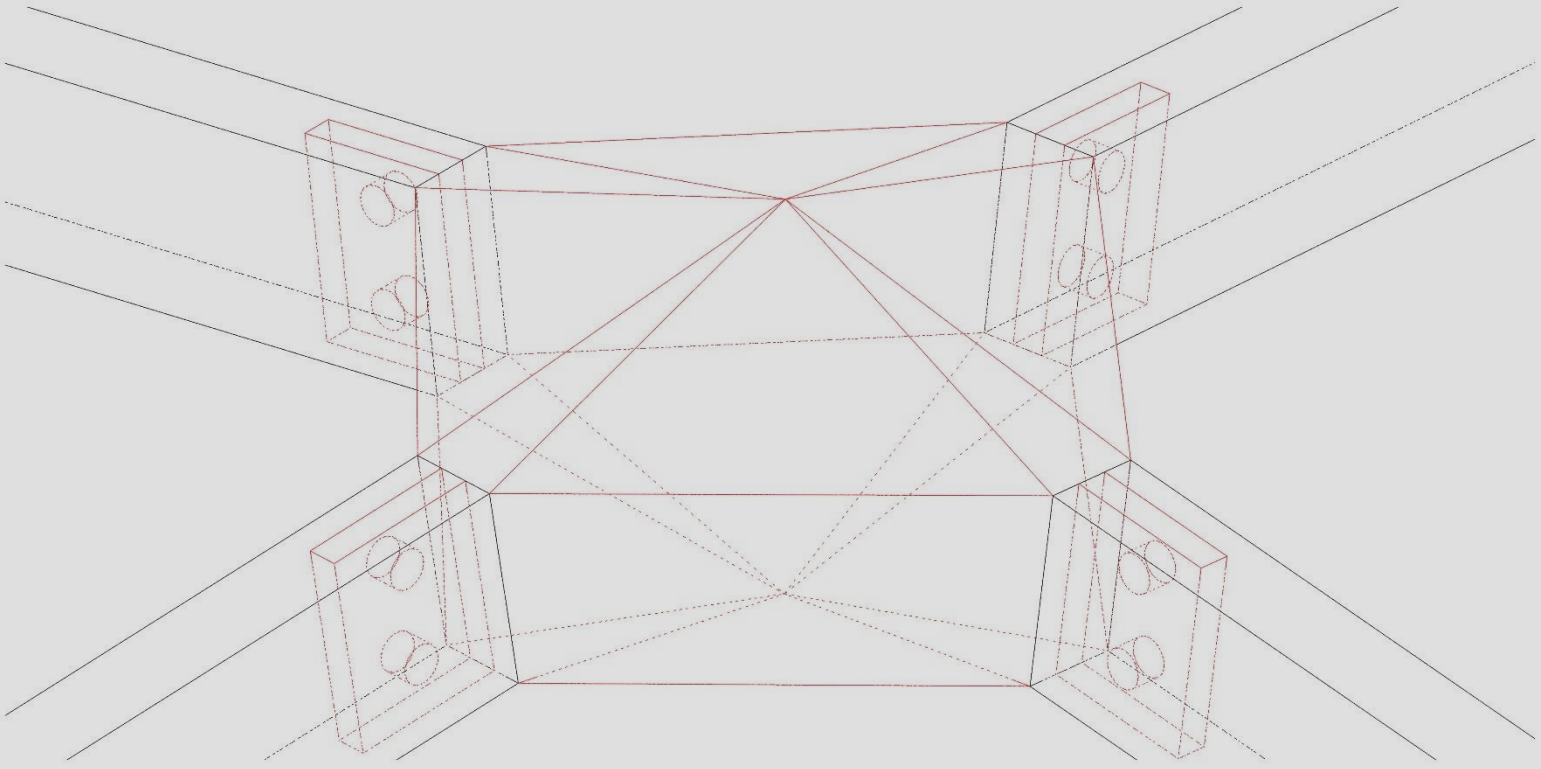

5.4 Nodes Topology Optimization

The general idea of structural optimization is to optimize a structural performance and efficiency of certain elements to its own specific function. However, structural elements in architecture are supposed to be flexible in terms of its structural function, and should be able to cater into different unintended function which might take place in the building's lifetime. The hypothesis of this research is that on top of the structural optimization specific to its predetermined architectural function, there should be a generalized structural criteria in the optimization parameters. Thus, the optimization process is divided into two parallel process which in the end combined into one optimized structure: the standardized optimization process and the definite optimization process specific to its architectural function.

1. Optimization parameters and constraints

- Material properties

The material property of the 3D printed element especially using the FDM machine could be considered as an orthotropic material. The stiffness on Z-print axis is lower than the X and Y axis. On a carbon fibre reinforced filament this issue is even more obvious since the carbon fibre reinforcement is embedded in each layer while connection between layers is mostly related to the plastic adhesion when it is solidify. For this research, the generalized rules was applied that the elastic modulus of the material in Z direction is 85% lower than in X and Y direction. The same principle also applies to its shear modulus.

Figure 5-21 Build orientation axis determines different material properties on each direction (orthotropic material)

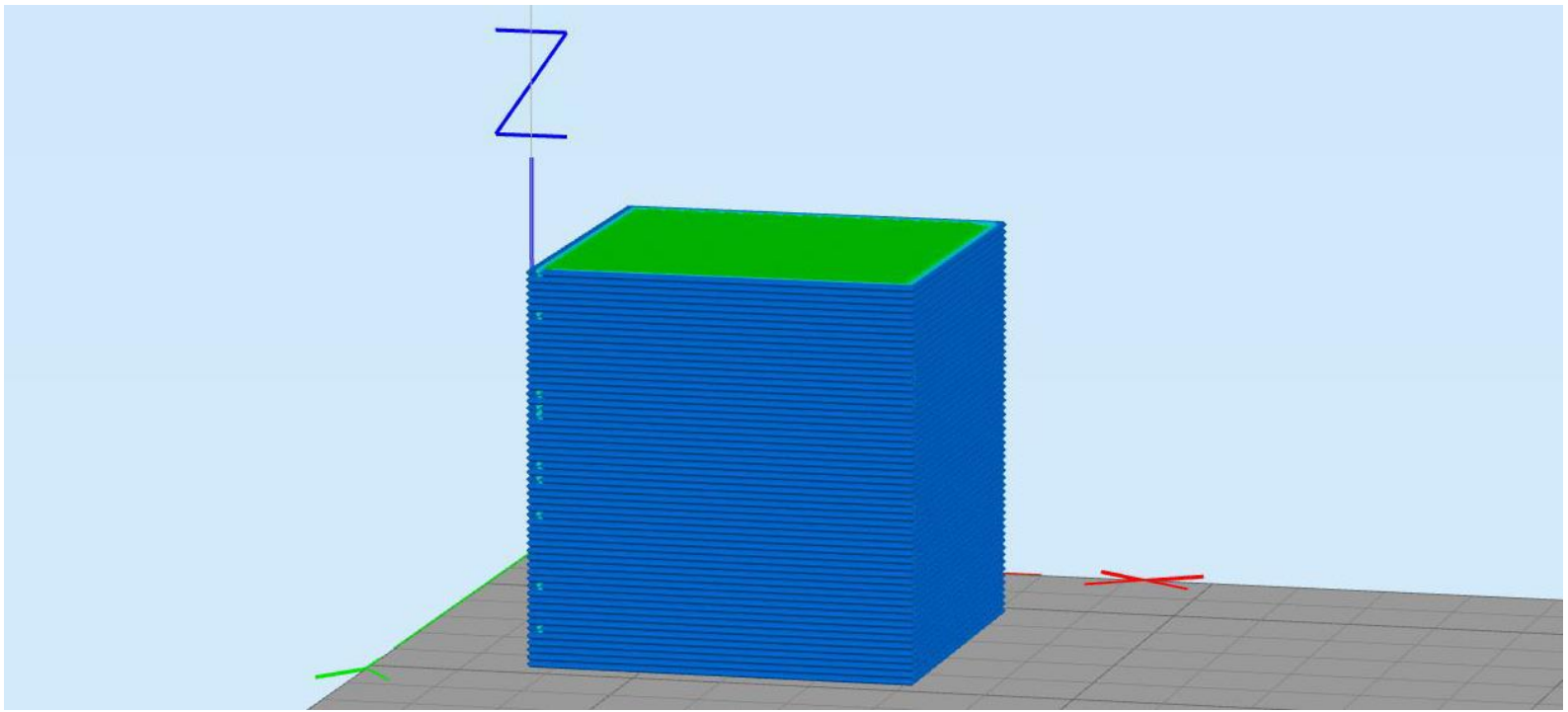

There are several crucial parameters needed as an input for performing the topology optimization calculation, they are:

- Elastic modulus (E) in 3 axis (X, Y, and Z)
- Poisson's ratio (NU) in 3 planes (XY, YZ, and ZX)
- Shear modulus (G) in 3 planes (XY, YZ, and ZX)
- Density (Rho) of the material

The elastic modulus for this calculation is replaced with the material's flexural modulus, which was obtained by testing the specimen on pure bending. This step is usually applies to plastic material with a high differences of stiffness in tension and compression. The flexural modulus is used as the average value which could represent the general properties of the material.

While the flexural modulus and density of the material is available from the material data sheet provided by the manufacturer, there is no available data for Poisson's ratio and shear modulus of the material. Moreover, a physical test to measure those value is not possible to do within the time span of this research. Therefore, the missing data was replaced by an available data of a different material with a similar composition and properties which is available in the CES Edupack material database. The chosen material was Polycarbonate + polyethylene terephthalate with 20% glass fibre blend. Finally, the composition of material properties used for the optimization calculation is listed below:

- Ex : 6.2 GPa
- Ey : 6.2 GPa
- Ez : 4.96 GPa
- NUxy : 0.36
- NUyz : 0.36
- NUzx : 0.36
- Gxy : 1.9 GPa
- Gyz : 2.38 GPa
- Gzx : 2.38 GPa
- Rho : 1.35e3 kg/m^3

- Optimization parameters

The topology optimization calculation and form-finding is performed in OptiStruct's topology optimization function. The tool performs density method of topology optimization where the design space is divided into smaller mesh elements and applied with different virtual density values. In general the parameters used in the calculation are listed below:

- Mesh type : tetramesh
- Mesh element size : 3 mm
- Volume fraction constraint : 5%
- Optimization objective : Minimize compliance (maximize stiffness)
- Minimum element dimension : 4 mm
- Discrete control : 1.5
- Maximum iteration : 100
- Density penalization limit : 0.2

2. Standardized optimization design

The standard node design is generated on a generic and symmetrical node condition that represent the whole node. The model is built separately from the main prototype model while still using the same beam dimension. The result of the optimization form-finding then reinterpreted into a parametric design geometry which can be applied to different node conditions. The load condition applied to the standard node design are generic bending and compression force subjected to the node as different loadcase.

The forces are applied directly to the node's end without the presence of beams. Each ends of the nodes are connected to a virtual spring element with low stiffness. The springs are connected to the end surface of the node with a rigid body element. This method allows running an equal forces at each four ends. It is crucial to have an equilibrium on all forces to avoid large displacement on the spring elements.

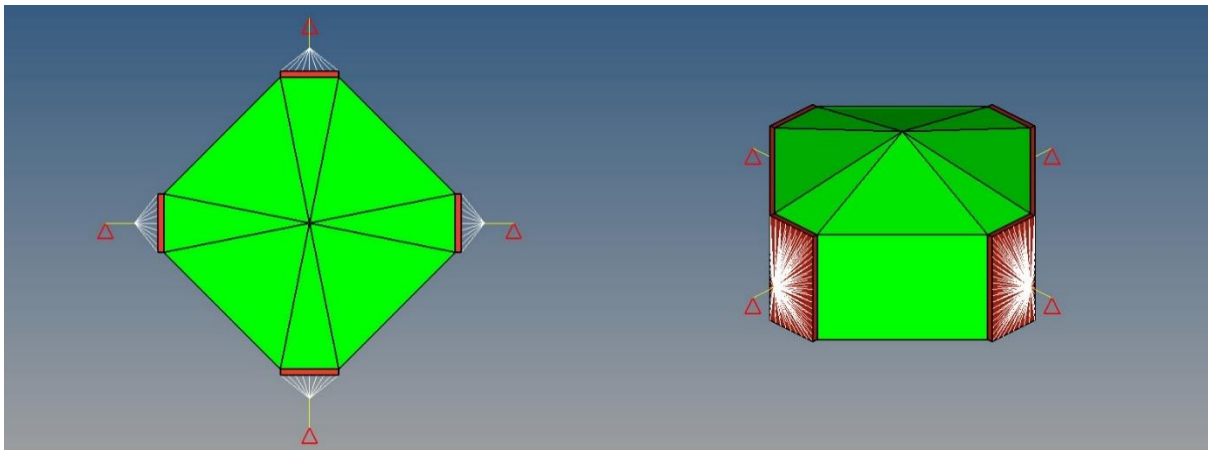

Figure 5-22 Boundary condition of the standard node model. Green object: optimized volume; Red object: non-optimized volume; Red triangle: fixed constraint; Yellow lines: spring elements; White lines: rigid body element

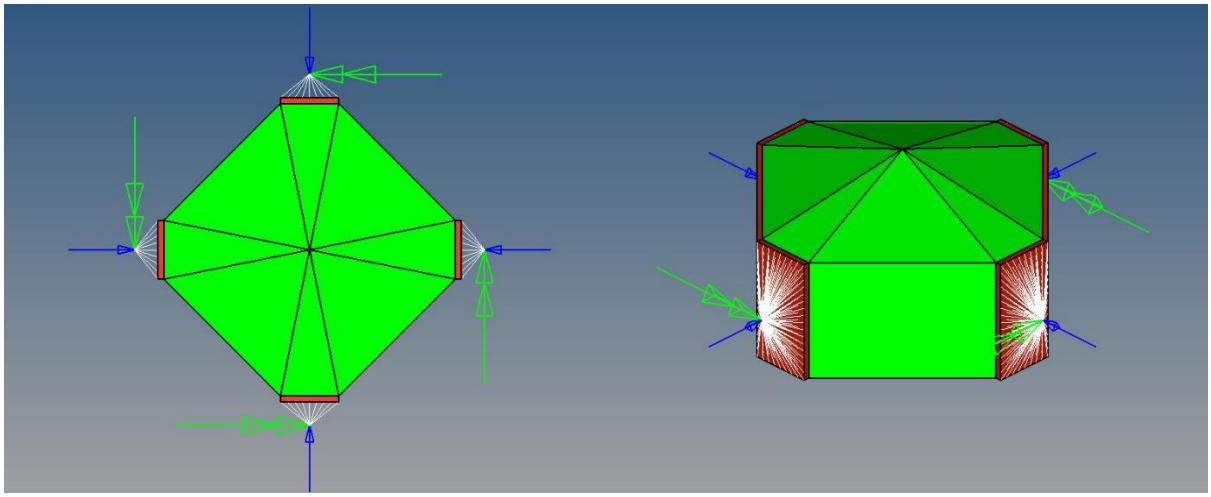

Figure 5-23 Load cases of the standard node model. Blue arrows: compression forces; Green arrows: moments

The OptiStruct topology optimization calculation runs for 73 iteration until it reaches convergence. The calculation result is shown in the figure below.

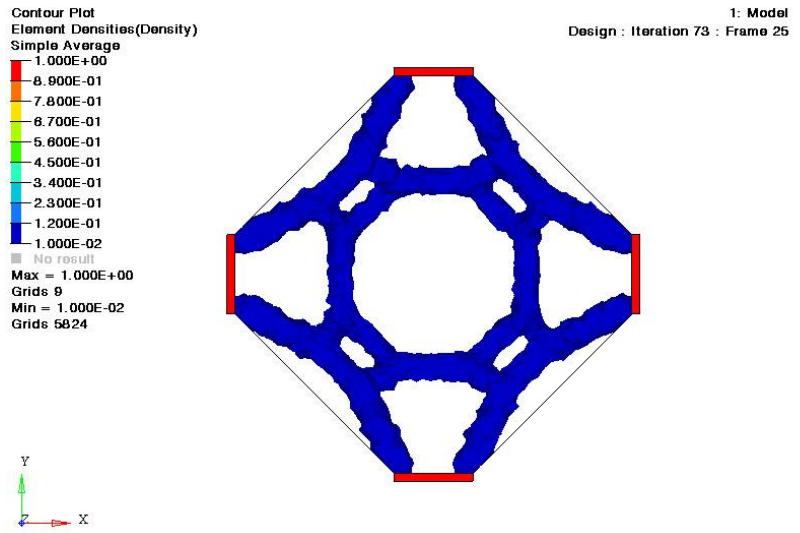

Figure 5-24 Optimization result visualized with iso density threshold 0.1

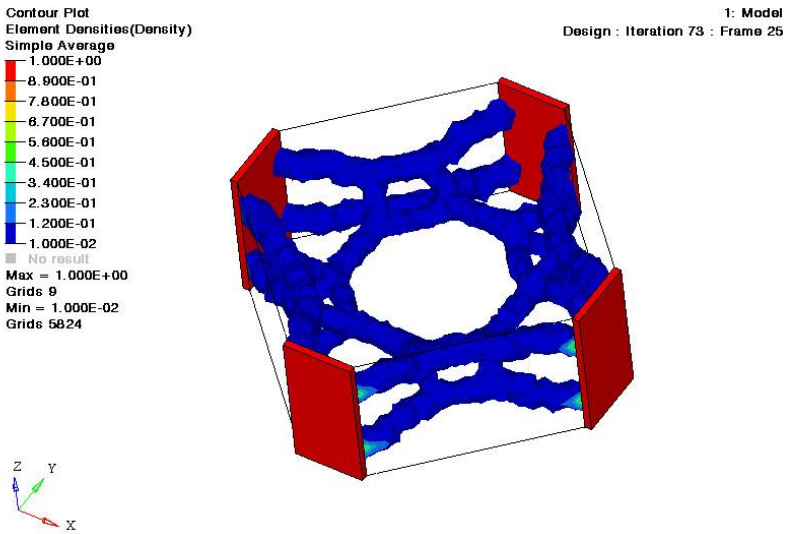

Figure 5-26 Optimization result visualized with iso density threshold 0.2

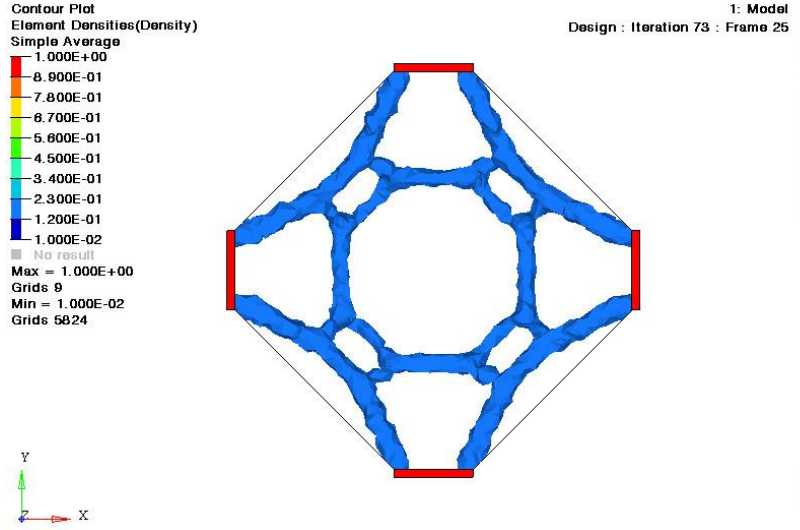

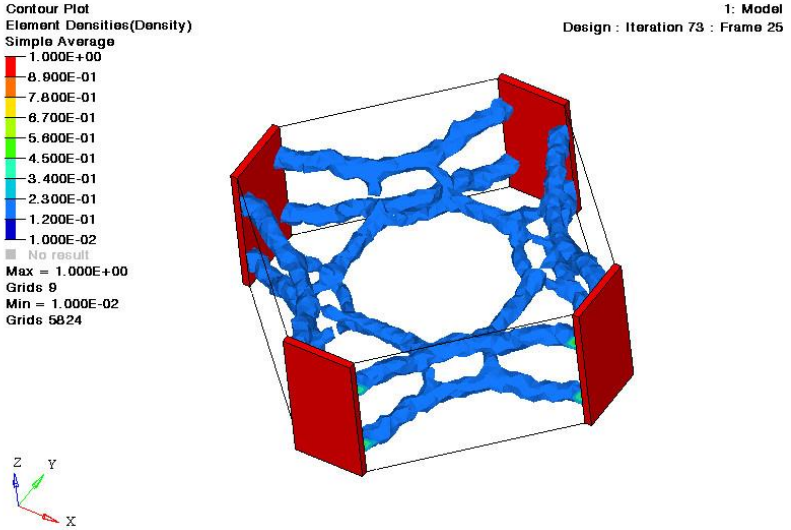

Figure 5-25 Load analysis of the optimized result (displacement and stresses)

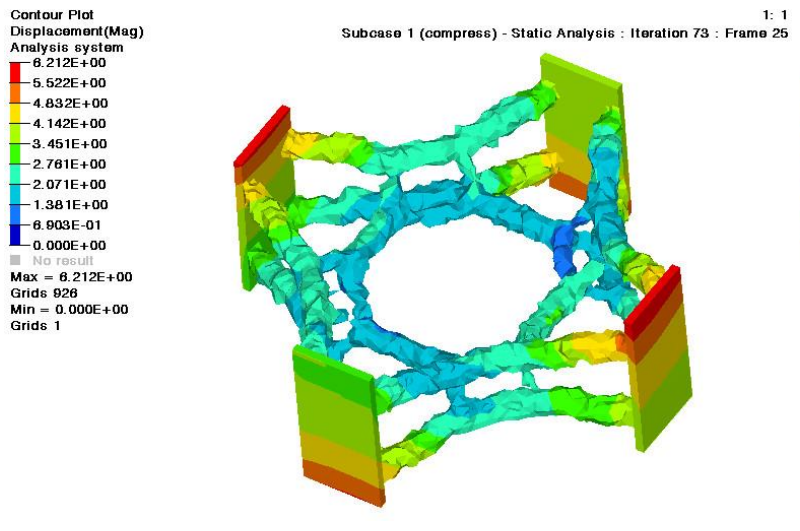

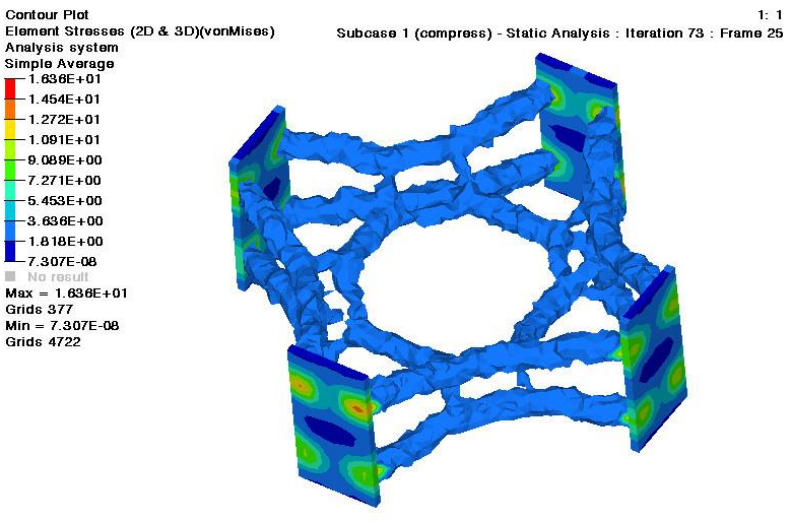

Afterwards, the optimized standard node design is directly interpreted as a parametric model which can be applied to any node situation. The parametric modeling process of the standard nodes stated by interpreting the optimized result into a series of connected lines which is then given a certain thickness roughly follows the scale of the optimized result from OptiStruct. The important tool in this modeling process is Kanggaro with ExoWireframe plug-ins which convert wireframe into skeletal mesh structure.

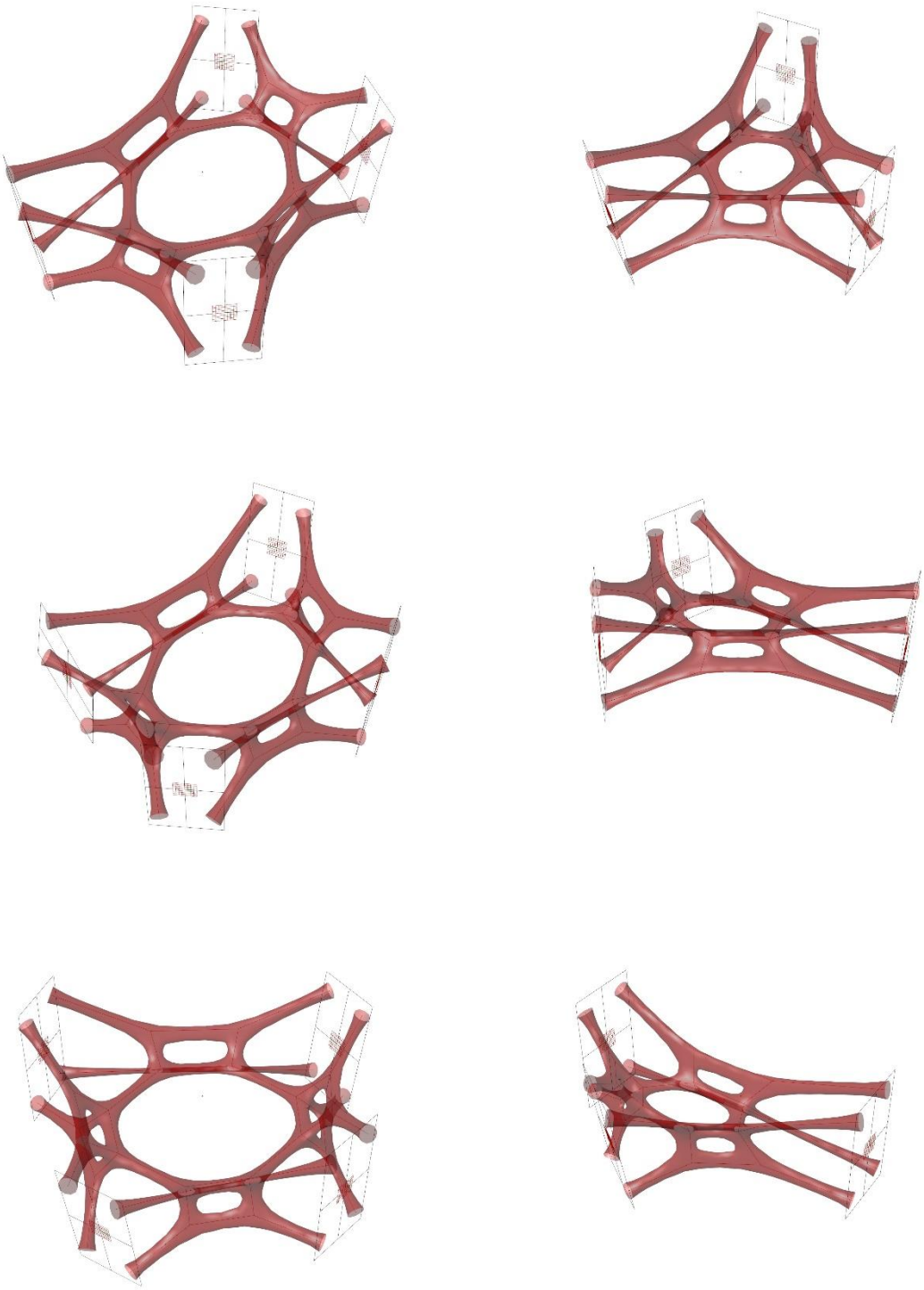

Figure 5-27 Parametric interpretation design of the standard optimized node on different node conditions

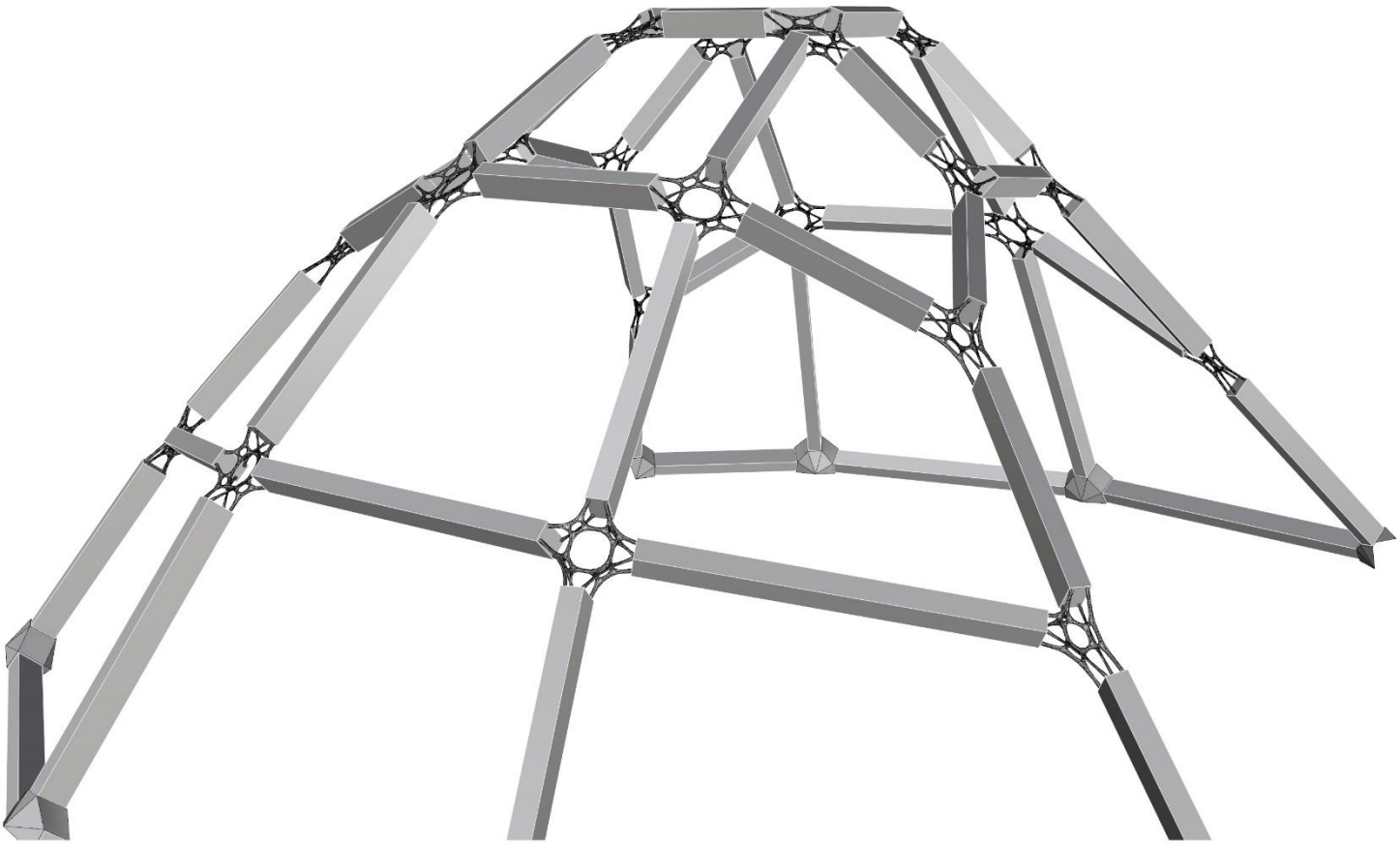

Figure 5-28 The standard optimized node applied on the prototype structure design

The parametric model of the standard node was made to fit on both four and three beams connection. The model is then applied to the main prototype model according to its nodes conditions. The standard node is not applied to the bottom base connection because it requires special design treatment on how the structure connect to the base tension ring.

3. Special optimization design

The special optimization calculate the topology optimization of the specific structural case that take place on the case study. The optimization runs on the whole elements of the structure and calculates every nodes as different optimization design space in one single solid model. This method provides direct feedback to the result of the topology optimization into the boundary conditions and element properties of the structural model. The main drawback of this method is that it requires a significant amount of computing power and time.

Even though every nodes are fabricated using the same material, each node has its own specific 3D printing build orientation. The build orientation determines the orthotropic material properties of each nodes. Therefore each node has a local axis which determines the orthotropic orientation which is important for the topology optimization calculation.

To simplify the calculation model, the bolted connection details are omitted from the calculation model. Instead, the nodes are connected with fix bonded connection to the beams. On the other hand, to simulate the real practical situation of the support condition of the prototype structure, the tension ring base are modeled with only one degree of freedom (3rd DOF) and only has one vertex fixed point to analyze the behavior of the base ring under the load.

Figure 5-29 Visualization of 3D printer' bounding box and print orientation of each node

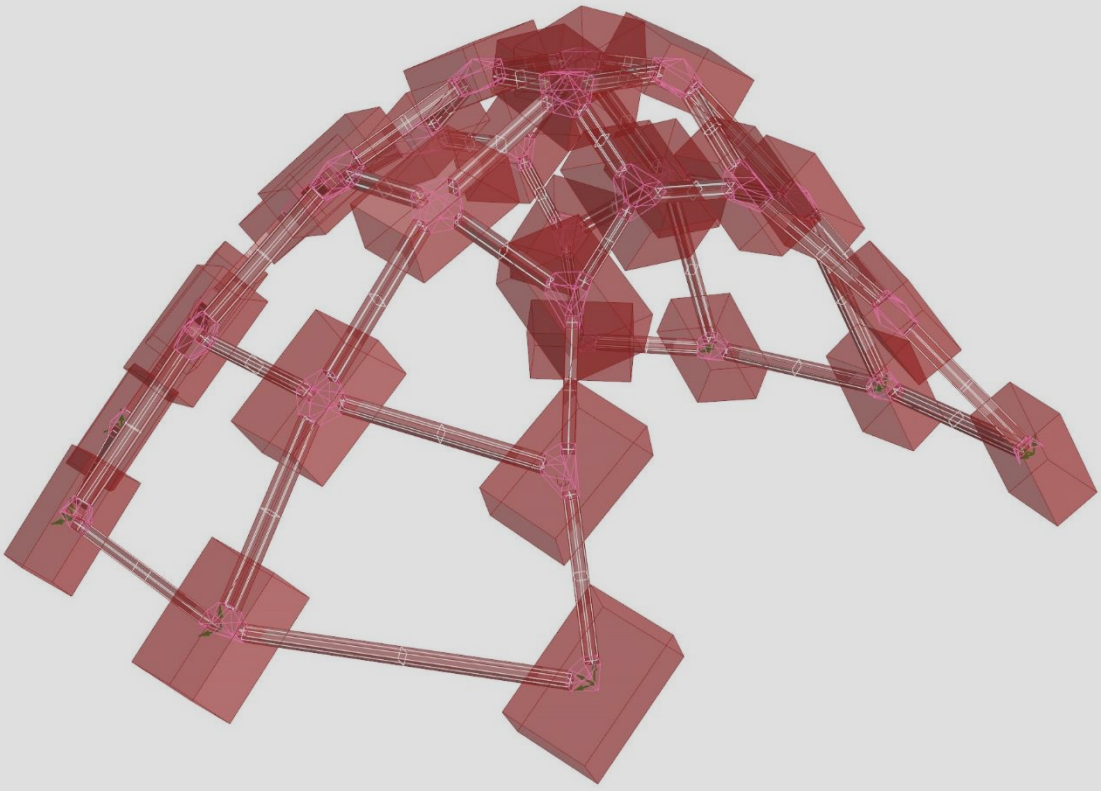

Hyperworks model setup:

- Constraint:

The whole base surface of the ring beam was set with only 1 DOF on Z axis, allowing movement on X and Y axis. However, one vertex point, which can be located in any location of the surface, must have 3 DOF constraints. This will prevent the structure moving away into infinity.

- Node's material properties

The material properties of the nodes are similar to the standard optimization. However, each of the node has its own coordinate axis since it is an orthotropic material.

- Load cases

There are two load cases applied to the structure. They are a force of a person weighted 100 kg standing on top of the structure. Each load cases represents different position of the person's feet while standing. The forces were modeled as a single point load force which applied to RBE (Rigid Body Element) connected to the beams.

- Optimization parameters

The parameters used are similar to the standard optimization design. The difference is only in this case the objective is weighted compliance. The compliance for 2 load cases are weighted equally.

Figure 5-31 Constraint model on base surface

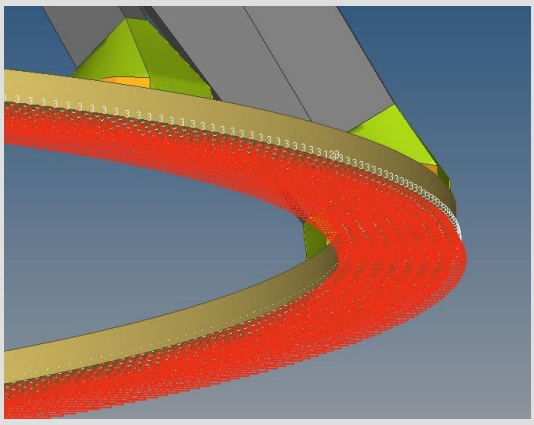

Figure 5-30 Each node has its own material orientation axis

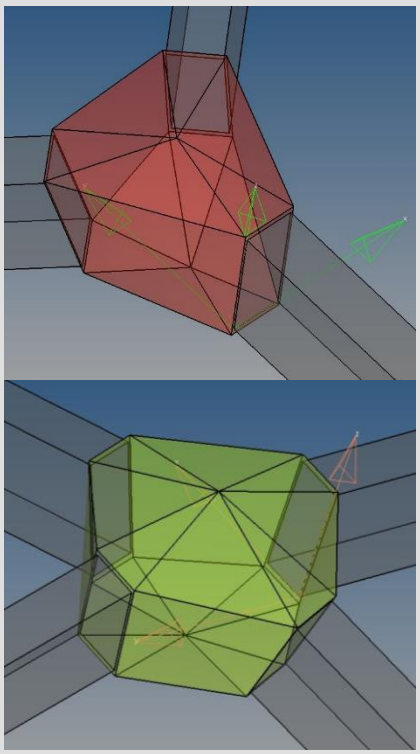

Figure 5-32 Two load cases of different standing position

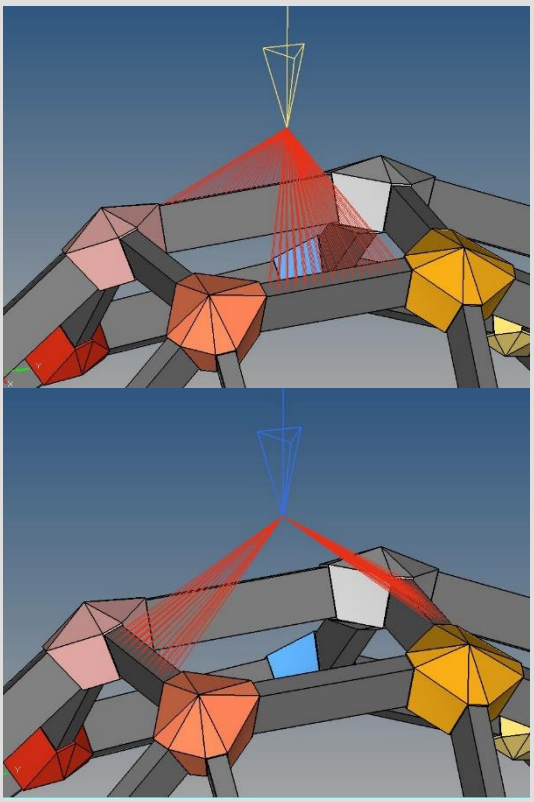

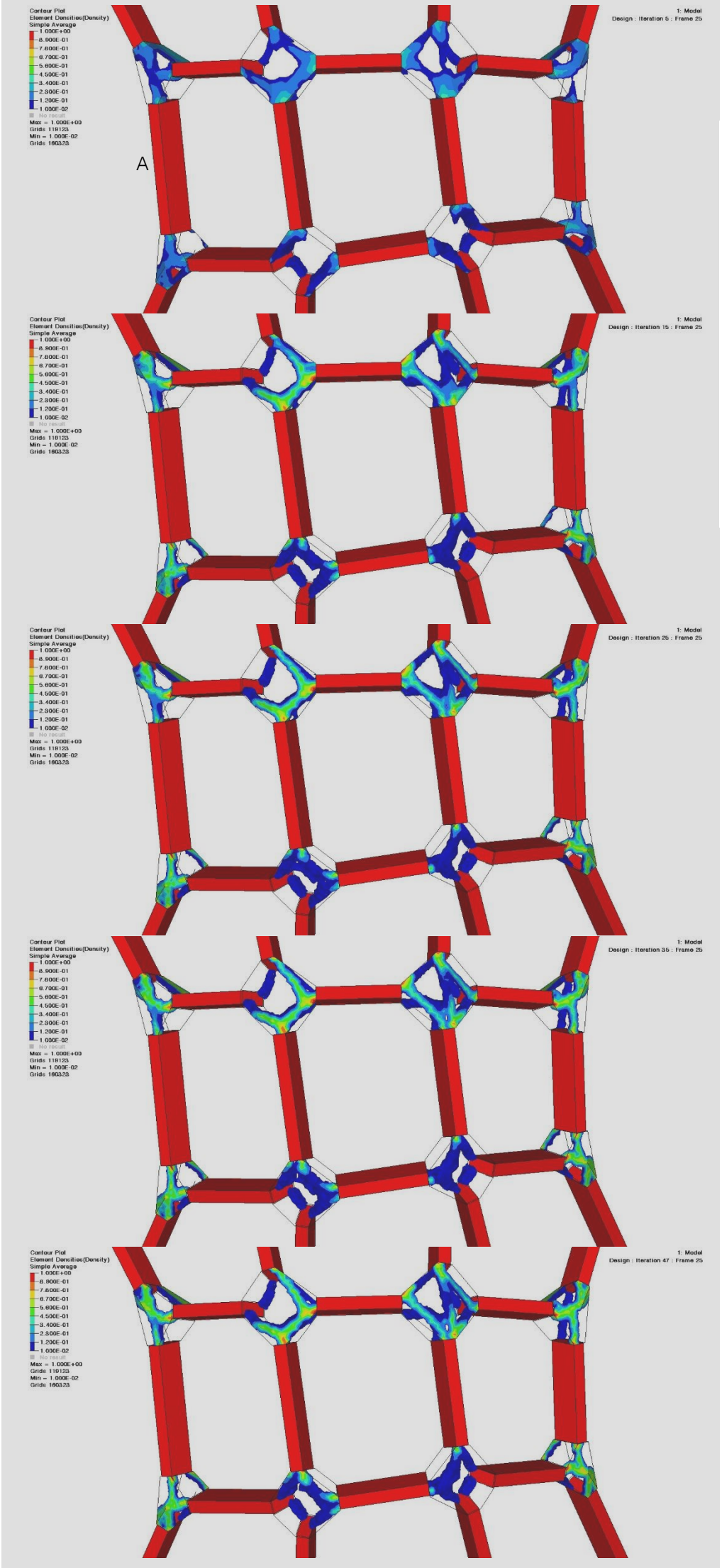

Figure 5-33 The optimization process runs for 47 iteration. These are the generated shape on iteration 5, 15, 25, 35, and 47.

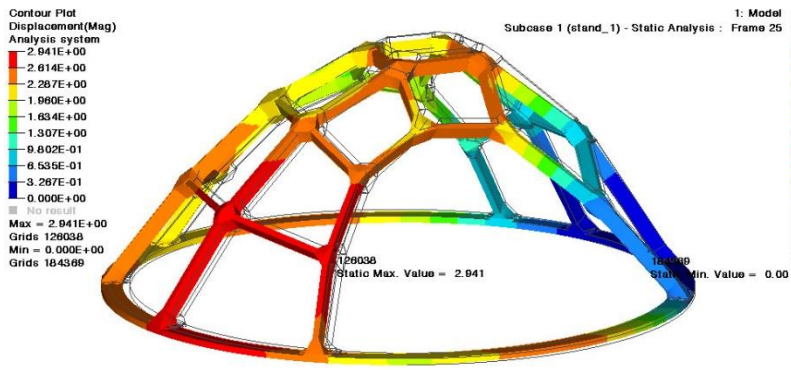

Figure 5-34 Loadcase 1 max displacement 2.9 mm

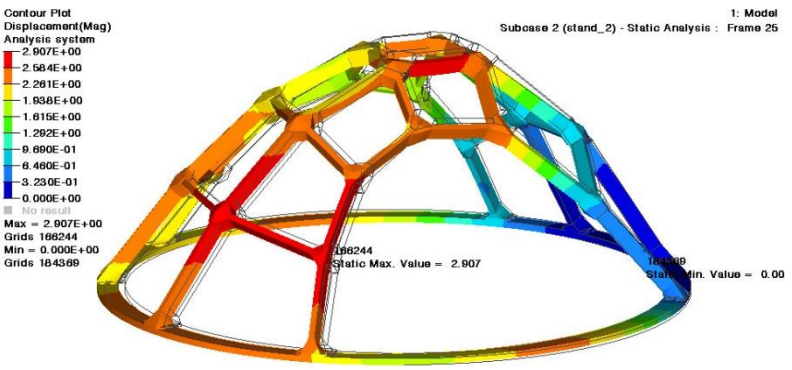

Figure 5-35 Loadcase 2 max displacement 2.9 mm

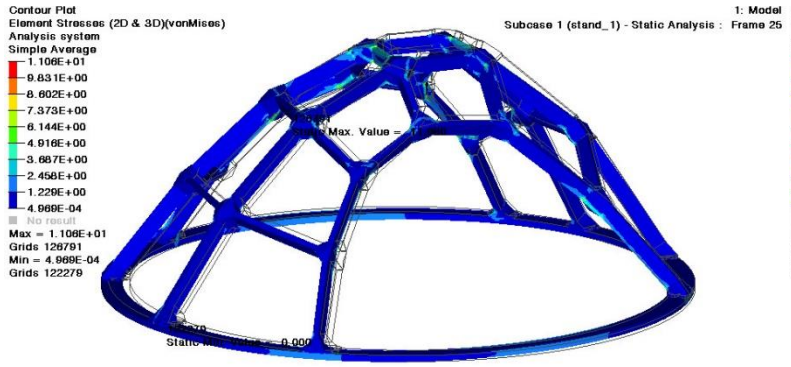

Figure 5-37 Loadcase 1 max von mises stress 11 N/mm2

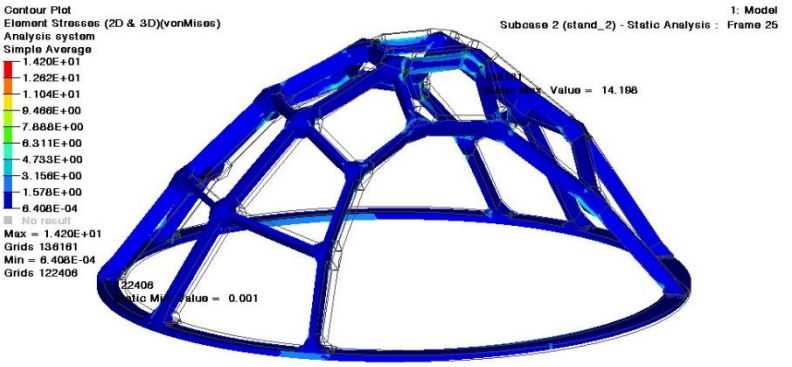

Figure 5-36 Loadcase 2 max von mises stress 14 N/mm2

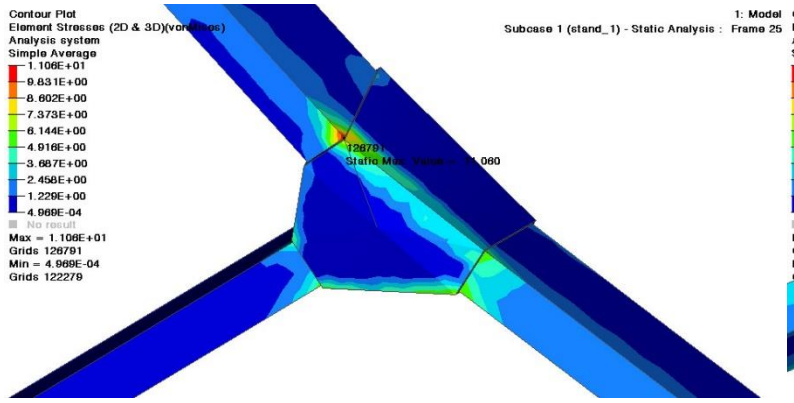

Figure 5-39 Max stress location on loadcase 1

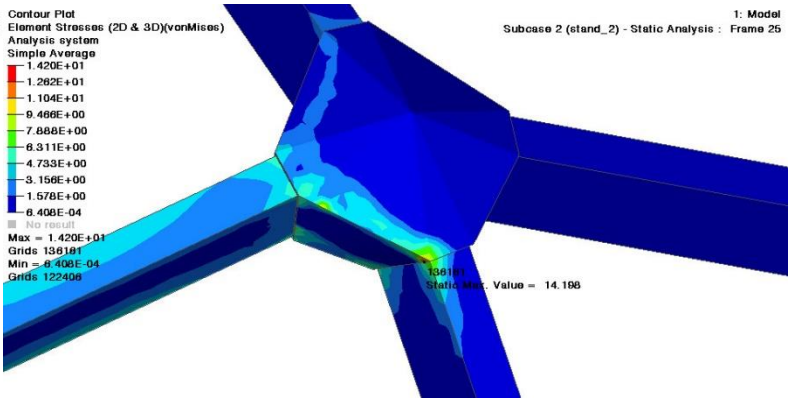

Figure 5-38 Max stress location on loadcase 2

4. Final optimized design

The finalized design of the nodes are a combination of the geometry from both optimization process. The mesh model was exported from the Optistruct workspace with Hyperworks mesh features called OSSmooth. The tool convert the 3d mesh finite element model into a solid mesh geometry in STL format. The settings for OSSmooth export was:

Isosurface threshold	: 0.1
Laplacian smoothing iteration	: 10
Feature angle	: 30

The mesh models were combined in a mesh modelling software from Autodesk called Meshmixer (http://meshmixer.com/). Meshmixer is a powerful free-software for mesh editing especially for 3D printing works. The software is used from this point on for post processing before the slicing process in Simplify3D.

5. Post processing

The post processing mainly consist of combining the models of special optimized design, standard optimized design, and the connection detail. Moreover, it consists a surface smoothing to achieve a more acceptable look of the node. If necessary, manual sculpting of the mesh geometry is executed to remove sharp edges on the node, flatten out local bumps, and thickening shapes which are too thin for printing.

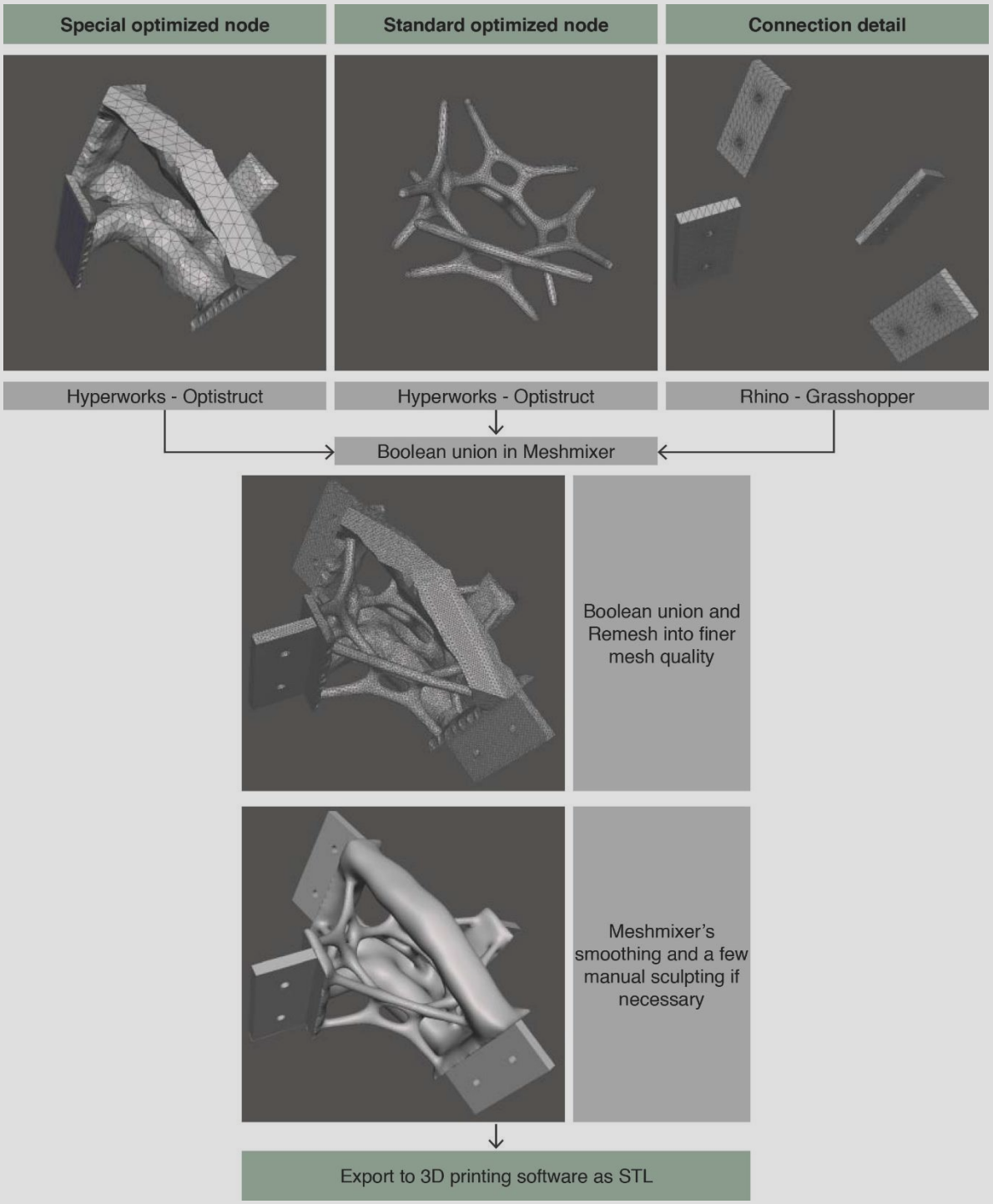

Figure 5-40 The general figure of the post-processing of each node design

5.5 Construction

1. Non-AM parts

The wooden beam is a standard building construction solid wood with 44 x 18 mm profile (vurenhout). However, the wooden profiles are roughly have a dimension tolerance as much as 2 mm. The first step is to cut the wood into the specific accurate length based on the parametric model. The woods were cut with handsaw machine, the highest effort was tried to cut the wood as accurate as possible. In the end, the length of the beams are roughly still have at least 1 mm discrepancy for a few beams after a final measurement.

The second step is to make the connection of the wooden beam to the optimized nodes. First, 2 holes needed to be drilled at each ends of the beams. The bolt used was standard M5 bolt with 20 mm length. Other options which were considered was to use a more sophisticated chamfered bolt and fitted metal pin connection.

The next step is to provide the space for the extruded part of the nodes to allow the connections. The dimension of the extrusion is 20 mm deep with 4 mm wide. A special tool was made to simplify the cutting process of the wood. It is basically a clamp that holds the beams in place on the table saw so it will always cut the end parts of the beam accurately according to the dimension required.

The ring base structure is more complicated to build than the wooden beams. The ring has a thickness of 18 mm, outer radius of 840 mm and inner radius of 760 mm. It was constructed from 8 pieces of quarter-circles of 9 mm plywood which are sandwiched together to form a complete circle. The quarter-circle was cut from a 1220x610 mm plywood board. The cutting process was done using a router which was attached to a guide with a fixed radius. The wooden ring base is expected to have a lot of stress while holding the weight, therefore the 8 quarter-circles was attached together not only with wooden glue but also with many screws that holds the wood together forming a complete ring structure.

Figure 5-41 The wood profiles is cut according to the length of the beams

Figure 5-42 Two drilled holes for the bolt connection

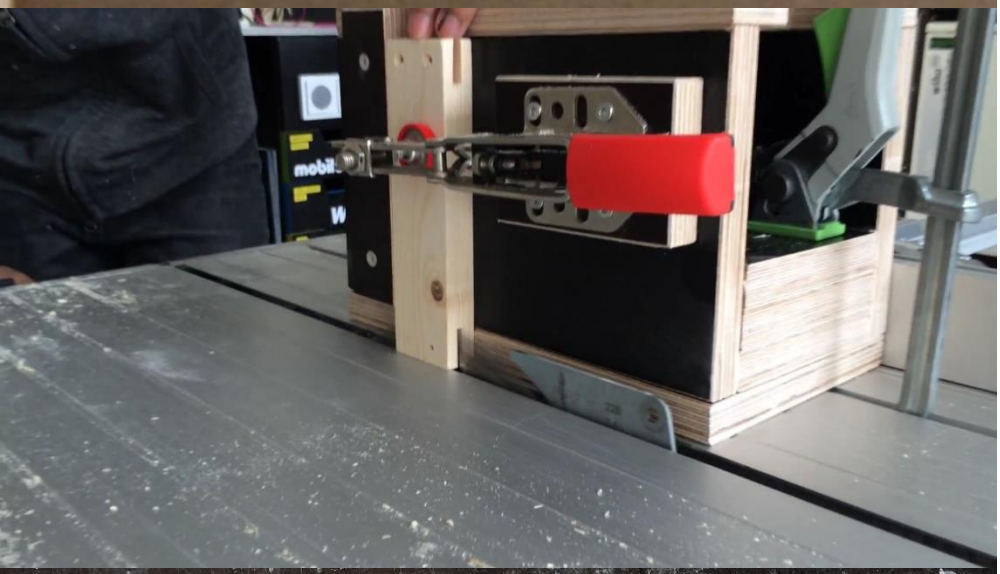

Figure 5-43 Cutting out the space for connection with table saw

Figure 5-44 In total there are 39 wooden beams with different length

Figure 5-45 A router is fixed to a specific radius to cut the plywood

Figure 5-47 Each plywood creates 3 of quarter-rings

Figure 5-46 The final ring beams showing the first impression of the structure's scale

2. AM nodes

The node models were sliced using Simplify3D, a special 3d printing software. Below is the setting used for the 3D printing process with the software for the Leeuwenhoek 3d printer:

Nozzle diameter	: 0.8 mm (stainless steel nozzle)
Temperature	: 250 degree Celsius
Printing speed	: 30 mm/s
Layer height	: 0.3 mm
Perimeter shells	: 3
Infill	: 60%
Extrusion multiplier	: 0.8
Extrusion width	: 0.96
Retraction distance	: 4 mm
Retraction speed	: 40 mm/s

The printing time of each nodes varies depends on the geometry of the nodes. The fastest print is approximately 4 hours while the longest print time of some nodes were up to 8 hours.

There are many problems encountered during the printing process. One of the biggest problem is the first layer issue. The Leeuwenhoek 3D printer is not equipped with a heated bed, therefore many alternatives were used to improve the first layer adhesion to the printer bed such as using glue stick, masking tape, and hair-spray. Overall the most effective way is to use glue stick with careful manual inspection at the few first layer of the prints. Most of the nodes printed encountered problems which resulted to failed prints on the few first layer, therefore it is very recommended to carefully inspect the printing process in the first one to two hours of the prints.

Figure 5-48 Preview of the sliced model in Simplify3D

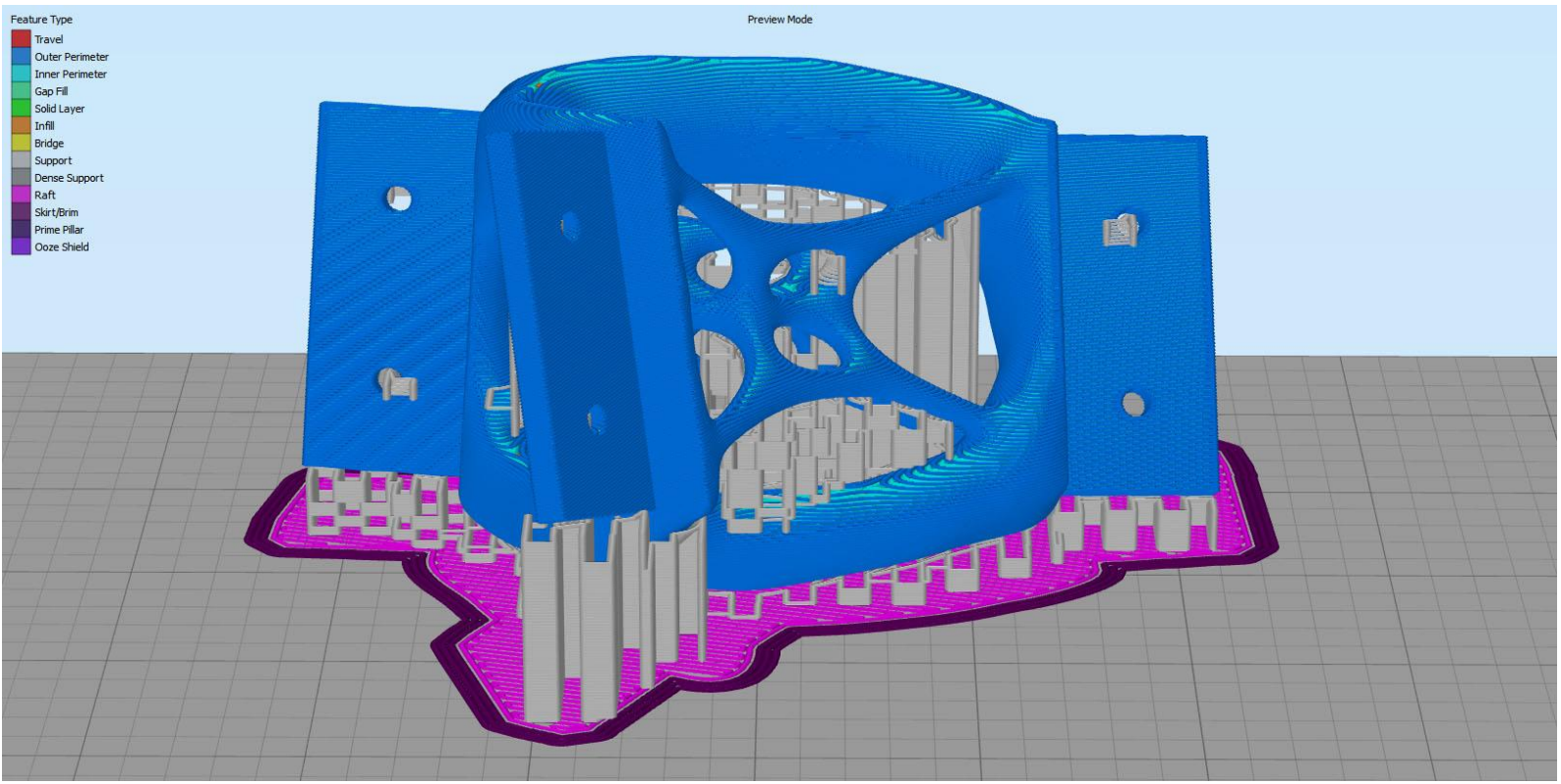

Figure 5-49 3D printing process of the carbon fibre infused filament

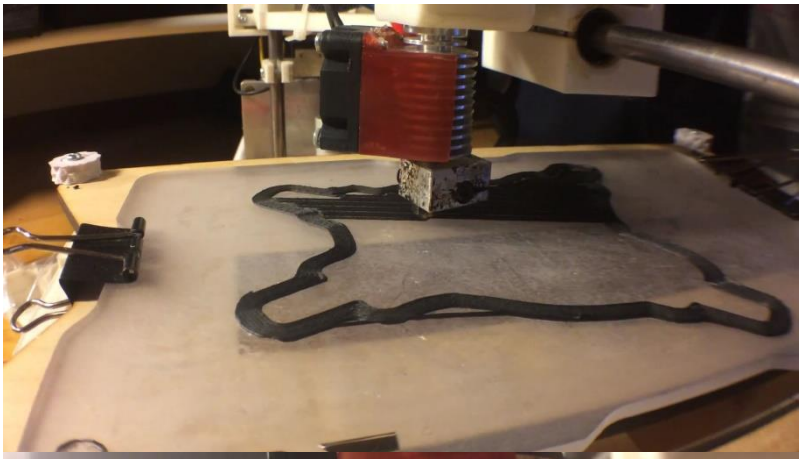

Figure 5-53 A manual clean-up of the nozzle is often necessary

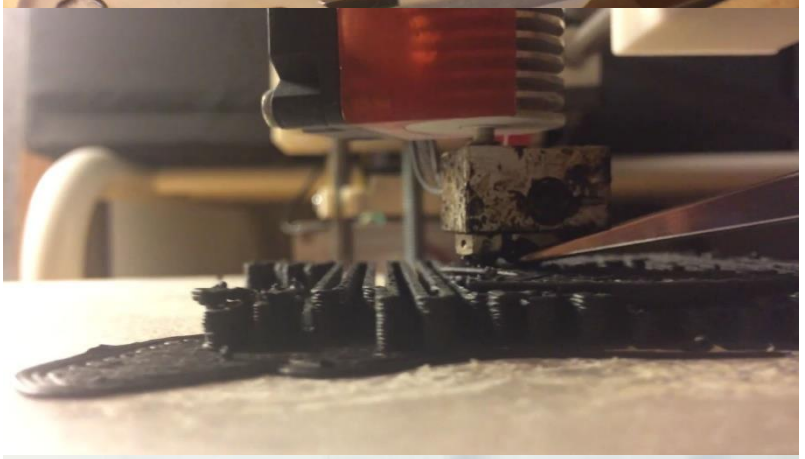

Figure 5-52 Some of the finished prints

Figure 5-51 Removal of the scaffolding structure

Figure 5-50 Final polishing with sand paper

5.6 Final built result and testing

The prototype was built in a time span of roughly one month. The structure in the end is able to take a person on top of it with 65 kg of weight. Although, displacement is quite large and it was close to fail. The biggest problem were the bolted connection details. Lack of precision and inaccuracy of the AM node and woodworking cause incorrect alignment which brings high local stress on the connection.

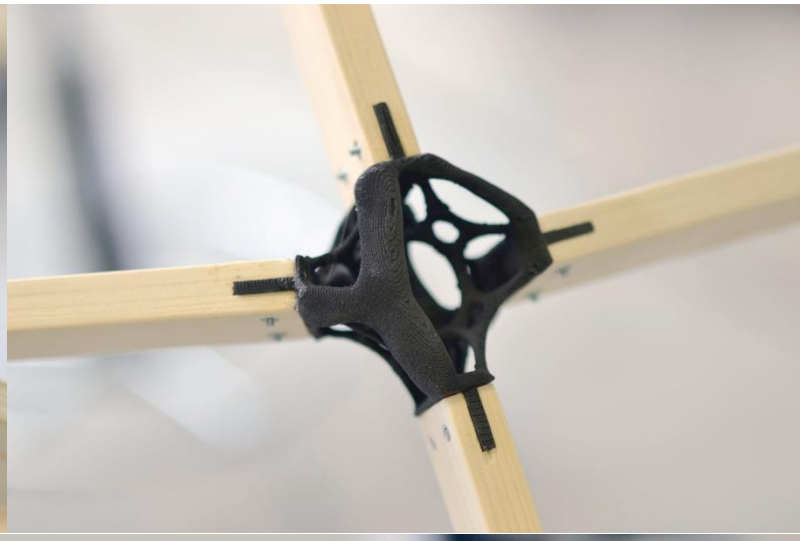



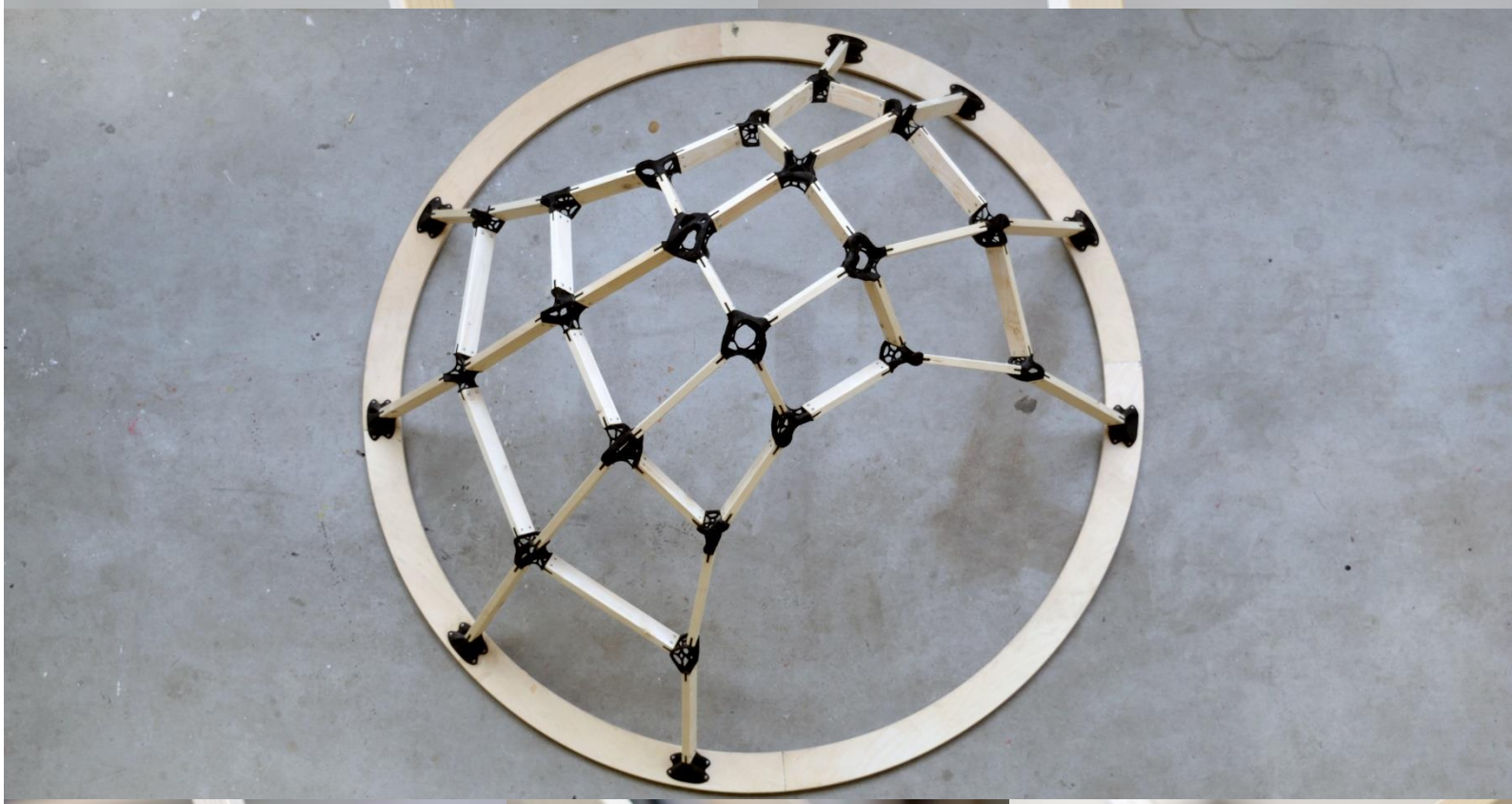




5.7 References

Autodesk. (n.d.). Meshmixer is state-of-the-art software for working with triangle meshes. Retrieved June 20, 2016, from http://meshmixer.com/

Bislip, A. (n.d.). Home of the RepRap Leeuwenhoek project - an open-source, compact, all-in-one 3D printer. Retrieved June 20, 2016, from http://dymensional.nl/

ColorFabb XT-CF20. (n.d.). Retrieved June 20, 2016, from http://colorfabb.com/xt-cf20

Galjaard, S., Hofman, S., & Ren, S. (2014). New Opportunities to Optimize Structural Designs in Metal by Using Additive Manufacturing. *Advances in Architectural Geometry 2014,* 79-93. doi:10.1007/978-3-319-11418-7_6

Letcher, T., & Waytashek, M. (2014). Material Property Testing of 3D-Printed Specimen in PLA on an Entry-Level 3D Printer. *Volume 2A: Advanced Manufacturing*. doi:10.1115/imece2014-39379

Print Quality Troubleshooting Guide | Simplify3D. (n.d.). Retrieved June 20, 2016, from https://www.simplify3d.com/support/print-quality-troubleshooting/

Prohasky, D., Williams, N., Crolla, K., & Burry, J. (2015). SmartNodes: 'Light-weight' parametric structural design process with BESO. *Proceedings of the International Association for Shell and Spatial Structures (IASS)*.

RepRap wiki. (n.d.). Retrieved June 20, 2016, from http://reprap.org/

Tymrak, B., Kreiger, M., & Pearce, J. (2014). Mechanical properties of components fabricated with open-source 3-D printers under realistic environmental conditions. *Materials & Design, 58*, 242-246. doi:10.1016/j.matdes.2014.02.038

DESIGN RESEARCH: CASE STUDY

6

DESIGN RESEARCH – CASE STUDY

6.1 Case study: Baku Airport canopy

The design methodology based on the design research in this project is applied to the real architecture project case study to further develop the potential of topology optimization with additive manufacturing on freeform envelope design as part of the research objective and to answer the research question. The case study chosen is one of ARUP's projects, an outdoor canopy located at Baku international airport in Azerbaijan. The canopy was built to cover the front end of an airplane covering the passenger going in and out of the airplane. The roof canopy has a surface area of 417 square meters with the tallest soffit height of 9.18 meters and length of 29.5 meters.

Figure 6-1 The freeform canopy at Baku international airport in construction process

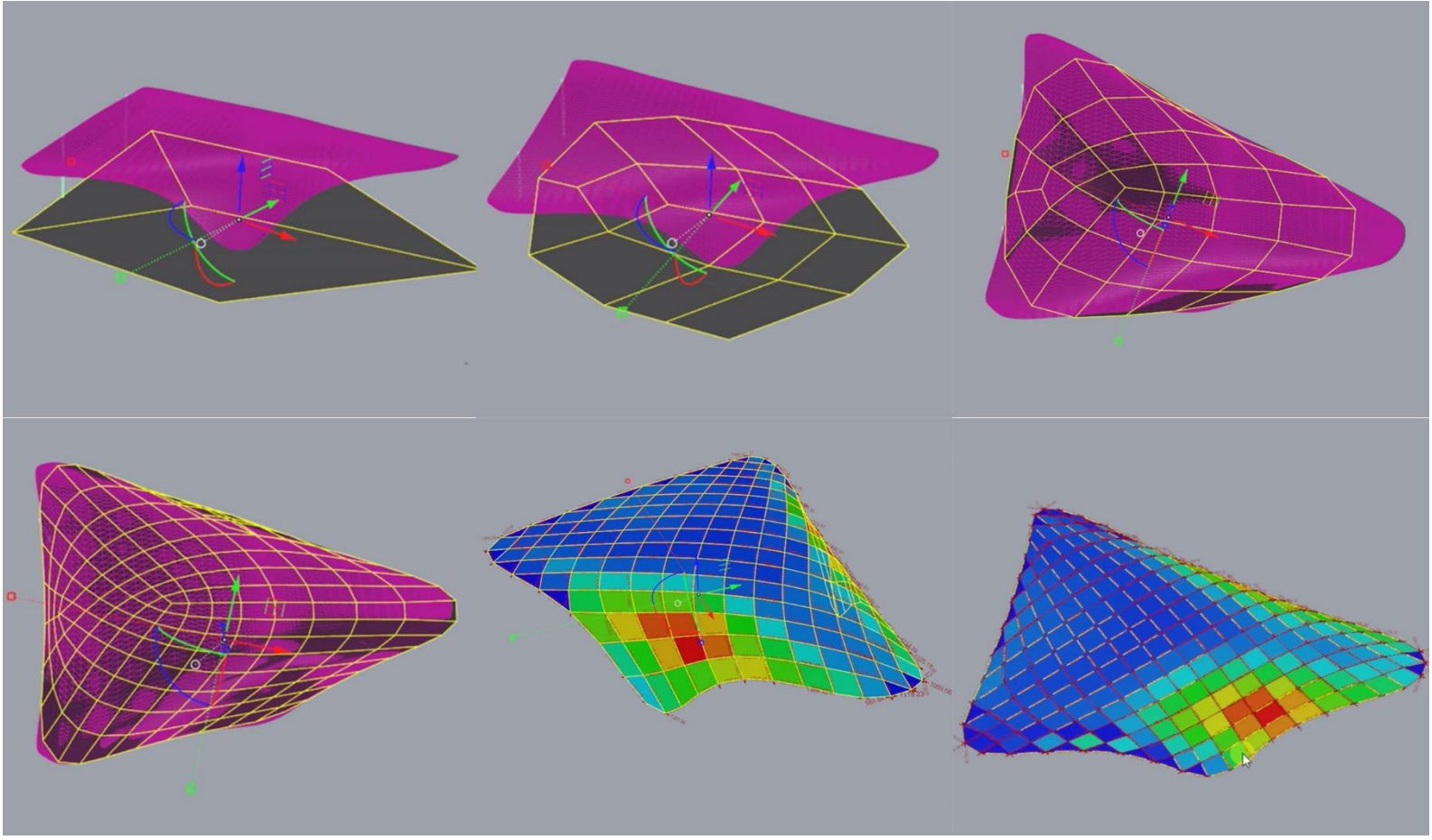

Figure 6-2 Iteration steps of aplplying the desired mesh topology onto the reference surface (Purple coloured))

6.2 Free-form rationalization with planar quadrilateral facets

The design strategy of rethinking the design method of freeform surface by utilizing quad panels instead of triangular panels. It is not possible to apply quad panel on any given freeform surface, therefore parametric adjustment was needed to be applied to modify the given surface while keeping a certain limit of deviation of the panel's planarity. The process was made easier with a high performance tool called Evolute Tools Lite (http://www.evolute.at/). The tool works by performing a number of different algorithms to a target mesh geometry with the desired topology, in this case a quad tessellation. The algorithm adjust the target mesh iteratively to get as close as possible to the reference geometry, in this case the original design surface by ARUP.

Although the process relies heavily on the algorithm, it is not necessarily a hands off parametric process. Along the geometry adjustment iteration, some manual alterations were very much necessary to achieve the best possible tessellation layout design. For example, manual alterations were needed to add or remove specific panels, rows of grid, and also adjusting the edge panels into triangular panels.

The final geometry made with Evolute's algorithm has a higher surface area and a more evenly distributed curvature along the whole surface. The maximum deviation of the quad panel is 49 mm as shown on the following figure with the red color. The panels with the higher deviation are located on the top of the surface. This condition is more architecturally acceptable since it is less visible from human eye level.

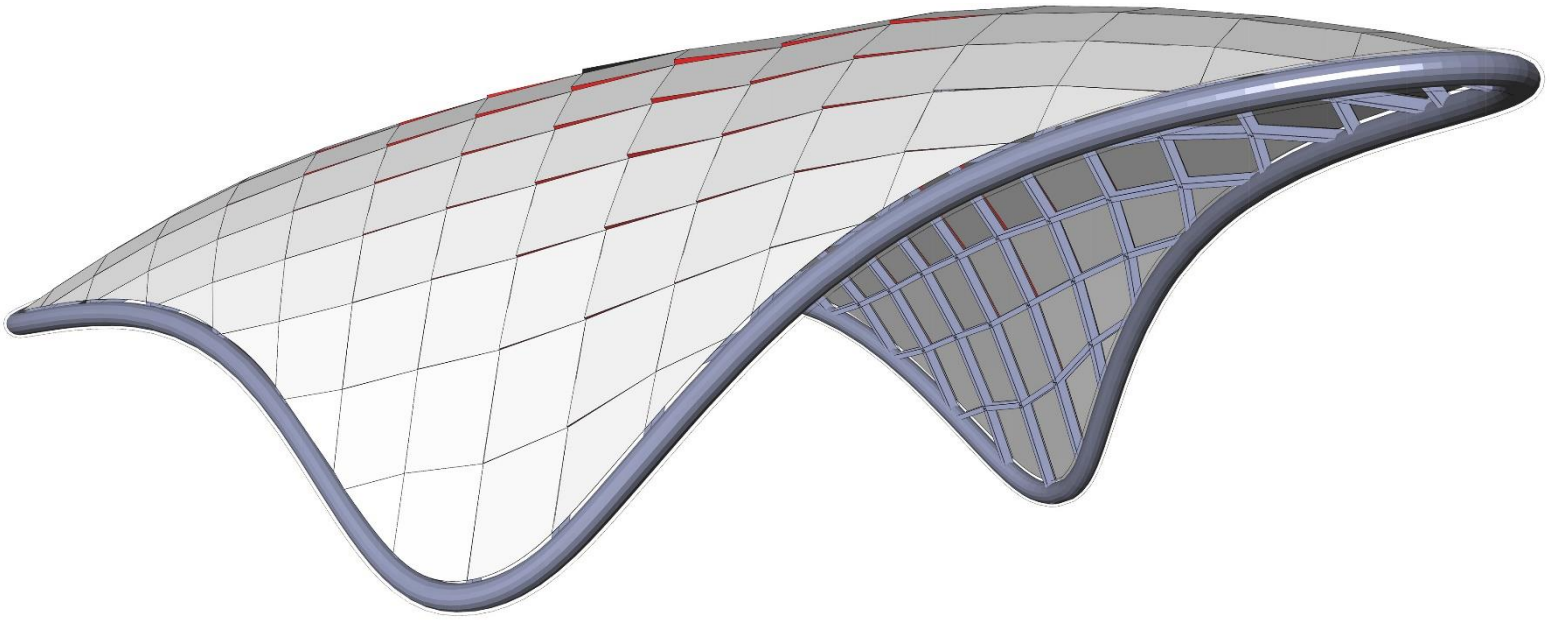

Figure 6-3 Drawings of the final redesign of the canopy with quad panelling

Figures on the next page show the comparison of the original design of the canopy (blue color) with the adjusted quad panel geometry (red color). One of the important feature is that the panels along the edges are triangular because the deviation was too large if they were forced to have quad panels.

Figure 6-4 Final quad panelling geometry with curvature analysis of each panels

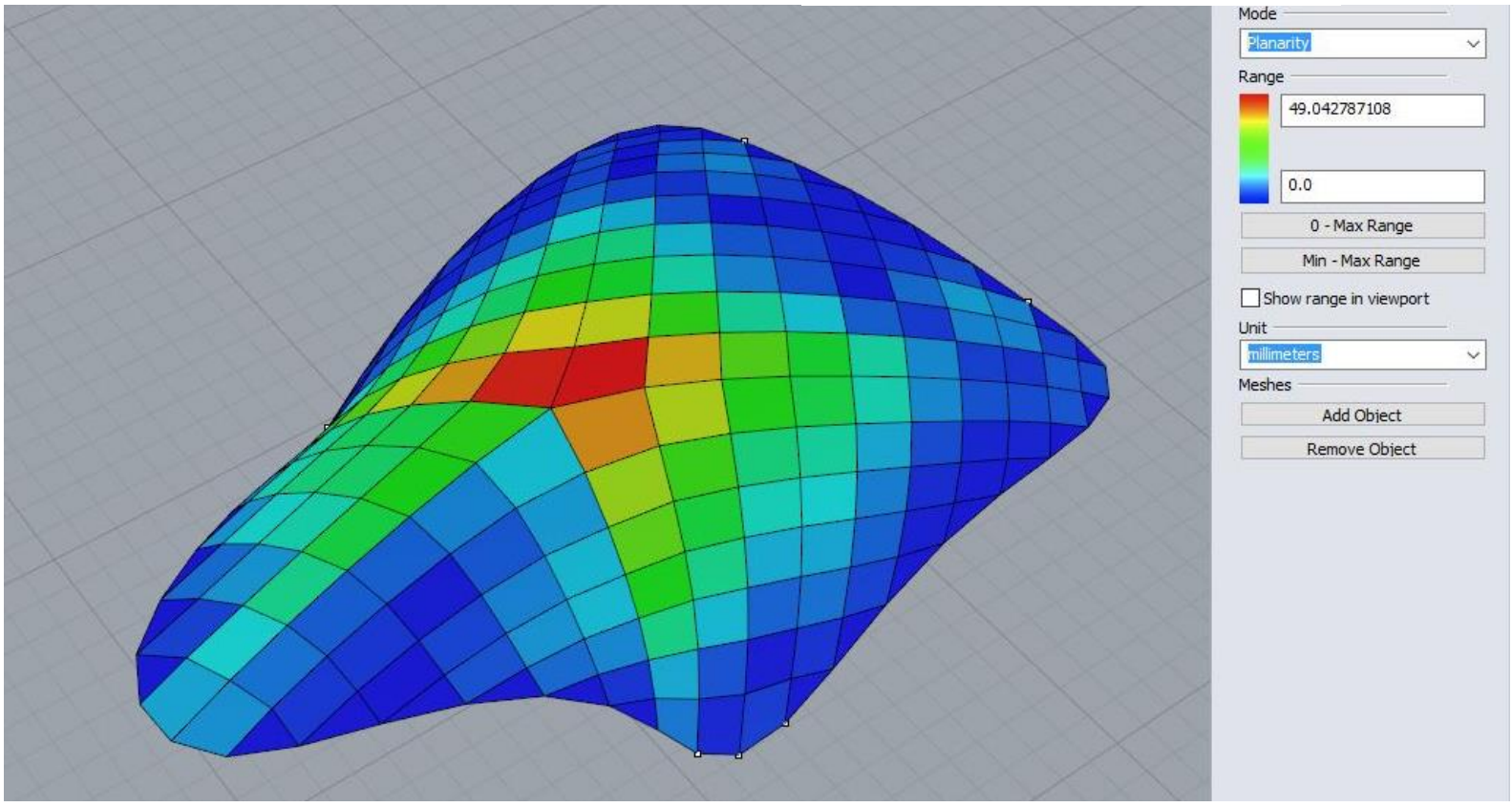

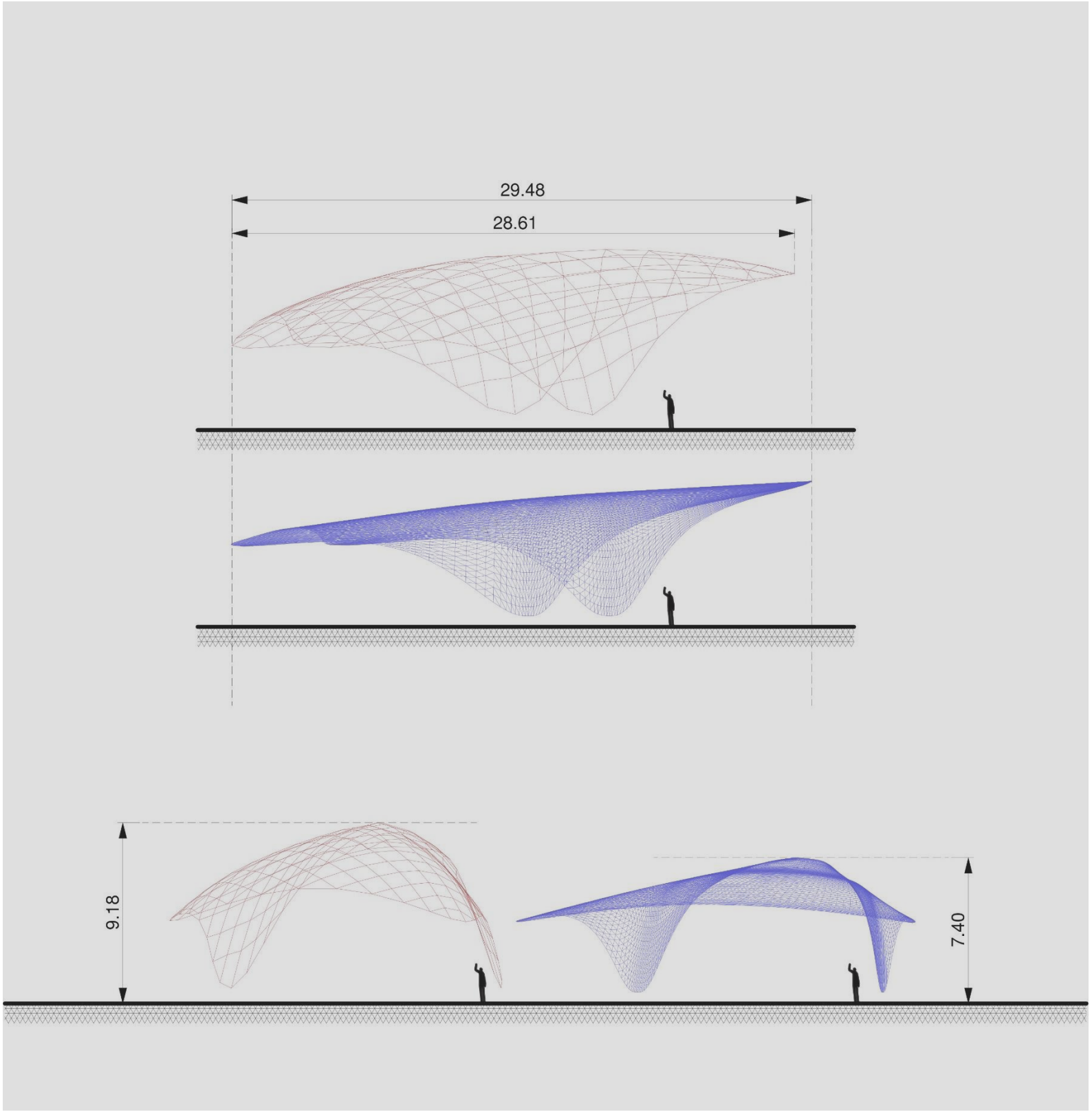

Figure 6-5 Comparison of original design intent with the final quad panel geometry

6.3 Structural design

The structural design development of the canopy is carried out with a simple conceptual structural analysis. Several assumption had to be taken into account since the lack of data available of the project.

There are five load cases which are taken into account to analyze the structural performance of the canopy with the quad paneling design in general and also for topology optimization of the node. The following load cases will be calculated:

LC1 : Dead load + Live load

LC2 : Dead load + Live load + Snow load

LC3 : Dead load + Live load + Wind load (uplift)

LC4 : Dead load + Live load + Lateral load (X)

LC5 : Dead load + Live load + Lateral load (-X)

Lateral load in this case was considered because the structure is located in the seismic zone. However, the calculation was carried in a very conceptual manner, enough to see the general behavior of the structure under that specific load.

On the following page, conceptual structural analysis of the 6 different loadcase are presented as utilization diagram on the left (red color showing compression forces and blue representing tension forces), while on the right are the displacement diagrams.

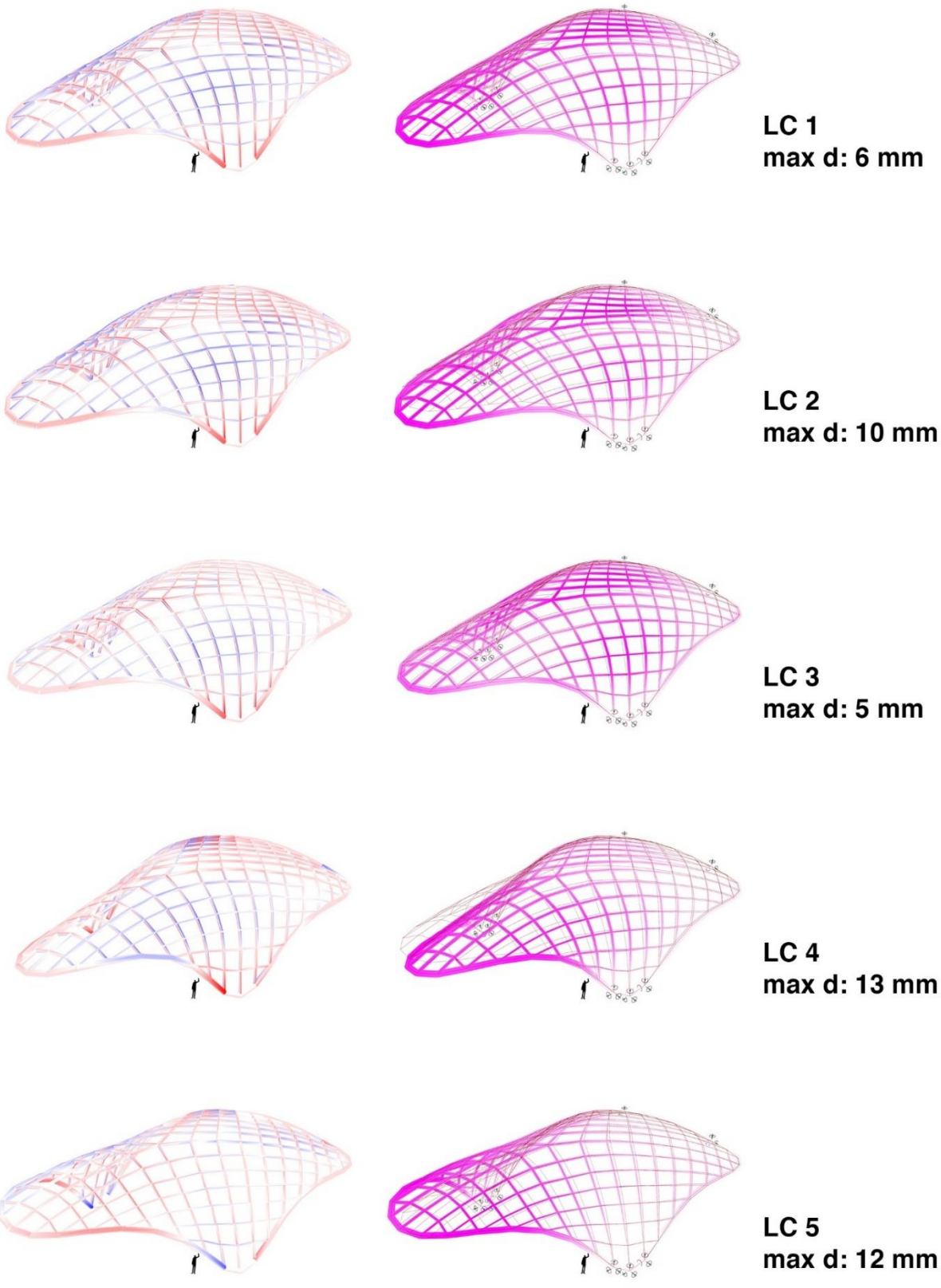

Figure 6-6 Conceptual structural analysis in Karamba for beam's utilization (left) and displacement (right)

The dimension of the beams were determined by parametric analysis with Grasshopper plugin Karamba, mainly by considering the displacement and principal stresses. In the end, it was decided to have a similar RHS beam member size throughout the structure and a large continuous CHS as ring beam similar to the original design of the built project. Dimension of the beam members:

RHS 200x100x8

CHS 400x10

The structure is supported by two footings on the side where the geometry is bent down, and also a V-shaped column supported at the back-side of the structure which functions as tension structure counter balancing the weight on the cantilever part of the structure at the front-side.

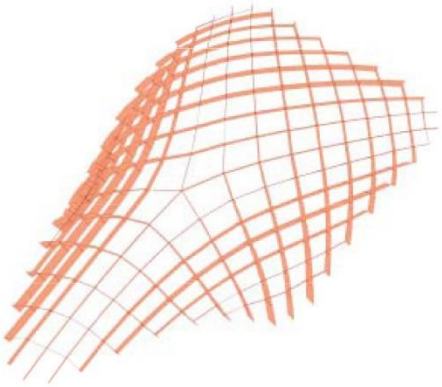

Nx: Normal (axial) forces on beam's local X-axis

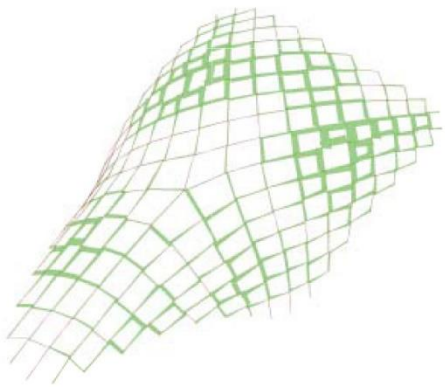

Vy: Shear forces on beam's local Y-direction (in plane shear)

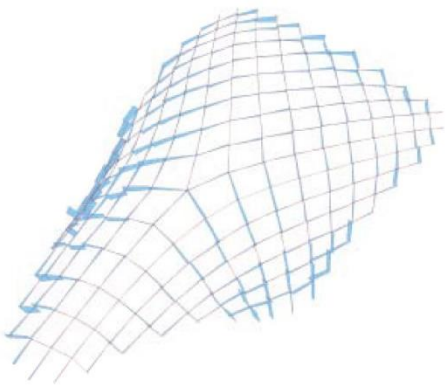

Vz: Shear forces on beam's local Z-direction (out of plane shear)

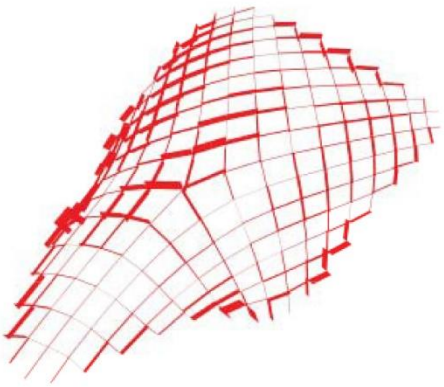

Mx: Torsional moment on beam's local X-axis

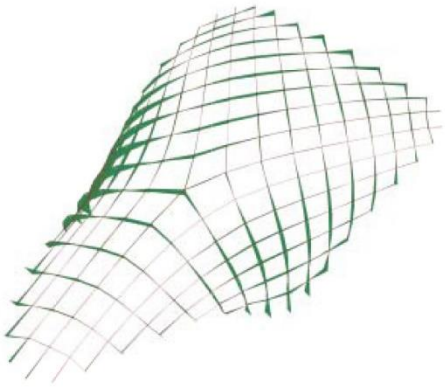

My: Bending moment on beam's local Y-axis (out of plane bending)

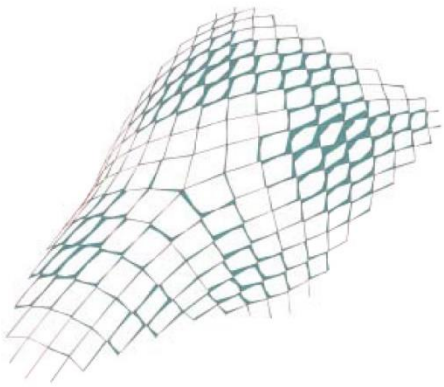

Mz: Bending moment on beam's local Z-axis (in plane bending)

6.4 Optimized node design

1. Hyperworks model

The case study is a project that has an entirely different scale and level of detail compared to the prototype structure on the previous chapter. Even though the general design method of utilizing topology optimization and additive manufacturing are generally similar, there are many significant differences in terms of technical process of the design workflow.

In this project, it was not possible to perform the global calculation method shown in the previous chapter. The amount of computational power available for this research is not sufficient to handle the size of the model. The number of elements, load cases, and level of detail makes a very large FEA model which requires a professional-grade computing power, presumed with distributed processor calculation or cloud computing calculation.

Therefore, the optimization was only performed on one node, by taking the numerical data of different forces which happened in the node from the analysis in Karamba. The Hyperworks model is made as a single independent node, where every single forces were modeled manually.

Figure 6-7 The chosen node for optimization with diagrams of forces on adjacent beams

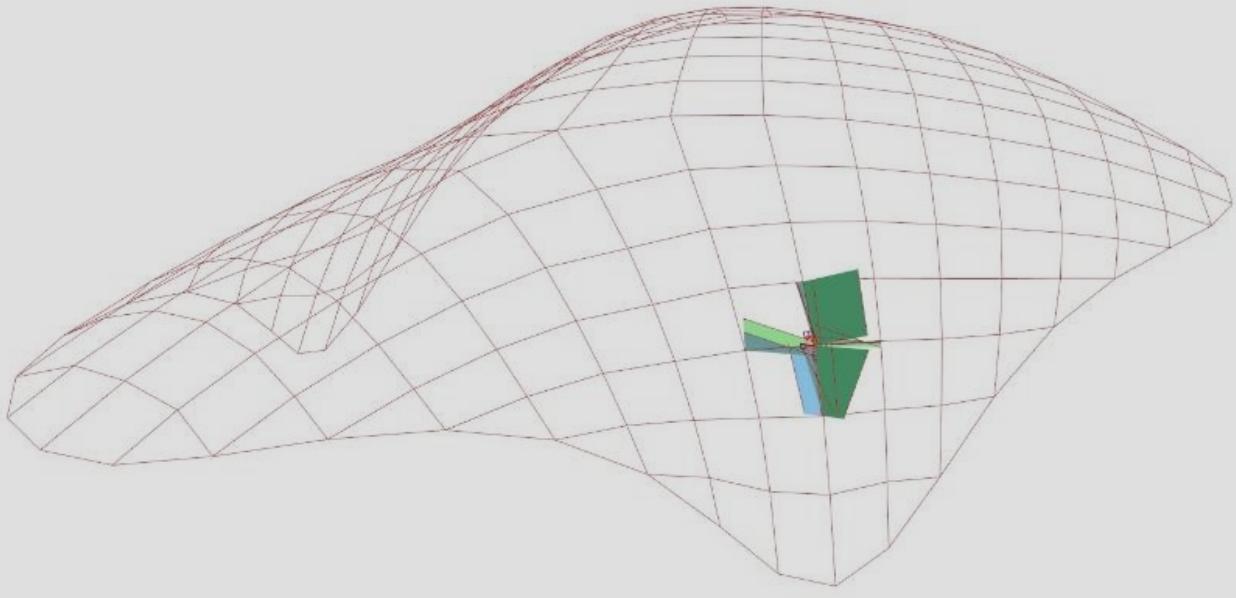

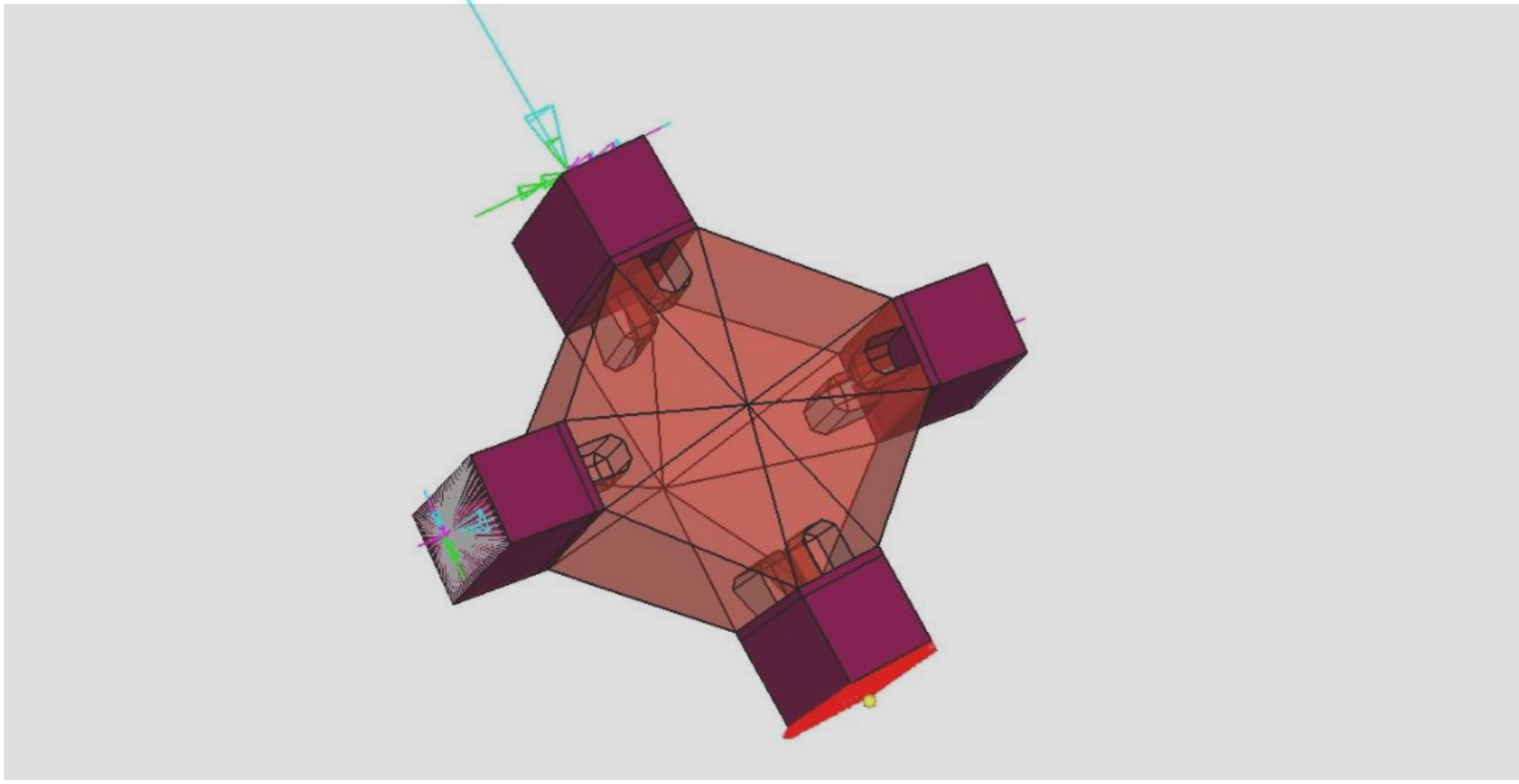

Figure 6-8 Hyperworks model for topology optimization of 5 load cases

The forces are applied on 100 mm section of beams connected to the node. Rigid Body Elements were attached to the beam's end surface where the loads and moments are applied. The forces are not equilibrium, therefore a fixed constraint is applied to the lower beam. Each beam has 3 point loads and 3 moment loads for each load case. In total, there are 90 different forces modeled. In terms of mesh detail, the model has 623,375 FEA mesh elements and 117,719 nodes.

The parameters used in the calculation are listed below:

- Mesh type : tetramesh
- Mesh element size : 5 mm
- Volume fraction constraint : 5%
- Optimization objective : Minimize weighted compliance (maximize stiffness)
- Minimum element dimension : 8 mm
- Discrete control : 1.5
- Maximum iteration : 100
- Density penalization limit : 0.2

The optimization was calculated with weighted compliance objective, with the compliance important as follows:

LC1 : 1.0
LC2 : 0.6
LC3 : 0.8
LC4 : 0.6
LC5 : 0.6

2. Material properties

The material assigned for the node is a direct metal laser sintering material manufactured by EOS called EOS Stainless Steel GP1. The beams are using RHS section grade S355.

Node material properties:

E modulus	: 1.8e5 N/mm2
Poisson ratio	: 0.3
Yield strength	: 530 N/mm2

Beam material properties:

E modulus	: 2.1e5N/mm2
Poisson ratio	: 0.3
Yield strength	: 355 N/mm2

The node's material is modeled as isotropic material since the properties in different print orientation is less significant in DMLS printing method.

Figure 6-9 Mesh model for topology optimization in Optistruct

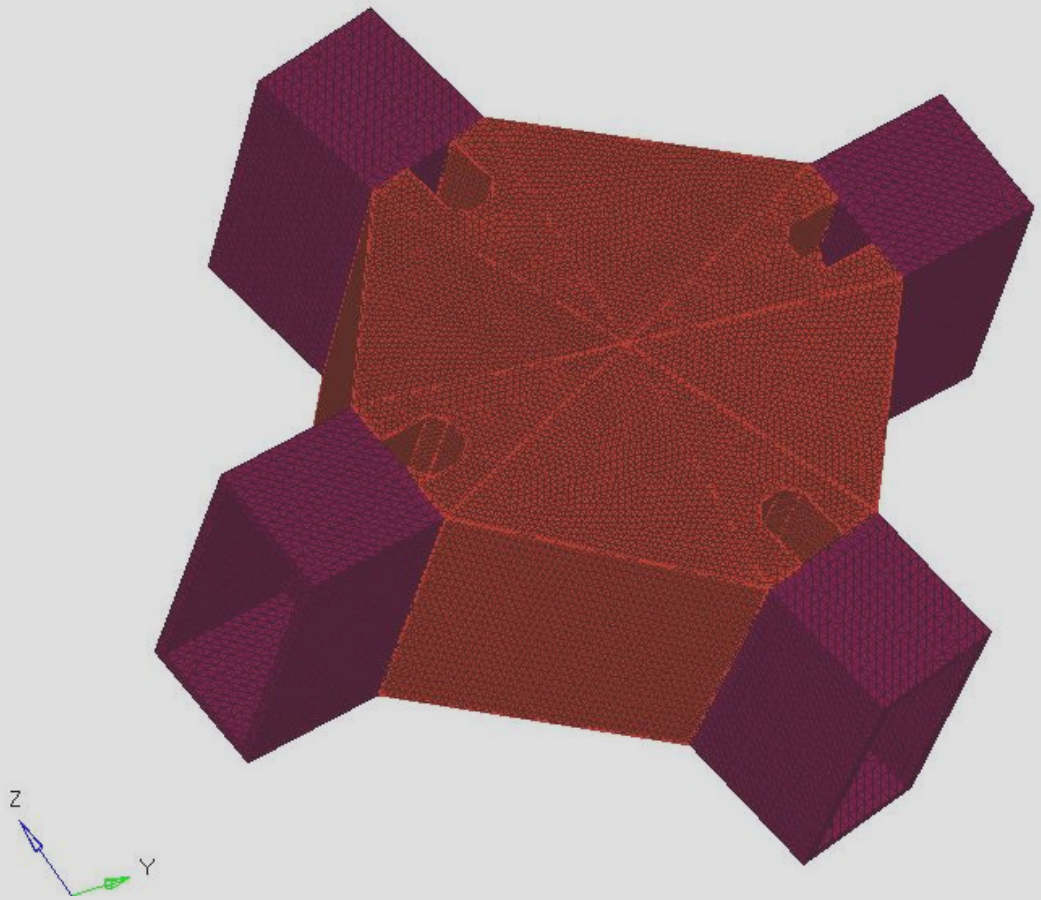

3. Optimization process

The calculation runs until 38 iterations. The following describes the summary of the calculation:

Objective function at the first iteration: 0.796E+05 J
Objective function at the last iteration: 0.302E+04 J
Objective function change: -96.2 %
Maximum constraint violation: 0.00 %

Loadcase 1

Maximum displacement is 0.588 mm at grid 30464.
Maximum 3-D element stress is 69.5 N/mm2 in element 59543.

Loadcase 2

Maximum displacement is 1.02 mm at grid 30971.
Maximum 3-D element stress is 123 N/mm2 in element 56145.

Loadcase 3

Maximum displacement is 0.524 mm at grid 28021.
Maximum 3-D element stress is 62.1 N/mm2 in element 84201.

Loadcase 4

Maximum displacement is 0.556 mm at grid 30971.
Maximum 3-D element stress is 58.2 N/mm2 in element 63486.

Loadcase 5

Maximum displacement is 0.773 mm at grid 66286.
Maximum 3-D element stress is 65.6 N/mm2 in element 66752.

Figure 6-10 Optistruct topology optimization density distribution at iteration 5, 10, 15, 25, 30, 38

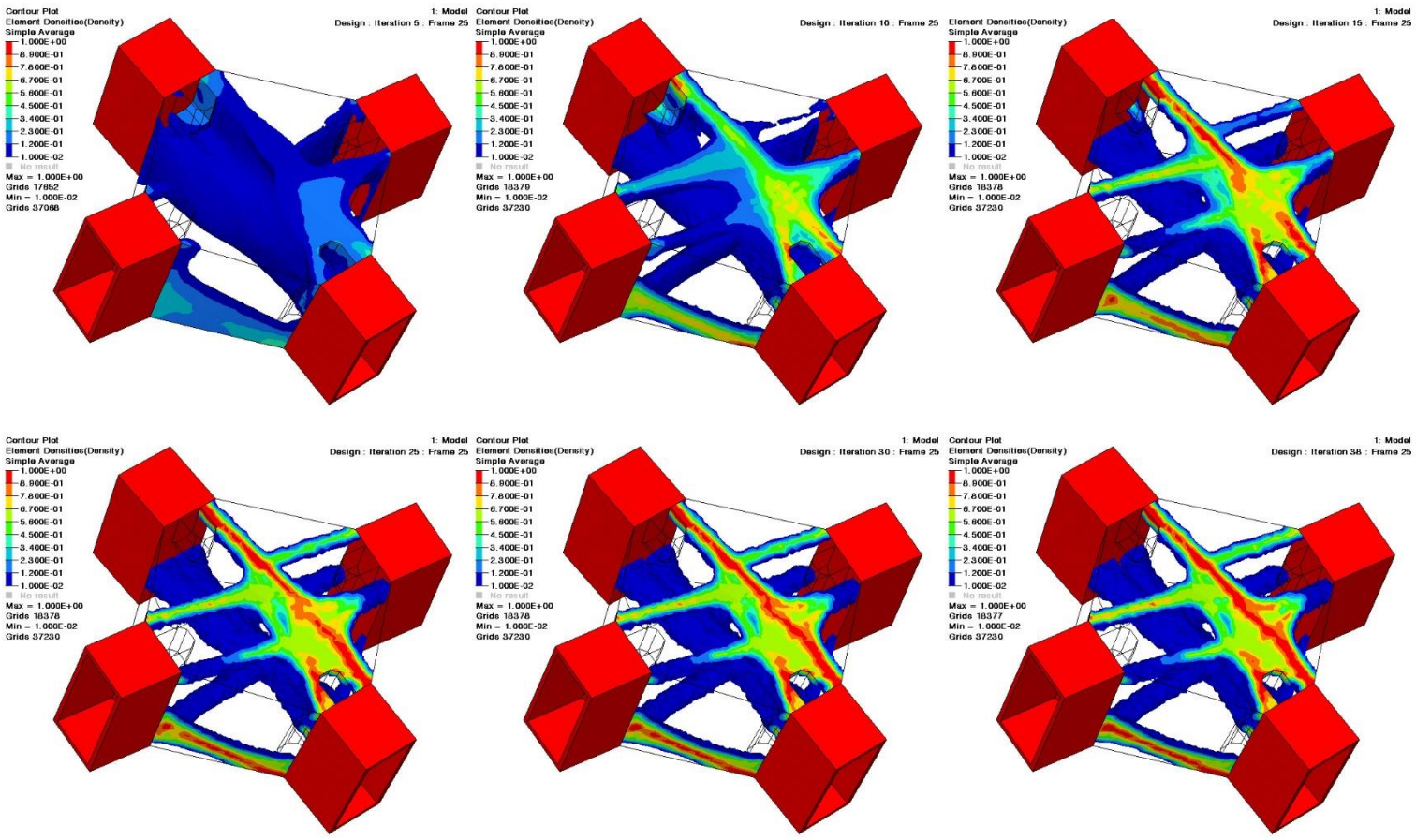

4. Post-processing

Since the case study optimization design is focused on one node, the post processing are treated differently form the prototype structure project. Instead of using automated mesh smoothing, the process was done manually with a free-form modelling tools T-Splines, a plugin for Rhinoceros software.

T-Splines tool is a great software to produce freeform geometry with more control over the curvature of the surface compared to a standard NURBS modelling process. Even though it has a steeper learning curve to master the tool, the resulting geometry is more elegant in terms of general looks compared to the automatic smoothing in Meshmixer.

A standard optimization design using the similar method with the prototype structure is also equipped on the node. The shape was generated using the same parametric model used in the prototype structure design.

Figure 6-11 Mesh output from Hyperworks combined with the standard node design (left), and the smooth final design after T-Splines modelling (right)

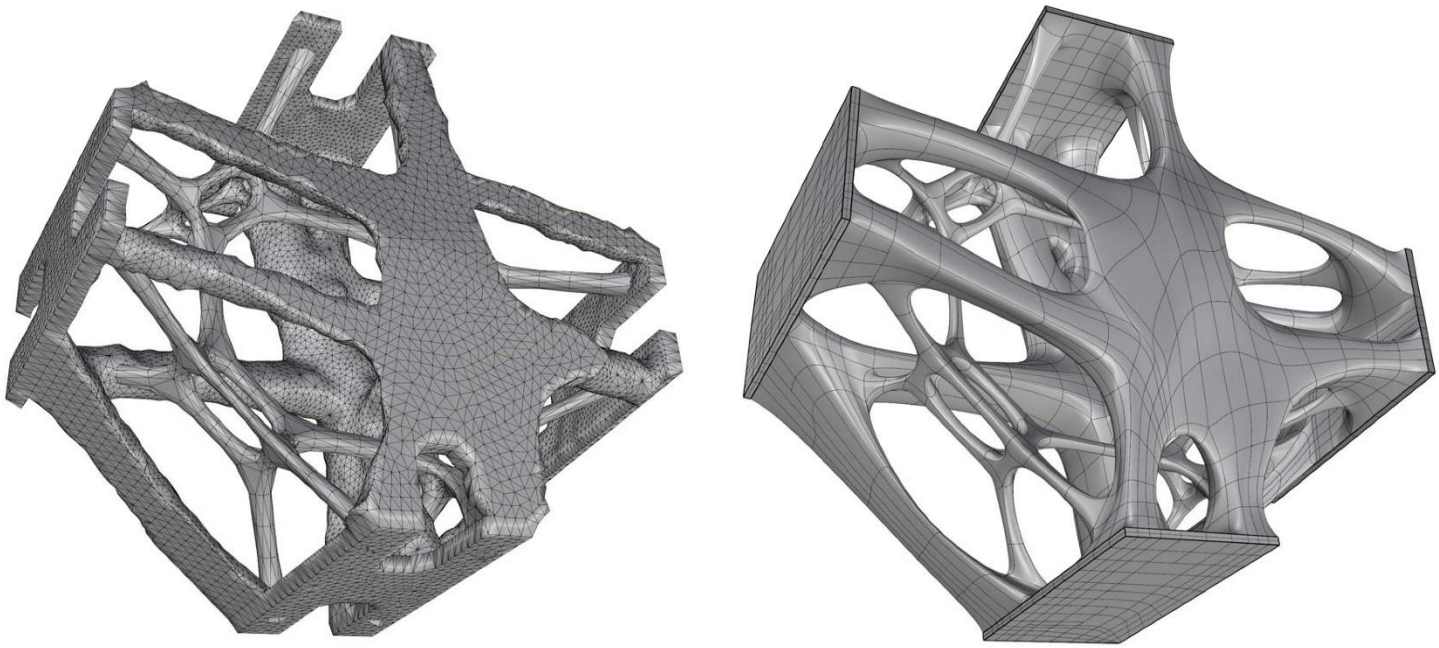

6.5 Construction

The node was designed to have bolt connection with the beams, with 2 holes provided for each beams. It is also possible to have welded connection considering the material properties of EOS Stainless Steel GP1, depends on more detailed structural analysis which is beyond the scope of this research.

The glazing connection could use the similar design as the Portrait gallery roof with the stepped glazing. A triangular mount is placed on top of the beam giving space for the gap of the stepped panels. The detailing of the optimized node in this research is presented conceptually. Further detailed research is required for the optimal design and strategy of façade construction utilizing the potential of additive manufacturing.

Figure 6-12 Connection detail of the Portrait gallery roof

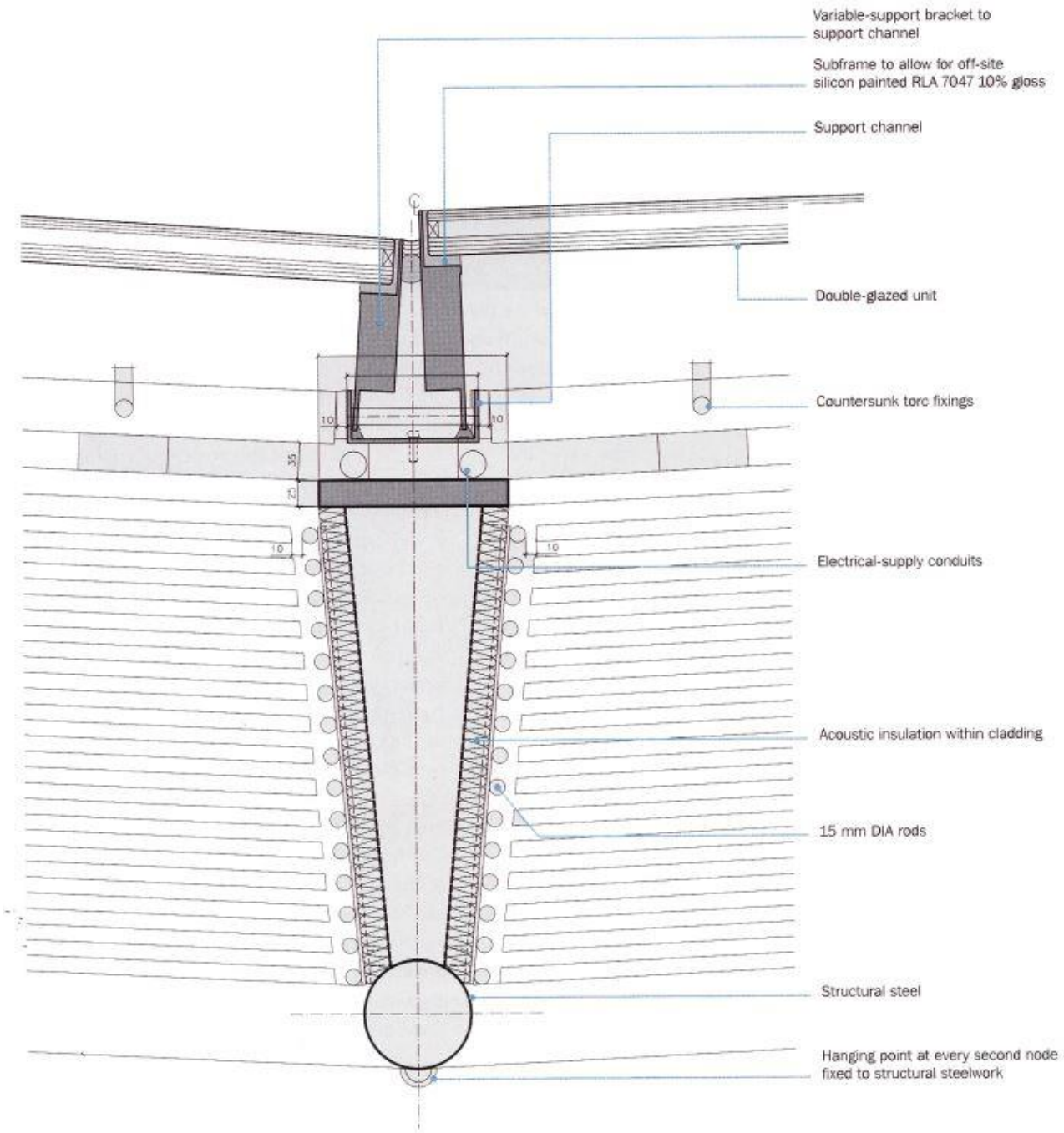

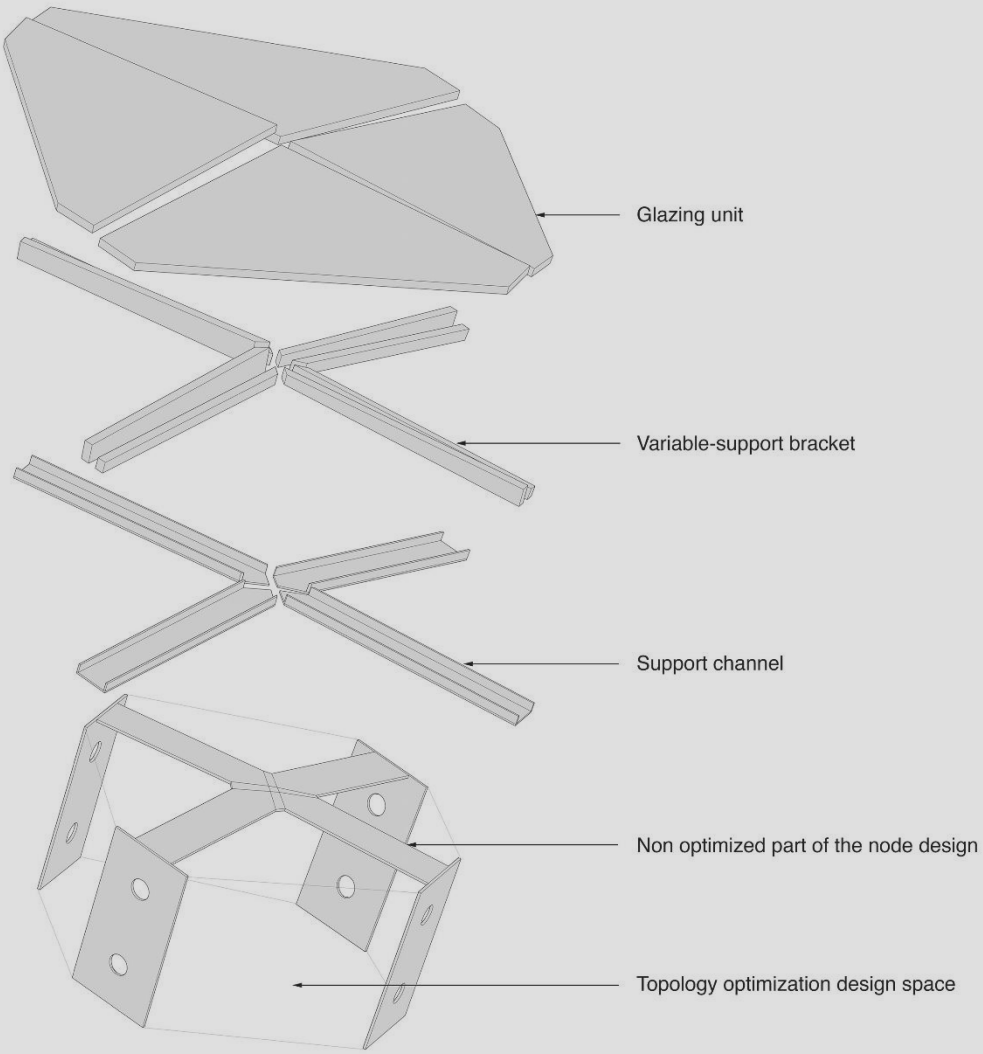

Figure 6-14 Exploded detail of the glazing connection

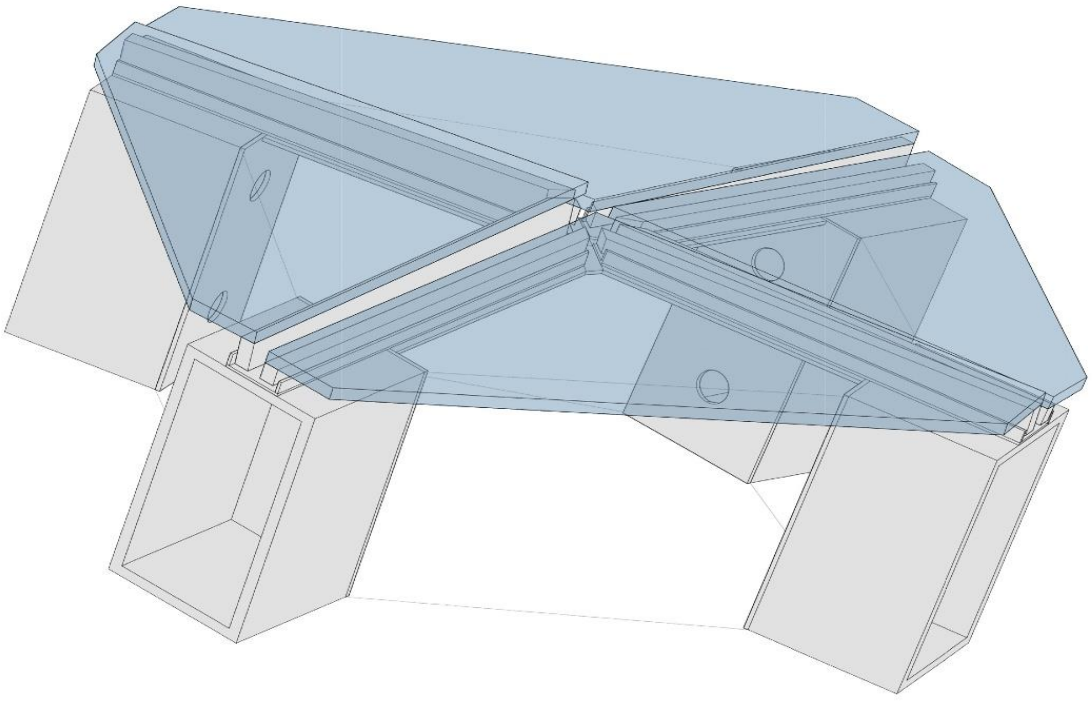

Figure 6-13 Conceptual connection detail of the glazing

6.6 Prototype node

The node is manufactured in 1:4 scale with approximate dimension of 100 mm. It was printed by Shapeways, a company which has service of 3D printing of multiple different material and methods. The metal printing process was done in binder jetting of stainless steel powder with 40% infused of bronze powder instead of direct laser sintering. In general the process is cheaper than DMLS method, even though the material is not pure stainless steel and the stiffness of the parts if approximately 2/3 lower than DMLS stainless steel.

Certain modification of the model was necessary after it was scaled down 25%. One of the main issue was that the standard optimization design part was too thin for the metal printing and it has a high chance for failure. In the end a certain parts were simplified and thin members were made thicker on thte T-Splines model before sending for the manufacturer.

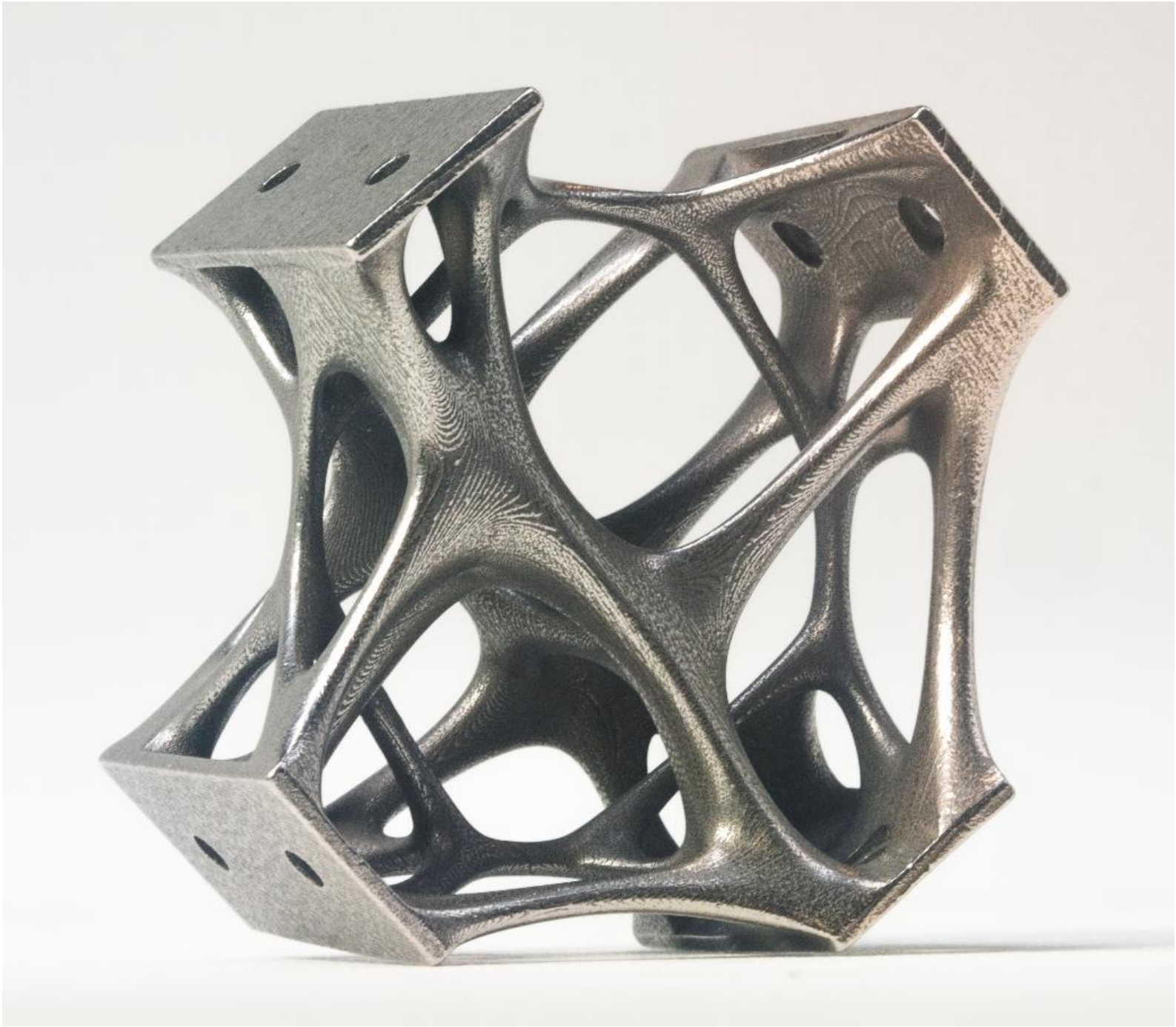

6.7 Comparison

Since the 3d model of the built project is not available, the design of the original structure is remodeled with approximation and some assumption. The total weight of all nodes is averaged using only one node model, further research of detailed comparison in terms of weight and cost is still required.

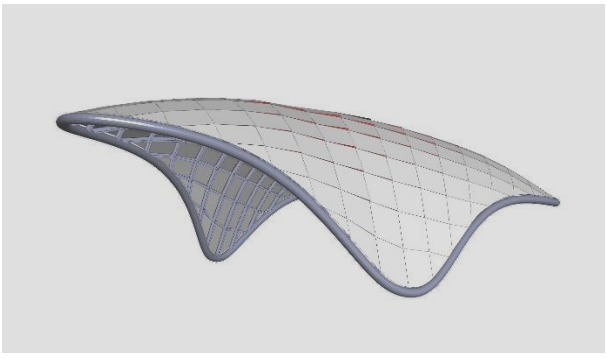

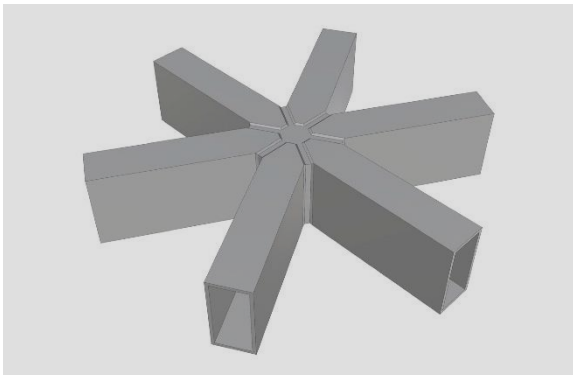

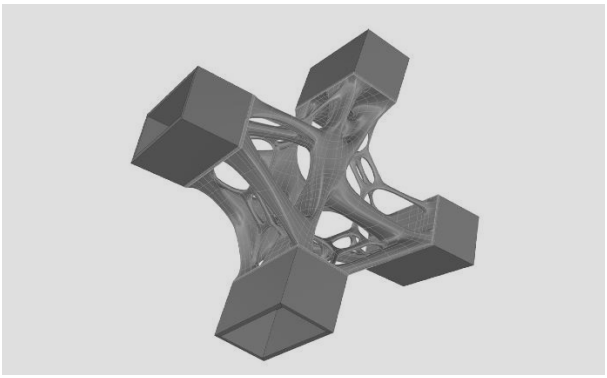

Original design	
Glazing area	: 417 sqm
Beam count	: 503
Total beam length	: 847 m
Total net beam mass	: 30.2 ton
Node count	: 202
Net node mass	: 23.5 kg
Total net node mass	: 4.7 ton
Total structure mass	: 34.9 ton

Optimized design	
Glazing area	: 423 sqm
Beam count	: 392
Total beam length	: 490 m
Total net beam mass	: 17.5 ton
Node count	: 222
Net node mass	: 28.3 kg
Total net node mass	: 6.2 ton
Total structure mass	: 23.7 ton
Weight reduction	: 32%

6.8 References

Blaauwendraad, J., & Hoefakker, J. H. (2013). *Structural shell analysis: Understanding and application* (Solid Mechanics and Its Applications, v.200; Solid mechanics and its applications, v.200). Dordrecht: Springer. doi:10.1007/978-94-007-6701-0

Donnell, J. O., Sefi, H., Sitler, B., Williams, N., Crolla, K., & Xie, Y. M. (2015). Smart Nodes Pavilion – Bi-Directional Evolutionary Structural Optimization and Additive Manufacturing. Proceedings of the International Association for Shell and Spatial Structures (IASS) Symposium 2015, Amsterdam, (August).

D. Anderson, Z. Czajewski, S. Clarke, I. Feltham, P. Geeson, M. Karczmarczyk, R. Kent, D. Killion, Z. Kotynia, M. Lewonowski, R. Lindsay, P. Monypenny, C. Murgatroyd, J. Ojeil, R. Orlowski, A. Sitko, and D. Woolf, "Zlote Tarasy, Warsaw , Poland," *Arup Journal*, vol. 1, 2008.

Evolute | the geometry experts. (n.d.). Retrieved June 16, 2016, from http://www.evolute.at/

Galjaard, S., Hofman, S., & Ren, S. (2014). New Opportunities to Optimize Structural Designs in Metal by Using Additive Manufacturing. *Advances in Architectural Geometry 2014,* 79-93. doi:10.1007/978-3-319-11418-7_6

Knippers, J., & Helbig, T. (2009). Recent Developments in the Design of Glazed Grid Shells. International Journal of Space Structures, 24(2), 111-126. doi:10.1260/026635109789043205

Linden, L. (2015). Innovative joints for gridshells. *Master Thesis Faculty of Civil Engineering TU Delft*.

CONCLUSION &DISCUSSION

7

CONCLUSION & DISCUSSION

7.1 Topology optimization method: global calculation for local optimization

The topology optimization design method developed in this prototype project was to perform the calculation on the whole structure as a complete solid FEA model. The calculated result is more reliable since the optimization calculates directly to the problem existed on the structure. The issues with the conventional method where forces are translated from a separate structural frame model analysis (for example in Karamba), is that the initial structural analysis was modeled as 1 dimension beam element while on the other hand, topology optimization only works for 3D solid elements. By modeling the whole structure as solid elements, the calculated stresses and behavior of the structure throughout the whole iteration on the non-design space are taken into calculation for the topology optimization design space. There is also an issue of software interoperability when the initial analysis is done in different software with the TO software, where some of the analysis could 'lost in translation' especially if the initial calculation was executed in a conceptual tool such as Karamba.

The main drawback of using this method is that the mesh element need to be very fine with consistent scale especially for the design space geometry. Unlike the conventional FEM analysis model where the mesh can be adjusted to have a high level of detail only where the high stresses is expected, in TO process the mesh need to be detailed on all areas for consistent material penalization. As a result, the model will have a very large amount of finite element which makes a high calculation cost. In general, the issue is simply lies in computational power. It is recommended to invest in a high-end computer machine with high performance processor and large internal memory, or a distributed cloud computation to perform the calculation.

7.2 AM method for TO's 'organic' complex geometry

Topology optimization has been around for quite some time and is used for structural design in many different engineering industry. However, the conventional method is to use the generated shape as a reference to see the general structure behavior, and then the engineer will design the parts according to what is the available manufacturing method. The complex shape from TO was considered as a direct design output only with the availability of additive manufacturing. It is proven that Direct Metal Laser Sintering could produce the most complex shape while at the same time having structural material properties. The scaled mock-up node shows a high quality and accuracy of AM method considering the complexity of the shape, even though the fabrication method was hybrid binder jetting instead of the DMLS.

However, there are many technical issues encountered during the production of the carbon fiber prototype nodes. There are many features of the optimized geometry that are just too difficult for FDM machine. Most of the time spent on the production was consumed for technical tinkering of the machine and finding the suitable print setting which can work for the material. There is also an issue of extensive waste material produced for the support structure. It is concluded that the complex geometry of the optimized structure is more suitable for powder based laser sintering method which it is much better at handling smaller wall thickness and lower support required for overhang parts.

7.3 Additive manufacturing for building structure: localized complexity

Most of the question asked for research on Additive Manufacturing is that whether it will replace the traditional fabrication process. This research tried to answers that question from a different perspective. Instead of simply replacing the original design and applying the method of TO and AM, it is more recommended to take a step back and establish a new design method based on the opportunities and constraints offered by TO and AM technology. In the context of freeform envelope, the geometric and structural complexity are taken by the nodes and solved with the TO and AM design. The idea of localized complexity is to push in most of the complexity into the smallest detail where it can utilize the potential of AM, while reducing the general complexity of the structure where AM method is not an option.

7.4 Beyond weight reduction

There are already a few of previous research that concludes the potential of TO and AM in reducing structural weight compared to the conventional design. However, this research aims to go beyond replacing the conventional manufacturing method and completely change the whole design intent utilizing the potential of TO and AM. With a simple approximate calculation, the Baku airport canopy new design is 32 % lighter than the original structure design, even though it has more envelope surface area. Moreover, the quad paneling design reduces the amount of connection detail elements required compared to the triangular design in terms of bulk volume and it increase the efficiency of glazing manufacturing. There are more significant factor to be considered when designing with TO and AM. First, the lead time of AM fabrication is lower than traditional manufacturing. Secondly, it is easier to design for simpler connection method with AM design, such as bolted connection. This means most of the assembly process can be done on site, reducing the needs to transport large pre-assembled structural parts which requires larger means of transportation. Furthermore, fabrication with AM method can greatly reduce the overall construction time which could have a significant impact in reducing general construction cost. In conclusion, design with TO and AM should not be compared directly in terms of only weight reduction or volume differences. An extensive comparison should be evaluated since design with TO and AM could change the whole process from design to construction in architecture.

7.5 Further research suggestions

- Application of TO and AM in other architecture elements

Freeform envelope is just one of the context of architectural element where the technology of TO and AM can be applied. There are still many possibilities to explore its potential in the building industry. With the concept of localized complexity, the same idea can be applied to façade design, building utilities system, building primary or secondary structure and interior design.

- Quad glazing assembly detail integration with AM

While in this research a conceptual design of glazing connection was developed, a more extensive research is required to further explore the potential of design with AM to integrate structural design and façade design by considering more design parameters such as glazing insulation properties, glazing manufacturing process, façade secondary structure, and waterproofing.

- Extensive advanced structural analysis

The scope of structural analysis level of detail in this research was limited to simple linear analysis calculation. To further validate the design concept, it is required to do more advanced calculation for non-linear behavior such as buckling analysis.

- Shape optimization for AM constraints

There are many opportunities to further optimize the material efficiency in AM fabrication, especially in FDM method. Support material or scaffolding structures sometime takes a large amount of material and time relative to the actual printed part itself. Meshmixer has developed a smart algorithm to generate more efficient support structures. However, when we have a complete freedom of geometry on the design, there is a potential in using an algorithm which modify the design itself, for example reducing the overhang and bridges geometry in the design parts.

- Extensive physical test for AM materials

The physical test done in this research was a schematic proof of concept method. It is still required to do a comprehensive test on the carbon fiber infused filament material. It is also interesting to explore further different FDM print setting in relation to material mechanical properties.

- Extensive cost analysis

The final question was always is it worth it to use metal 3D printing for buildings? Further cost analysis is still required to compare the new design method with the traditional method. The comparison should consider not only quantitative but also qualitative comparison to see its impact as part of architectural design elements.

7.6 Discussion

When computers take over your job

Topology optimization in general is a part of structural form-finding computational design method. The technology was meant to inspire designer and engineer create their designs. It is a design tool which helps designers in making a design decision, with respect of other design requirement that influenced the performance and the purpose of the design. In the other industry such as aerospace and automotive, topology optimization generated design is arguably could replace the engineer's job in designing the structural shape. Moreover, the additive manufacturing process made it possible to greatly reduce the needs of alteration from raw computer generated design to functional physical object. The bigger question would be: Are we going to have a product which was designed and manufactured completely by computer and software?

Relevance in architecture

If we are talking about a specific performance driven products such as parts of an airplane or car, which have highly regulated performance criteria for specific functions, perhaps the answer is yes, machines and artificial intelligent could provide a complete design and manufacturing solutions while human is merely needs to prepare the problem to solve. However, architecture and the built environment industry works in a much bigger scale of social context. There is never been a single definite solution for one architectural problems, including the building structural problems. Buildings are meant to last for generations

Sketched by computer software

However, as it was observed in this research, there are still some design steps after the optimized design resulted from the topology optimization algorithm can be considered as a finished design product. If the result of topology optimization is a science approach where the solution is pure numerical calculation giving the most optimal answers, the integration of the standard optimization design node and manual geometry smoothing with T-Splines is considered as engineering and design intervention, where engineers and designers' intuition based on knowledge and experience took part in finalizing the design. In conclusion, I would argue that the algorithm simply provides a design sketch. In the end, designers are still responsible for the design, while considering other important factor into the calculation such as manufacturability, functional intent, and especially aesthetic, an area where even the most advanced algorithm couldn't compete with human designer.

8

BIBLIOGRAPHY

Books

Adriaenssens, S. (2014). *Shell structure for architecture: Form finding and optimization*. Abingdon: Routledge - imprint of Taylor & Francis Group.

Bendsoe, M., & Sigmund, O. (2003). *Topology optimization: Theory, methods, and applications*. Berlin: Springer.

Blaauwendraad, J., & Hoefakker, J. H. (2013). *Structural shell analysis: Understanding and application*. Dordrecht: Springer.

Chua, C. K., & Leong, K. F. (2015). *3D Printing and additive manufacturing: Principles and applications.* New Jersey: World Scientific.

Christensen, P. W., & Klarbring, A. (2008). *An introduction to structural optimization*. Dordrecht: Springer.

Gibson, I., Rosen, D., & Stucker, B. (2015). *Additive manufacturing technologies: 3D printing, rapid prototyping, and direct digital manufacturing* (Second edition.). New York, NY: Springer.

Knaack, U., Strauss, H., & Bilow, M. (2010). Rapids (Imagine, 04). Rotterdam: 010 Publishers.

Pawlyn, M. (2011). *Biomimicry in architecture*. London, UK: Riba Publishing.

Philippe, B., & Knippers, J. (2015). *Advances in architectural geometry 2014*. Cham: Springer.

Schober, H., & Schaffert, C. (2015). *Transparent shells: Form, topology, structure*. Wiley.

Articles & Research papers

Anderson, Z. D; Czajewski, S. (2008). Zlote Tarasy, Warsaw, Poland. *Arup Journal, vol 1*

Donnell, J. O., Sefi, H., Sitler, B., Williams, N., Crolla, K., & Xie, Y. M. (2015). Smart Nodes Pavilion – Bi-Directional Evolutionary Structural Optimization and Additive Manufacturing. Proceedings of the International Association for Shell and Spatial Structures (IASS) Symposium 2015, Amsterdam, (August).

Galjaard, S., Hofman, S., & Ren, S. (2014). New Opportunities to Optimize Structural Designs in Metal by Using Additive Manufacturing. *Advances in Architectural Geometry 2014,* 79-93. doi:10.1007/978-3-319-11418-7_6

Glymph, J., Shelden, D., Ceccato, C., Mussel, J., & Schober, H. (2004). A parametric strategy for free-form glass structures using quadrilateral planar facets. *Automation in Construction, 13*(2), 187-202.

Guido A. O. Adam Detmar Zimmer, (2015),"On design for additive manufacturing: evaluating geometrical limitations", Rapid Prototyping Journal, Vol. 21 Iss 6 pp. 662 – 670

Huang, X., Xie, Y. M., & Wiley InterScience (Online service). (2010). *Evolutionary topology optimization of continuum structures: Methods and applications.*Chichester, West Sussex: Wiley.

Knaack, U. (2007). *Facades: Principles of construction*. Ba: Birkha¨user. http://public.eblib.com/choice/publicfullrecord.aspx?p=336679

Knippers, J., & Helbig, T. (2009). Recent Developments in the Design of Glazed Grid Shells. International Journal of Space Structures, 24(2), 111-126.

Langelaar, M. (2016). Topology Optimization of 3D Self-Supporting Structures for Additive Manufacturing. *Additive Manufacturing*, (5-8). doi:10.1016/j.addma.2016.06.010

Langelaar, M., & Keulen, F. (2015). Topology optimization. A natural counterpart of additive manufacturing. *TU Delft Lecture Notes*.

Letcher, T., & Waytashek, M. (2014). Material Property Testing of 3D-Printed Specimen in PLA on an Entry-Level 3D Printer. *Volume 2A: Advanced Manufacturing*. doi:10.1115/imece2014-39379

Linden, L. (2015). Innovative joints for gridshells. *Master Thesis Faculty of Civil Engineering TU Delft*.

Lundgren, J; Palmqvist, C. (2012). *Structural Form Optimization Methods of Numerical Optimisation and Applications on Civil Engineering Structures.* Chalmers University of Technology.

Oxman, N., Laucks, J., Kayser, M., Tsai, E., & Firstenberg, M. (2013). *Freeform 3D Printing: Toward a Sustainable Approach to Additive Manufacturing. Green Design, Materials and Manufacturing Processes.*

Prohasky, D., Williams, N., Crolla, K., & Burry, J. (2015). SmartNodes: 'Light-weight' parametric structural design process with BESO. Proceedings of the International Association for Shell and Spatial Structures (IASS).

Sigmund, O., & Maute, K. (2013). Topology optimization approaches. Struct Multidisc Optim Structural and Multidisciplinary Optimization, 48(6), 1031-1055. doi:10.1007/s00158-013-0978-6

Sischka, J; Biro, Wagner. (2008). Mesh match: Stories of seminal skins - Case study: The British Museum, London. *The Journal of the Society of Façade Engineering, 4.*

Suzuki, K., & Kikuchi, N. (1991). A homogenization method for shape and topology optimization. Computer Methods in Applied Mechanics and Engineering, 93(3), 291-318.

Strauss, H., Knaack, U., & Techen H. (2013). *AM Envelope: The Potential of Additive Manufacturing for facade constructions*. TU Delft.

Tymrak, B., Kreiger, M., & Pearce, J. (2014). Mechanical properties of components fabricated with open-source 3-D printers under realistic environmental conditions. Materials & Design, 58, 242-246. doi:10.1016/j.matdes.2014.02.038

Wang, M. Y., Wang, X., & Guo, D. (2003). A level set method for structural topology optimization. Computer Methods in Applied Mechanics and Engineering, 192(1-2), 227-246

Zegard, T., & Paulino, G. H. (2016). Bridging topology optimization and additive manufacturing. Structural and Multidisciplinary Optimization, 53(1), 175-192. doi:10.1007/s00158-015-1274-4

Weblinks - Softwares

Altair Hyperworks – Advanced engineering software with TO features (OptiStruct)
http://www.altairhyperworks.com/

Evolute – Freeform surface paneling tool
http://www.evolute.at/

Kangaroo - Live Physics engine for simulation, optimization and form-finding with Grasshopper
http://www.grasshopper3d.com/group/kangaroo

Milipede – TO algorithm as Grasshopper plugin
http://www.sawapan.eu/

Meshmixer - Software for working with triangle meshes
http://meshmixer.com/

Solidthinking Inspire – TO concept generation software
http://www.solidthinking.com/Inspire2016.html

Simplify3D – 3D printing slicing software
https://www.simplify3d.com/

T-Splines – Advanced free-form modelling tools
http://www.tsplines.com/

AM service providers

3D hubs, online local 3D printing service
https://www.3dhubs.com/

3DSystems (UK) http://uk.3dsystems.com/

ExOne (Germany) http://www.exone.com/

Fit-Prototyping (Germany) http://www.fit-prototyping.de/

i.Materialise (Belgium)
https://i.materialise.com/

Laserproto (UK) http://www.laserproto.com/

Protolabs (USA) https://www.protolabs.com/

Rapidobject (Germany)
https://www.rapidobject.com/

Rapidmade (USA)
http://www.rapidmade.com/

Shapeways (Netherlands)
https://www.shapeways.com/

Star-Prototype (China) http://www.star-prototype.com/

Stratasys (USA)
https://www.stratasysdirect.com/

Miscellaneous

3D printing news, trends, and resources
http://www.3ders.org/

Colorfabb filament manufacturer
http://colorfabb.com/

EOS AM systems http://www.eos.info/en

Leeuwenhoek open-source FDM 3D printer
http://dymensional.nl/

RepRap open-source 3D printer
http://reprap.org/wiki/Main_Page

RM Platform: European collaboration on Rapid Manufacturing http://www.rm-platform.com/

TED Talk by Neri Oxman - Design at the intersection of technology and biology
https://www.ted.com/talks/neri_oxman_design_at_the_intersection_of_technology_and_biology?language=en

.

9

APPENDICES

9.1 Example case of topology optimization

In order to understand the design methodology of structural elements with Topology Optimization, multiple test calculation was done on a simple cantilever beam case study.

The test model was a rectangular box 100 x 60 x 70 mm beam, with a fixed support at one side.

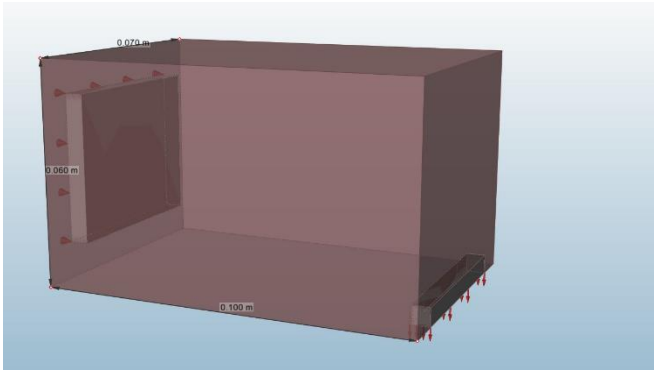

Material: Aluminum (2024) E: 75 GPa Yield Stress: 75 MPa

Load : 3 kN

1. Minimize mass with safety factor constraint

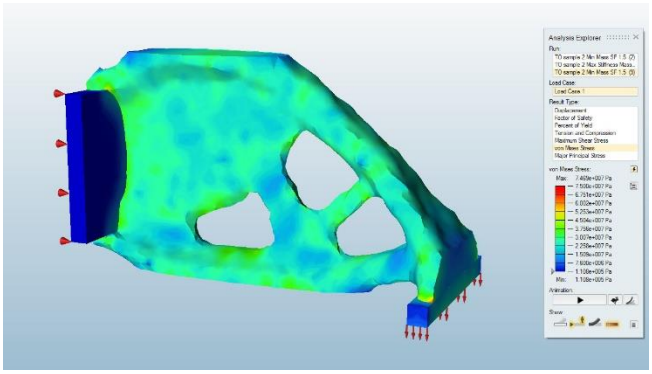

TO result with safety factor target of 1.5

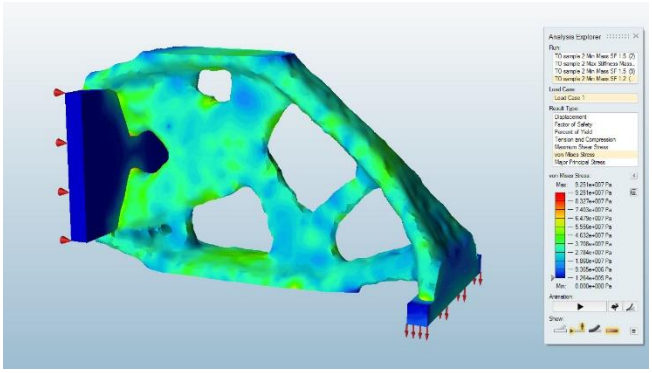

TO result with safety factor target of 1.2

2. Maximize stiffness with percentage of design space volume constraint

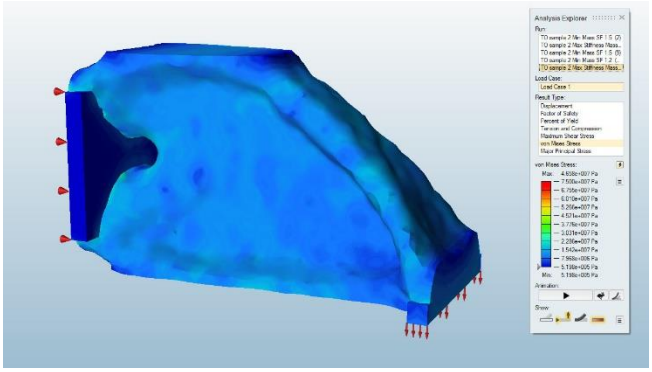

TO result with 20% target mass

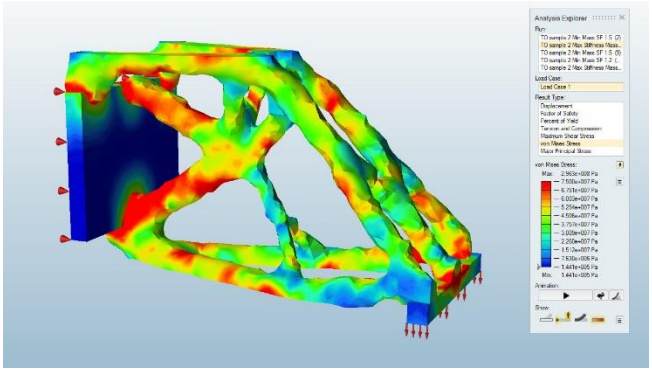

TO result with 5% target mass

Structural loadcase

Another test done was to apply different type of loads to cantilever beam. The test results show different optimized geometry according to each specific load types.

Original structure member: 300mm long RHS100x50x5

TO design space: 240mm long in the middle of the member

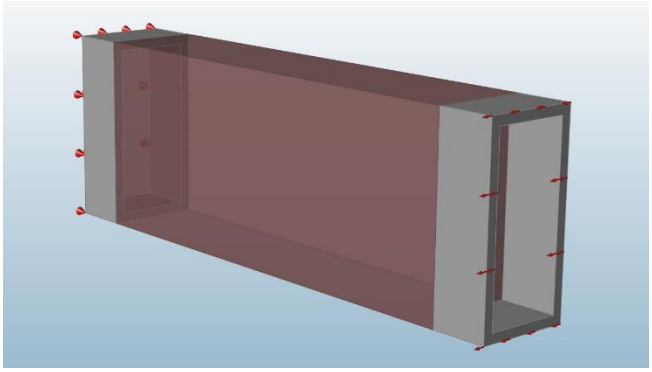

1. Normal force x-axis

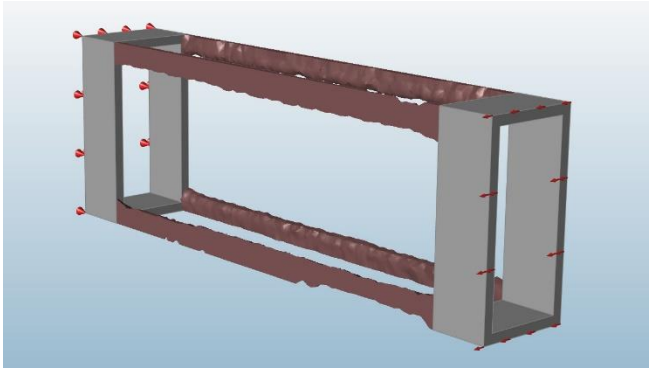

2. Shear force y-axis

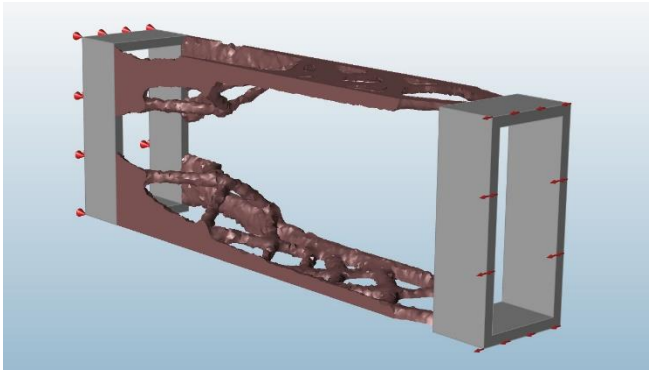

3. Shear force z-axis

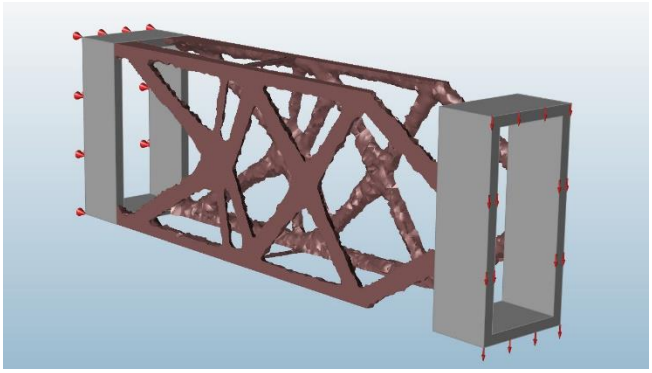

4. Torsion around x-axis

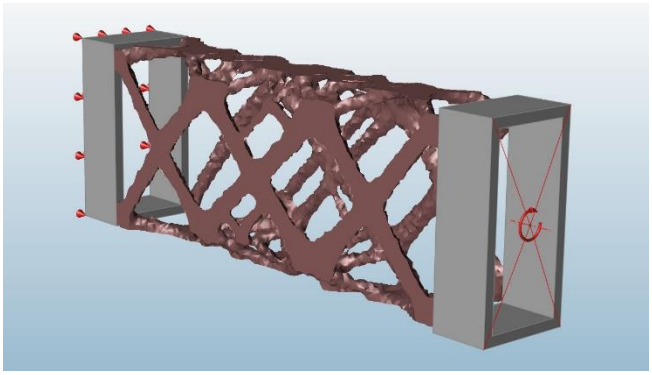

5. Moment around y-axis

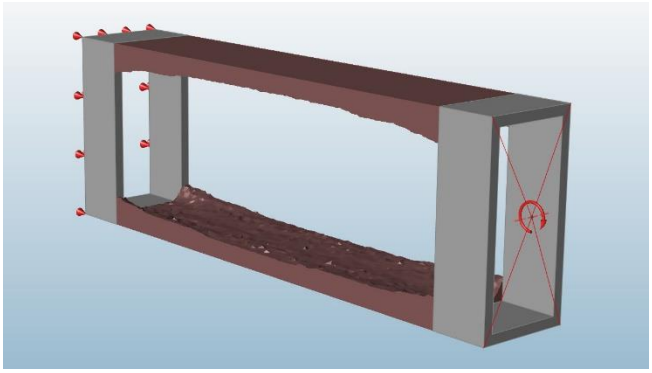

6. Moment around z-axis

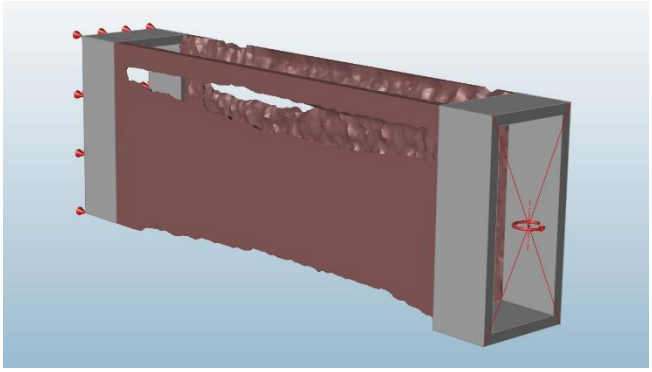

7. Combination loads

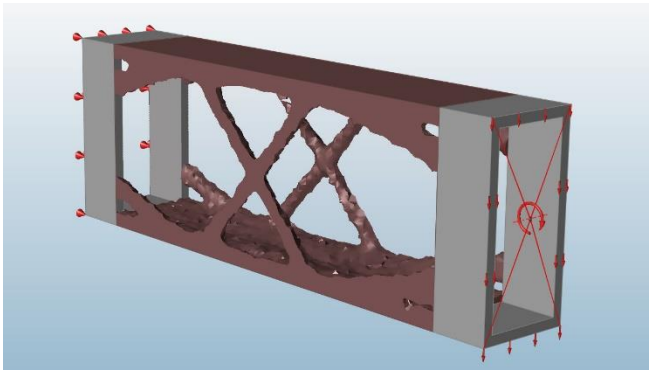

Overview

Each of the result of the optimized geometry are quite reasonably make sense in terms of its structural requirements. The result came close to what was imagined before with engineering intuition. In average, each of the optimization calculation with Solidthinking Inspire takes around 15 to 30 minutes with an average-laptop computing power. The constraints with the software is that the output geometry is too rough and coarse to be used directly as a final product.

Another case that was not possible to be done in Solidthinking Inspire was to apply multiple load cases with importance weight. It will need a multi-objective optimization algorithm to run the calculation. Further studies will be needed on a more advanced software such as Hyperworks OptiStruct with more computing power.

9.2 Sample prototype for Additive Manufacturing

One of the result of the sample topology optimization case was developed further to fulfil the requirements of Additive Manufacturing. The output geometry was remodelled with T-Splines modelling tools in Autodesk Fusion. Further design optimization was done by adjusting the geometry in order to minimize the need of support material in the printing process. The geometry was modelled with the basic principle of design for DMLS and SLM method.

The model was sent to multiple AM service companies all around the world and quotation was requested. The objective was to get the basic idea of the cost of metal AM in different metal materials available on the market. The model was also fabricated in PLA plastic as a comparison model.

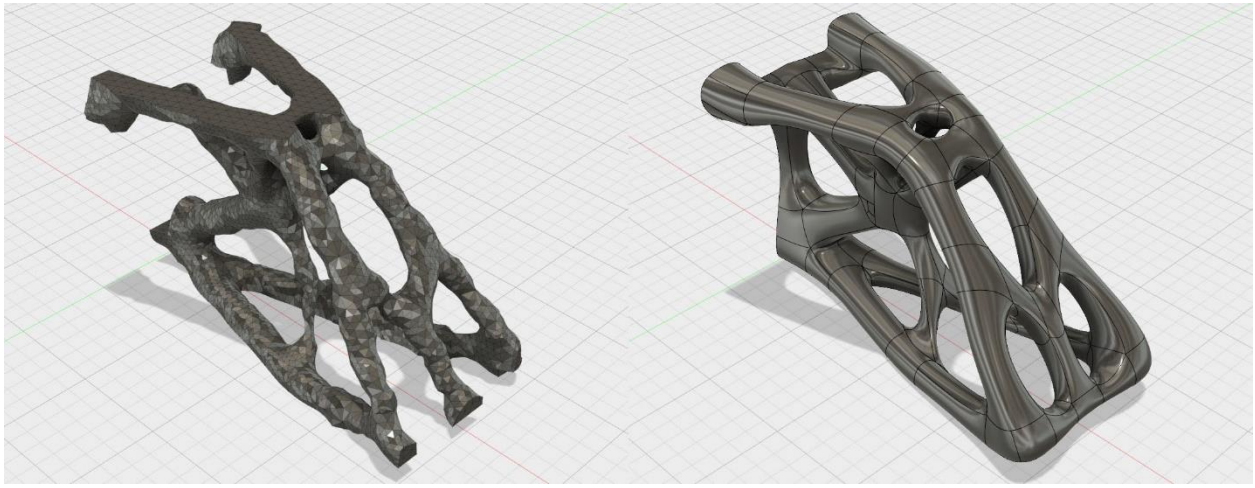

Original TO result (left) and remodeled result (right)

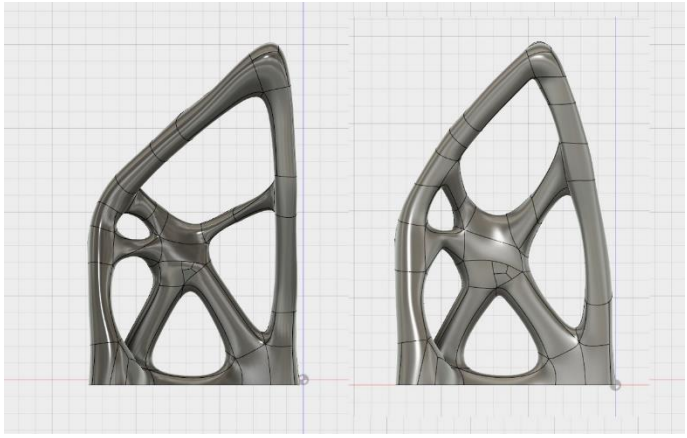

First remodeling result (left), final optimized model for AM (right)

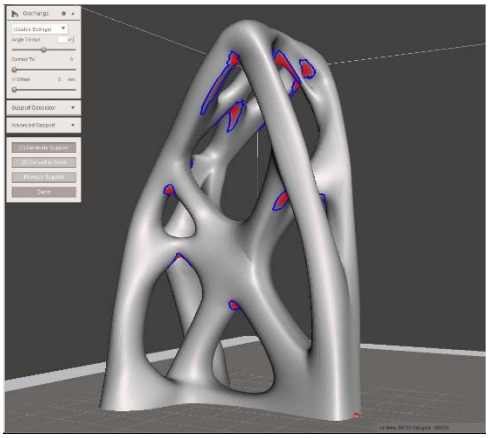

Overhang analysis, the red areas shows the possible need for support structure

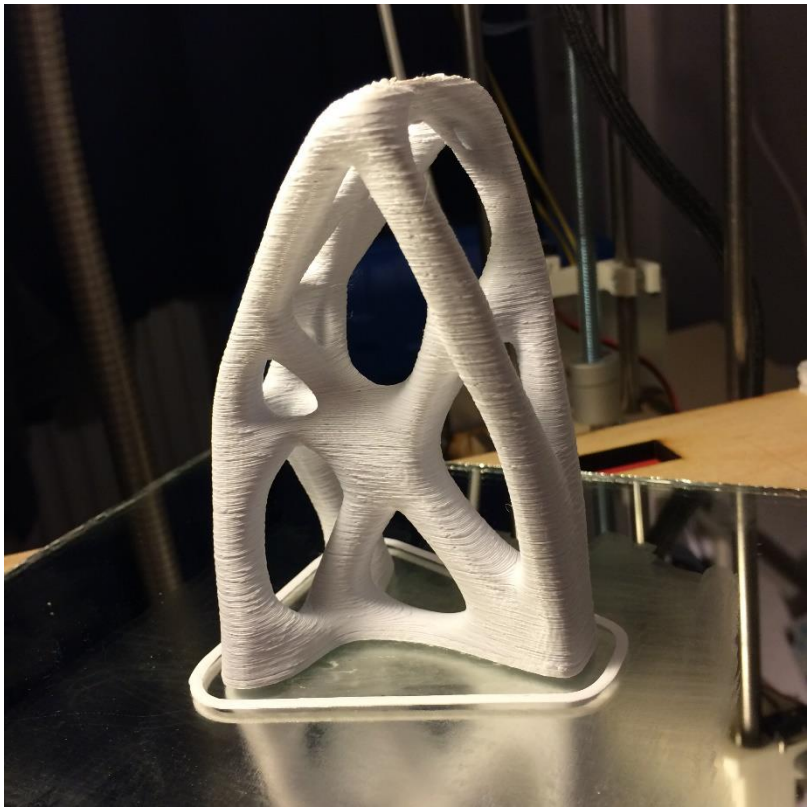

	Company	Country	Material	Ultimate Tensile Strength (MPa)	Price (EUR)
Binder jetting	Shapeways	NL	Stainless Steel 420 60% + Bronze 40%	682	229
	i.materialise	BE	Stainless Steel 420 60% + Bronze 40%	682	216
	ExOne	GER	Stainless Steel 420 60% + Bronze 40%	682	**125**
Direct Laser Melting	RapidObject	GER	Tool steel 1.2709	1100	757
	Stratasys	US	Stainless Steel 17-4 PH	980	1236
	Fit-Prototyping	GER	Stainless Steel 17-4 PH	980	930
	RapidObject	GER	Stainless steel 1.4542	930	924
	Stratasys	US	Stainless Steel 316L	675	1172
	Protolabs	UK	Stainless Steel 316L	675	1101
	Star-Prototype	CHN	Stainless Steel 316L	675	**642**
	Stratasys	US	Aluminum AlSi10Mg	400	1347
	Star-Prototype	CHN	Aluminum AlSi10Mg	400	1120
	Protolabs	UK	Aluminum AlSi10Mg	400	1044
	RapidObject	GER	Aluminum AlSi10Mg	400	428
	Fit-Prototyping	GER	Aluminum AlSi10Mg	400	350

Price comparison of the prototype model from different AM service companies

9.3 Material data sheet

1. Carbon fiber infused filament

Preliminary Data Sheet

20% milled carbon fibres
Latest revision: Januari 2015

Properties	Test methods	Units	carbon fibres
Physical properties			
Specific gravity	ISO 1183	g/cm^3	1,35
Water absorption at saturation, 23 °C	ISO 62	%	-
Humidity absorption, 23 °C/50 % r.h.	ISO 62	%	-
Mould shrinkage (flow direction, 3 mm)	ISO 2577	%	0,2 - 0,4
Mechanical properties			
Tensile strength (max.)	ISO 527	MPa	76
Elongation at break	ISO 527	%	7,5
Flexural strength	ISO 178	MPa	110
Flexural modulus	ISO 178	GPa	6,2
IZOD impact strength, notched	ISO 180/1eA	kJ/m^2	6
IZOD impact strength, unnotched	ISO 180/1eU	kJ/m^2	60
Thermal properties			
Heat distortion temperature (1,81 MPa)	ISO 75	°C	65
Relative temperature index, 3 mm, with impact	UL 746B	°C	-
Coefficient of linear thermal expansion	ISO 11359	$K\text{-}1 \cdot 10^{-5}$	-
Flammability			
Burning behaviour	IEC 60695-11-10	-	HB @ 3,2 mm
UL recognition	UL94	-	-
Electrical properties			
Surface resistivity	ASTM D257	□ /sq	10^9
Comparative tracking index	IEC 60112	V	-
Glow wire rating, 1,6 mm	IEC 695-2-1	°C	-

Processing conditions (injection moulding)

Drying conditions (dehumidifying drier)	:	3 - 5 Hours @ 65 °C
Maximum allowable moisture content	:	0,02 %
Melt temperature	:	235 - 255 °C
Mould temperature	:	60 - 75 °C
Screw speed	:	0,1 - 0,2 m/s
Back pressure	:	0 - 1,0 MPa
Injection pressure	:	Keep to a minimum
Injection speed	:	Fast ram speed
Hold pressure	:	Keep to a minimum

colorFabb
Noorderpoort 45
5916 PJ VENLO
The Netherlands

Tel: + 31 (0)77 - 398 09 09
Fax: + 31 (0)77 - 397 14 14
Email: sales@colorfabb.com
Website: colorfabb.com

Material data sheet

EOS StainlessSteel GP1 for EOSINT M 270

A number of different materials are available for use with EOSINT M systems, offering a broad range of e-Manufacturing applications. EOS StainlessSteel GP1 is a stainless steel powder which has been optimized especially for EOSINT M 270 systems. Other materials are also available for EOSINT M systems, and further materials are continuously being developed - please refer to the relevant material data sheets for details.

This document provides a brief description of the principle applications, and a table of technical data. For details of the system requirements please refer to the relevant information quote.

Description, application

EOS StainlessSteel GP1 is a pre-alloyed stainless steel in fine powder form. Its composition corresponds to US classification 17-4 and European 1.4542. This kind of steel is characterized by having good corrosion resistance and mechanical properties, especially excellent ductility in laser processed state, and is widely used in a variety of engineering applications.

This material is ideal for many part-building applications (DirectPart) such as functional metal prototypes, small series products, individualised products or spare parts. Standard processing parameters use full melting of the entire geometry with 20 µm layer thickness, but it is also possible to use Skin & Core building style to increase the build speed. Using standard parameters the mechanical properties are fairly uniform in all directions. Parts made from EOS StainlessSteel GP1 can be machined, spark-eroded, welded, micro shot-peened, polished and coated if required. Unexposed powder can be reused.

Typical applications:

- engineering applications including functional prototypes, small series products, individualised products or spare parts.
- parts requiring high corrosion resistance, sterilisability, etc.
- parts requiring particularly high toughness and ductility.

EOS GmbH - Electro Optical Systems
Robert-Stirling-Ring 1
D-82152 Krailling / München
Telephone: +49 (0)89 / 893 36-0
Telefax: +49 (0)89 / 893 36-28
Internet: www.eos.info

Technical data

General process and geometric data

Minimum recommended layer thickness	20 µm 0.8 mil
Typical achievable part accuracy [1]	
- small parts	± 20 – 50 µm 0.8 – 2.0 mil
- large parts [2]	± 0.2 %
Min. wall thickness [3]	0.3 - 0.4 mm 0.012 - 0.016 in
Surface roughness	
- after shot-peening	R_a 2.5 - 4.5 µm, R_y 15 - 40 µm R_a 0.1 - 0.2 , R_y 0.6 - 1.6 mil
- after polishing	R_z up to < 0.5 µm (can be very finely polished)
Volume rate [4]	
- standard parameters (20 µm layers, full density)	2 mm³/s 0.44 in³/h
- Inner core parameters (Skin & Core style, full density)	4 mm³/s 0.88 - 1.1 in³/h

[1] Based on users' experience of dimensional accuracy for typical geometries, e.g. ± 20 µm when parameters can be optimized for a certain class of parts or ± 50 µm when building a new kind of geometry for the first time.

[2] For larger parts the accuracy can be improved by post-process stress-relieving at 650 °C for 1 hour.

[3] Mechanical stability is dependent on geometry (wall height etc.) and application

[4] Volume rate is a measure of build speed during laser exposure. The total build speed depends on the average volume rate, the recoating time (related to the number of layers) and other factors such as DMLS-Start settings.

EOS GmbH - Electro Optical Systems
Robert-Stirling-Ring 1
D-82152 Krailling / München

Physical and chemical properties of parts

Material composition	steel including alloying elements Cr (15 – 17.5 wt-%) Ni (3 - 5 wt-%) Cu (3 - 5 wt-%) Mn (max. 1 wt-%) Si (max. 1 wt-%) Mo (max. 0.5 wt-%) Nb (0.15 - 0.45 wt-%) C (max. 0.07 wt-%)
Relative density with standard parameters	approx. 100 %
Density with standard parameters	7.8 g/cm³ 0.28 lb/in³

Mechanical properties of parts [5]

	As manufactured	Stress relieved (1 hour at 650 °C)
Ultimate tensile strength		
- in horizontal direction (XY)	min 850 MPa (123 ksi) typical 930 ± 50 MPa (135 ± 7 ksi)	typical 1100 MPa (160 ksi)
- in vertical direction (Z)	min 850 MPa (123 ksi) typical 960 ± 50 MPa (139 ± 7 ksi)	typical 980 MPa (142 ksi)
Yield strength		
(R_{eL}, Lower yield strength)		
- in horizontal direction (XY)	min 530 MPa (77 ksi) typical 586 ± 50 MPa (85 ± 7 ksi)	typical 590 Mpa (86 ksi)
- in vertical direction (Z)	min 530 MPa (77 ksi) typical 570 ± 50 MPa (83 ± 7 ksi)	typical 550 MPa (80 ksi)
(R_{eH}, Upper yield strength)		
- in horizontal direction (XY)	min 595 MPa (86 ksi) typical 645 ± 50 MPa (94 ± 7 ksi)	typical 634 MPa (92 ksi)
- in vertical direction (Z)	min 580 MPa (84 ksi) typical 630 ± 50 MPa (91 ± 7 ksi)	typical 595 MPa (86 ksi)

EOS GmbH - Electro Optical Systems
Robert-Stirling-Ring 1
D-82152 Krailling / München

Young's modulus	170 ± 30 GPa (25 ± 4 msi)	typical 180 GPa (26 msi)
Elongation at break		
- in horizontal direction (XY)	min 25 % typical 31 ± 5 %	typical 29 %
- in vertical direction (Z)	min 25 % typical 35 ± 5 %	typical 31 %
Hardness [6]		
- as built	approx. 230 ± 20 HV1	
- ground & polished [7]	approx. 250 - 400 HV1	

[5] Mechanical testing according to ISO 6892:1998(E) Annex C, proportional test pieces, Diameter of the neck area 5 mm, original gauge length 25 mm

[6] Vickers hardness measurement (HV) according to DIN EN ISO 6507-1. Note that depending on the measurement method used, the measured hardness value can be dependent on the surface roughness and can be lower than the real hardness. To avoid inaccurate results, hardness should be measured on a polished surface.

[7] Due to work-hardening effect

Thermal properties of parts

Coefficient of thermal expansion	
- over 20 - 600 °C (68 - 1080 °F)	14 x 10^{-6} m/m °C 7.8 x 10^{-6} in/in °F
Thermal conductivity	
- at 20 °C (68 °F)	13 W/m °C 90 Btu/(h ft² °F/in)
- at 100 °C (212 °F)	14 W/m °C 97 Btu/(h ft² °F/in)
- at 200 °C (392 °F)	15 W/m °C 104 Btu/(h ft² °F/in)
- at 300 °C (572 °F)	16 W/m °C 111 Btu/(h ft² °F/in)
Maximum operating temperature	550 °C 1022 °F

EOS GmbH - Electro Optical Systems
Robert-Stirling-Ring 1
D-82152 Krailling / München

Material data sheet

The quoted values refer to the use of these materials with EOSINT M 270 systems according to current specifications (including the latest released process software PSW and any hardware specified for the relevant material) and operating instructions. All values are approximate. Unless otherwise stated, the quoted mechanical and physical properties refer to standard building parameters and test samples built in horizontal orientation. They depend on the building parameters and strategies used, which can be varied by the user according to the application. Measurements of the same properties using different test methods (e.g. specimen geometries) can give different results. The data are based on our latest knowledge and are subject to changes without notice. They are provided as an indication and not as a guarantee of suitability for any specific application.
EOS®, EOSINT®, DMLS® and DirectPart® are registered trademarks of EOS GmbH.

EOS GmbH – Electro Optical Systems
Robert-Stirling-Ring 1
D-82152 Krailling / München

shapeways

STEEL

Material Data Sheet

Shapeways' 3D printed steel is Stainless Steel Alloy 420 infiltrated with Bronze (90% Cu/10% Sn). It is a matrix material composed of 60% stainless steel and 40% bronze.

60% 420 Stainless Steel + 40% bronze			
Property	**Value**	**Unit**	**Test Method**
Ultimate Tensile Strength (UTS)	496	MPa	ASTM E8
Yield Strength (0.2% offset)	427	MPa	ASTM E8
Elastic Modulus	147	GPa	ASTM E8
Elongation	7.0	%	ASTM E8
Hardness	93	HRb	ASTM E18
Density	7.86	g/cm^3	MPIF 42
Thermal Conductivity	22.6	W/m°K	ASTM E1530
Specific Heat	478	J/kg°K	ASTM E1263
Thermal Expansion Coefficient	13.4×10^{-6}	/°K	ASTM E228

Notes: *The values listed here should be used for reference only.*

TABLE OF FIGURES

BAYU PRAYUDHI

TUDelft

ARUP